1963

Optimization of the range of an unpowered space vehicle subjected to an aerodynamic heating constraint

Warren George Lambert
Iowa State University

OPTIMIZATION OF THE RANGE OF AN UNPOWERED SPACE VEHICLE SUBJECTED TO AN AERODYNAMIC HEATING CONSTRAINT

by

Warren George Lambert

A Dissertation Submitted to the

Graduate Faculty in Partial Fulfillment of

The Requirements for the Degree of

DOCTOR OF PHILOSOPHY

Major Subject: Theoretical and Applied Mechanics

Approved:

Signature was redacted for privacy.

In Charge of Major Work

Signature was redacted for privacy.

Head of Major Department

Signature was redacted for privacy.

Dean of Graduate College

Iowa State University
Of Science and Technology
Ames, Iowa

1963

TABLE OF CONTENTS

INTRODUCTION

With the advent of high speed aircraft, missiles, satellites, spacecraft, and the concept of lunar flights, there has arisen a host of problems which only a few years ago were unheard of. New areas of scientific investigation have been created and a whole new language has arisen such as astronaut, aerospace, space capsule, zero-g environment, etc. In order to solve many of the problems arising in the field of space technology, man has been forced into the position of reviewing old concepts in more detail and in many cases discarding the old and establishing the new. A classic example of this is the discarding of the Navier-Stokes equations of fluid motion, when one is investigating the viscid flow over a hypersonic airfoil in a rarified gas environment, in favor of a statistical analysis based on the probability of the number of molecular collisions per unit time.

One of the major problems encountered in high-speed flight is that of aerodynamic heating and the limiting of the heat flux at the stagnation point. This is a major problem particularly for reentry glide vehicles traveling at hypersonic speeds. Many of the heat flux equations now available are empirical and based on wind tunnel data. If one attempts to derive an expression for the stagnation heat flux using the classical approach, the classical equations of fluid dynamics must be greatly simplified if one derives a useful workable expression, hence, at the very best, the derived equation is only as good as the approximations used in the simplification. In this investigation, the classical approach is utilized, however, to derive a useful working expression, it was

necessary to make a number of not too unrealistic assumptions. The important fact, relative to this investigation, is that whether one uses a classical approach or an empirical relationship the resulting equation for the stagnation heat flux is independent of the angle of attack of the vehicle.

For a reentry glide vehicle subjected to aerodynamic heating, the optimum trajectory may be defined as the one for which the stagnation point heat flux never exceeds some preassigned value. A maximum range is also desired. The optimization of the trajectory involves the dynamics of a six degree of freedom reentry glide vehicle traveling at hypersonic speeds in a central force field and subjected to the action of aerodynamic forces. The motion of a reentry glide vehicle may be controlled by changing the angle of attack of the control surfaces since the aerodynamic forces and pitching moments acting on the vehicle are functions of the angle of attack. The control variable which is the angle of attack, while dominant in the aerodynamic forces and moment equations, does not appear in the stagnation point heat flux equation. This creates a problem and the problem of the optimum trajectory as stated is one of determining an angle of attack, which is somehow dependent upon the stagnation point heat flux.

If the usual maximum-minimum techniques are applied to the problem of the optimum trajectory as stated, the technique fails due to the fact that the constraint function, which will be considered as the maximum stagnation point heat flux, is independent of the angle of attack α.

If the classical variational Bolza technique is applied to the problem of the optimum trajectory as stated, this technique also fails due to the reason stated above.

One method of attack often utilized in problems involving the optimization of a missile intercept range is the steepest descent method. This method is successful when applied to the problem of the optimum trajectory as stated. The method involves the selection of the "best" values of a number of parameters. These "best" values of parameters are determined by sets of experiments, each set planned from information obtained from the preceding experiments. All significant factors are included and all constraints are satisfied in the initial experiment. Then, small variations in each parameter are used to measure the differential effects of each parameter upon the function to be maximized or minimized. The experiments are repeated until there is no longer a significant change in the function for each new set of experiments. This method lacks the sophistication of the classic variational method, and involves many experiments or computations(3).

The purpose of this investigation is to derive, by classical variational methods, the system of equations which will yield the optimum trajectory, as stated. All of the fundamental equations governing the aerodynamic heating and the flight mechanics of an unpowered reentry glide vehicle will be derived and these equations will then be subjected to recombination and analysis in terms of a classical variational control problem. Various conditions and an inequality constraint will be imposed upon the fundamental set of equations with the intention that the Lagrange multipliers, which are involved in this method of attack, serve as generating functions which generate an angle of attack such that the optimum trajectory, as stated, results.

LIST OF SYMBOLS

A	constant
A	area (where designated)
a_i	constants
a_i	acceleration (where designated)
a	sonic velocity
B	constant
$\bar{B}$	constant
c_p	specific heat at constant pressure
D_t	drag
D	diameter (where designated)
e_{ij}	strain rate component
E	energy
F	force
F_{ki}	view factor
g_c	a constant which relates force, mass, length and time
G	heat absorption capacity
h	altitude (where designated)
h	enthalpy (where designated)
I	inertia
i	free index
J	a constant which relates length, force, and thermal energy
j	summing index
k	specific heat ratio
k_c	thermal conductivity

L_i	lift
L_S	length of airfoil
m	mass of vehicle
M_{om}	moment
M	Mach number
M	mass (where designated)
Nu	Nusselt number
o	refers to stagnation point
P	pressure
Pr	Prandtl number
Q_R	radiant heat flux
Q_c	conducted heat flux
q_w	aerodynamic heat flux
R	general coordinate (where designated)
R_e	Reynolds number
R	gas constant (where designated)
R_o	earth radius
T	temperature
T_{ij}	stress component
t	time
U	free stream velocity
U_R	potential function
$\bar{u}$	internal energy
u	velocity component
u_{ij}	displacement rate
v	velocity component

V	velocity
W	weight
W	work (where designated)
x	general coordinate
y	general coordinate
z	general coordinate
α	angle of attack
$\alpha(Pr)$	a function of Prandtl number
ϕ	flight angle
ω	angular velocity
Γ_1	constant
ρ	density
σ	constant
σ	slope (where designated)
ϵ	emissivity
δ	boundary layer thickness
λ_i	Lagrange multipliers
μ	viscosity
$\bar{\mu}$	constant
θ	angular coordinate
$\bar{\gamma}$	kinematic viscosity
γ	angular coordinate
η	dimensionless velocity profile
η	normal (where designated)
τ_w	shear stress

τ	volume (where designated)
∞	refers to free stream

CENTRAL FORCE FIELD

A central force field is defined as a gravitational field which is produced by a perfectly homogeneous and perfectly spherical body. The central force field theory is of particular importance because it is usually adequate in performance analysis and in a great number of cases, for determining the basic flight path of an object within the field. The fundamental law of celestial mechanics is Newton's law of gravitation. Gravitation has been described by Newton as a force which is directly proportional to the mass of the attracting body and inversely proportional to the square of the distance from the center of the body. When considering a single point source of attraction in space one speaks of a central force field. The path of motion of a body acted upon by gravitation is called its orbit. In a central force field all orbits are geometrically defined as conics, i.e., ellipses, parabolas, or hyperbolas. Special cases of these orbits are radial motion i.e., free fall or vertical ascent, and the circular orbit. In general, in a central force field the orbit of a body is a conic path with the center of attraction at one focus of the conic.

Consider the following Figure 1.

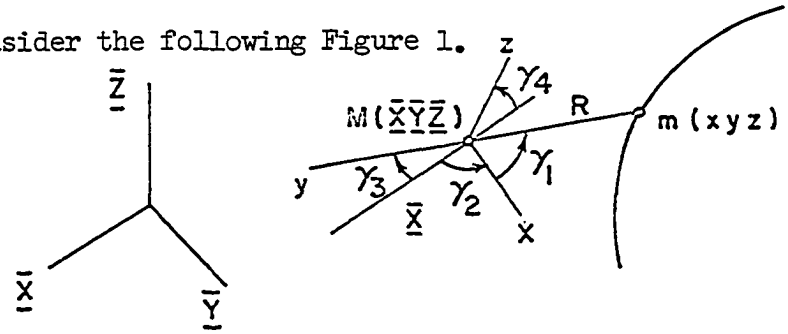

Figure 1. Coordinates of a central body and satellite body

M is the central body, m is the satellite body, and the inertial reference frame is defined by the $\bar{x}$, $\bar{Y}$, $\bar{z}$ coordinate system.

The central force acting on the mass m is

$$F = - \frac{k^2 M m}{R^2}. \qquad (1)$$

Consider now that the mass M is the earth and the mass m is an orbiting vehicle and that the inertial frame of reference is a set of fixed axes fixed within a non-rotating earth. These assumptions are made because the nature of the problem is such that the time from the start of reentry to impact will be small, i.e., the effects of a rotating, revolving earth will be assumed to be negligible.

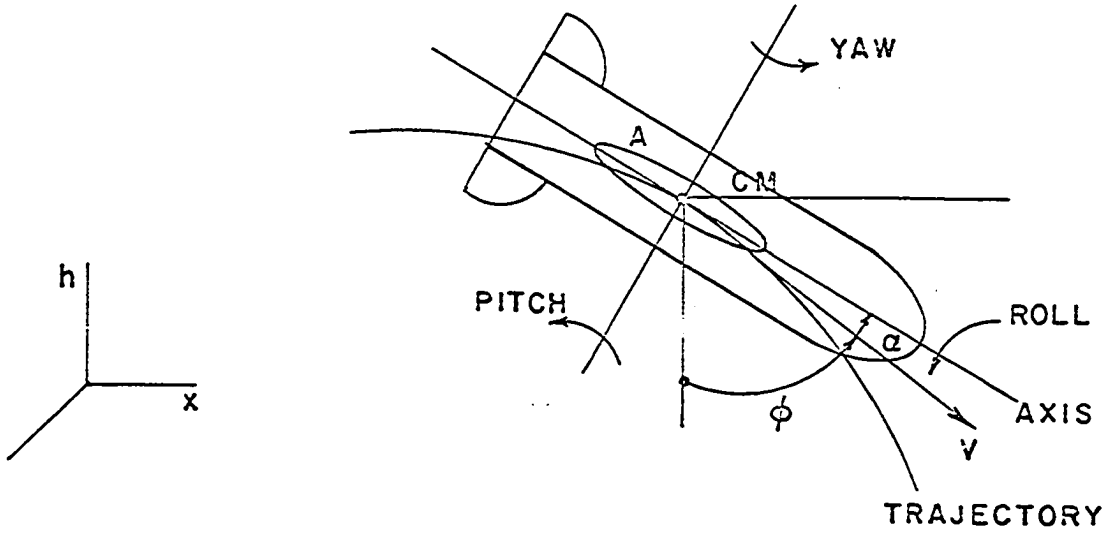

Figure 2. Vehicle flight configuration

where:

α = angle of attack

ϕ = flight angle

A = airfoil.

Initially, the orbiting vehicle will be traveling in an ellipitical orbit possessing both kinetic and potential energy by virtue of its velocity and position. Since the vehicle will be unpowered during reentry and since it is desired that the vehicle attain a maximum range subject to aerodynamic heating, it is obvious that the reentry trajectory should be a plane curve if a maximum range, based on an initial reentry total energy, is to be attained. All yaw pitch and roll motion should be kept at a minimum to reduce the energy requirement associated with these motions. The angle of attack should be small in order to reduce excessive drag.

The preceding statements justify the reducing of the vehicle to a system of three degrees of freedom. The yaw, roll, and the transverse trajectory motion will be assumed to be negligible due to energy considerations. The vertical and the horizontal trajectory coordinates will remain as well as the pitch motion. The pitch motion can be related to the flight angle and the angle of attack as indicated in Figure 2. Note that the flight angle is related to the slope of the trajectory and that the slope is a function of the vertical velocity divided by the horizontal velocity. If one assumes a small angle of attack as compared to the flight angle, it might be possible to reduce the vehicle to two degrees of freedom. At this point, however, the vehicle is considered to be a three degree of freedom system.

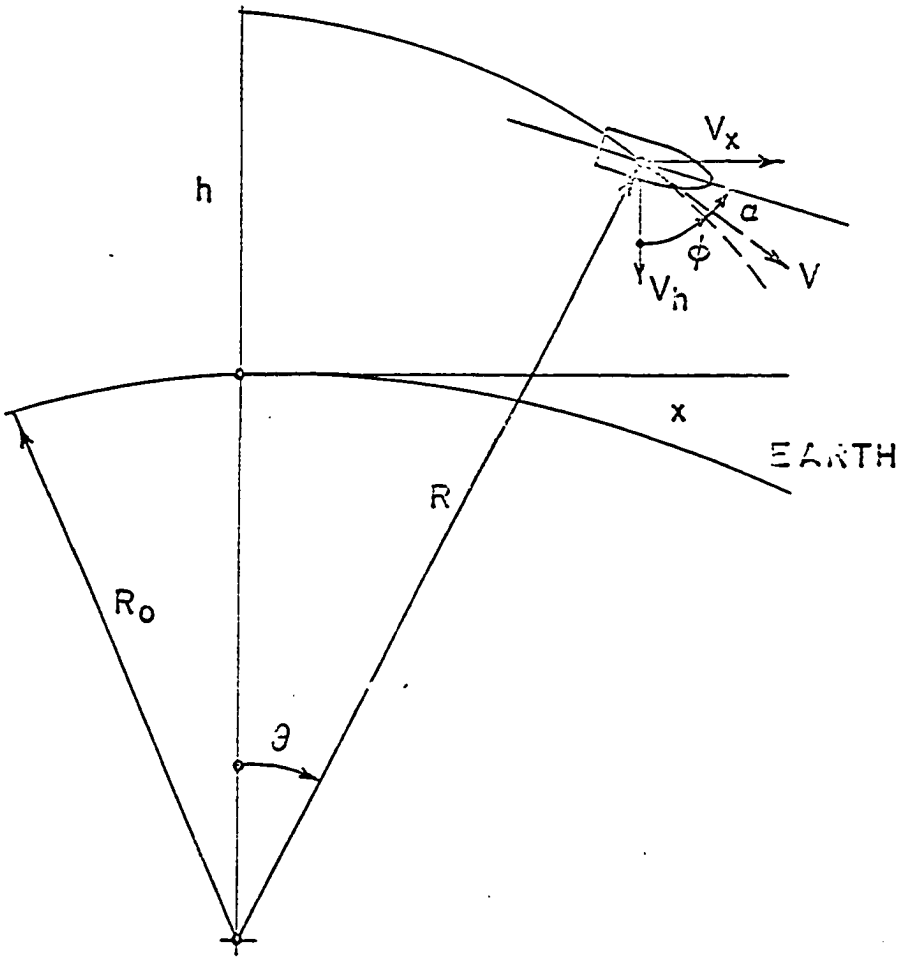

Figure 3. Central force field coordinates

$$\frac{dx}{dh} = \text{Tan } \phi \tag{2}$$

$$\frac{\frac{dx}{dt}}{\frac{dh}{dt}} = \frac{V_x}{V_h} = \text{Tan } \phi = \frac{-\dot{x}}{\dot{h}} \tag{3}$$

ϕ is the flight angle. The origin of the coordinates h and x is ground point directly below the point of reentry. The origin of the coordinates R and θ is at the center of the earth as indicated

in Figure 3. Useful relationships which are indicated in Figure 3 are

$$X = (R_o + h) \text{ Tan } \theta \tag{4}$$

$$X = R \sin \theta \tag{5}$$

from which:

$$R_o \text{ Tan } \theta + h \text{ Tan } \theta = R \sin \theta \tag{6}$$

$$h = \frac{R \sin \theta - R_o \text{ Tan } \theta}{\text{Tan } \theta} \tag{7}$$

$$h = R \cos \theta - R_o \tag{8}$$

also repeating Formula 1

$$F_R = - \frac{k^2 M m}{R^2}. \tag{9}$$

The force function of a vehicle located in a central force field is

$$F_{R_o} = - mg_c \text{ @ } R = R_o \tag{10}$$

$$- mg_c = - \frac{k^2 M m}{R^2_o} \tag{11}$$

or

$$g_c R^2_o = + k^2 M \tag{12}$$

hence

$$F_R = - mg_c \frac{R^2_o}{R^2} . \tag{13}$$

The potential function relative to the surface from which this force is derived is

$$U_R = - \int_{R_o}^{R} F_R \, dR \tag{14}$$

$$U_R = \int_{R_o}^{R} + mg_c R^2_o \frac{dR}{R^2} \tag{15}$$

$$U_R = + mg_c R_o \left(\frac{R - R_o}{R} \right). \tag{16}$$

The kinetic energy of a vehicle located in a central force field is

$$T = \frac{m}{2} (\dot{x}^2 + \dot{h}^2) + \frac{I}{2} (\dot{\phi} + \dot{\alpha})^2. \tag{17}$$

The Lagrangian function is

$$L = T - U_R \tag{18}$$

$$L = \frac{m}{2} (\dot{x}^2 + \dot{h}^2) + \frac{I}{2} (\dot{\phi} + \dot{\alpha})^2 - mg_c R_o \left(1 - \frac{R_o}{R}\right) \tag{19}$$

where,

$$R^2 = (R_o + h)^2 + x^2. \tag{20}$$

Since there are aerodynamic drag forces existing, the work which these drag forces do may be expressed as follows

$$\delta W = Q_i \, \delta X_i \, . \tag{21}$$

Hamilton's principle, stated in a most general form, is

$$\delta \int_{t_1}^{t_2} (L + W) \, dt = 0 \tag{22}$$

in which W is the work done by nonconservative (extraneous) forces, such as the aerodynamic drag forces mentioned above. Performing the indicated operation on the preceding equation leads to the Lagrange equation for the coordinate X_i

$$\frac{d}{dt} \left(\frac{\partial L}{\partial \dot{x}_i}\right) - \frac{\partial L}{\partial x_i} = Q_i \tag{23}$$

and

$$\frac{\partial L}{\partial \dot{x}_i} \, \delta x_i \Big|_{t_1}^{t_2} = 0 \tag{24}$$

where Q_i are non-conservative forces.

DERIVATION OF THE FUNDAMENTAL EQUATIONS REQUIRED FOR THE AERODYNAMIC HEATING ANALYSIS

All equations in this chapter will be derived by utilizing the compactness of the tensor notation.

The general equation of motion for a fluid particle is

$$T_{ij,j} + \bar{X}_i = \rho a_i \tag{25}$$

where T_{ij} is the component of the stress tensor $\bar{T}_i$.

The stress strain relationship may be expressed as (31)

$$T_{ij} = 2\,\mu\, e_{ij} + b\,\delta_{ij}\, e_{ii} - P\,\delta_{ij} \tag{26}$$

$$T_{ii} = (2\,\mu + 3\,b)\, e_{ii} - 3\,P. \tag{27}$$

For a static condition,

$$T_{ii} = -\,3P, \text{hence} \tag{28}$$

$$b = -\frac{2}{3}\,\mu, \text{ thus} \tag{29}$$

$$T_{ij,j} = (2\,\mu\, e_{ij})_{,j} + (b\,\delta_{ij}\, e_{ii})_{,j} - P_{,j}\,\delta_{ij}. \tag{30}$$

The strain-displacement rate relationship may be expressed as

$$e_{ij} = \tfrac{1}{2}\,(u_{i,j} + u_{j,i}) \tag{31}$$

$$e_{ij,j} = \tfrac{1}{2}\,(u_{i,jj} + u_{j,ji}) = \tfrac{1}{2}\,(\nabla^2 u_i + \theta_{,i}) \tag{32}$$

$$e_{ii,j} = u_{i,ij} = \theta_{,j} \tag{33}$$

hence, the general equation of motion becomes

$$(u_{i,j} + u_{j,i})\,\mu_{,j} - \frac{2}{3}\,\delta_{ij}\,u_{i,i}\,\mu_{,j} + \mu\,(\nabla^2 u_i + \theta_{,i}) - \frac{2}{3}\,\mu\,\delta_{ij}\,\theta_{,j} -$$

$$P_{,j}\,\delta_{ij} + \bar{X}_i = \rho a_i \tag{34}$$

$$(u_{i,j} + u_{j,i})\,\mu_{,j} - \frac{2}{3}\,u_{i,i}\,\mu_{,j} + \mu\nabla^2 u_i + \frac{\mu}{3}\,\theta_{,i} - P_{,i} + \bar{X}_i = \rho a_i. \qquad (35)$$

The last equation is known as the Navier-Stokes equation.

The equation of the conservation of mass, or continuity, may be derived as follows:

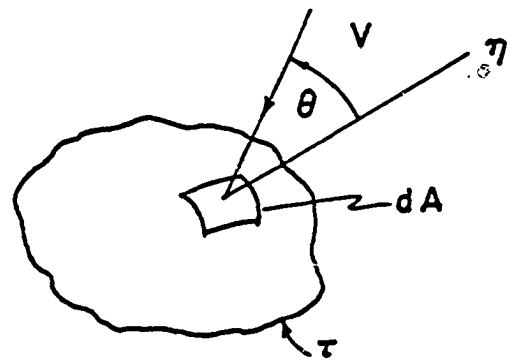

Figure 4. Reference volume

The net mass flow rate into the volume τ is

$$\int_A \rho v \cos\theta\, dA = \int_A \rho v \cdot \eta\, dA = \int_A (\rho v)_i\, \eta_i\, dA = \int_\tau (\rho v)_{i,i}\, d\tau. \qquad (36)$$

There may be sources or sinks within the differential volume. Let ψ be the source or sink function, i.e., the mass generated or dissipated per unit time per unit volume. The total mass generated or dissipated per unit time within the volume τ is

$$\int_\tau \psi\, d\tau. \qquad (37)$$

At any time t, the mass within the volume τ is

$$\int_\tau \rho\, d\tau, \qquad (38)$$

the time rate of change of the mass within the volume τ is

$$\int_\tau \frac{\partial \rho}{\partial t}\, d\tau. \qquad (39)$$

The sum of Equation 36, 37, and 39 should be equal to zero or

$$\int_\tau [(\rho v)_{i,i} + \psi + \frac{\partial \rho}{\partial t}]\, d\tau = 0. \qquad (40)$$

Since $d\tau$ is an arbitrary differential volume and the integral over the

volume τ is equal to zero, the value of the integrand must be equal to zero, hence, the continuity equation becomes

$$(\rho v)_{i,i} + \psi + \frac{\partial \rho}{\partial t} = 0. \tag{41}$$

The equation of the conservation of energy may be derived as follows:

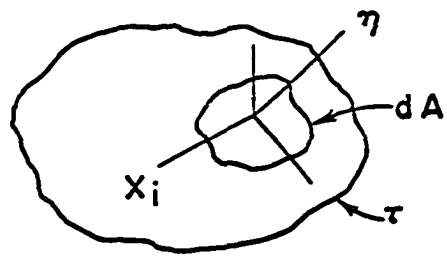

Figure 5. Reference volume

The net heat energy per unit time conducted into the volume τ is

$$\int_A - k \frac{\partial T}{\partial \eta} \, dA = \int_A - k \frac{\partial T}{\partial x_i} \frac{\partial x_i}{\partial \eta} \, dA = \int_A - (k \, T_{,i}) \, \eta_i \, dA =$$

$$\int_\tau - (k \, t_{,i})_{,i} \, d\tau. \tag{42}$$

The net radiant heat energy exchange per unit time (q_{NR}) is found by utilizing the net radiation method.

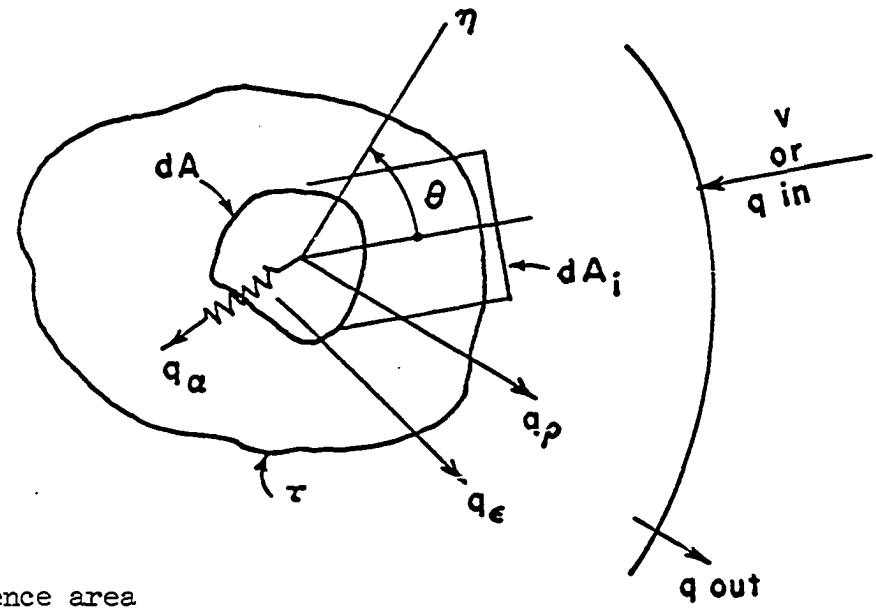

Figure 6. Reference area

The net radiant flux per unit time impinging on dA_i is

$$q_{in} - q_{out} = q_{NR} \tag{43}$$

$$q_{in} - (q_\rho + q_\epsilon) = q_{NR} \tag{44}$$

$$q_{in} - (1 - \alpha_{dA_i})\, q_{in} - \epsilon_{dA_i}\, \sigma\, T^4_{dA_i} = q_{NR} \tag{45}$$

$$\alpha_{dA_i}\, q_{in} - \epsilon_{dA_i}\, \sigma\, T^4_{dA_i} = q_{NR}. \tag{46}$$

The radiant flux "in" q_{in} may be expressed in terms of the radiant flux "out" $(q_{out})_k$ of the other surfaces A_k or

$$q_{in} = \sum_{k=1}^{S} (q_{out})_k\, F_{ki}. \tag{47}$$

F_{ki} is the geometric or view factor, i.e., the fraction of the space intercepted by the ith surface which the kth surface sees. Equation 46 becomes

$$q_{NRi} = \alpha_i \sum_{k=1}^{S} (q_{out})_k\, F_{ki} - \epsilon_i\, \sigma\, T_i^4. \tag{48}$$

The ith surface (dA_i) is also included in the summation if any part of the ith surface (dA_i) can "see" itself.

The net energy transport per unit time into the volume τ by virtue of mass transport is

$$\int_A \rho\, \bar{u}\, v \cos\theta\, d\, A = \int_A \rho\, \bar{u}\, v \cdot \eta\, dA = \int_A (\rho\, \bar{u}\, v)_i\, \eta_i\, dA = \int_\tau (\rho\, \bar{u}\, v)_i\, {}_{,i}\, d\tau. \tag{49}$$

The net energy transport per unit time into the volume τ by virtue of mass kinetic energy is

$$\int_A \left(\frac{\rho v^2}{2g_c J}\right) v \cos\theta \, dA = \int_A \left(\frac{\rho v^2}{2g_c J}\right) v \cdot \eta \, dA = \int_A \left(\frac{\rho v^2}{2g_c J}\right) v_i \, \eta_i \, dA =$$

$$\int_\tau \left(\frac{\rho v^2}{2g_c J} v_i\right)_{,i} d\tau. \tag{50}$$

The net energy transport per unit time into the volume τ by virtue of mass potential energy is

$$\int_A \left(\frac{gz_k}{g_c J}\right) \rho v \cos\epsilon \, dA = \int_A \left(\frac{gz_k}{g_c J} \rho\right) v \cdot \eta \, dA = \int_A \left(\frac{gz_k}{g_c J} \rho\right) v_i \, \eta_i \, dA =$$

$$\int_\tau \left(\frac{gz_k \rho}{g_c J} v_i\right)_{,i} d\tau. \tag{51}$$

Let E be the sum of the kinetic, potential and internal energy of a fluid particle of mass dm <u>within</u> the volume τ at any time t, then, the energy within the volume τ at time t is

$$\int_\tau \left(\frac{v_I^2}{2Jg_c} + \bar{u} + \frac{z_{kI} g}{Jg_c}\right) \rho \, d\tau = \int_\tau E \rho \, d\tau. \tag{52}$$

The increment in energy within the volume τ, per unit time, is

$$\int_\tau \frac{\partial}{\partial t} (E\rho) \, d\tau. \tag{53}$$

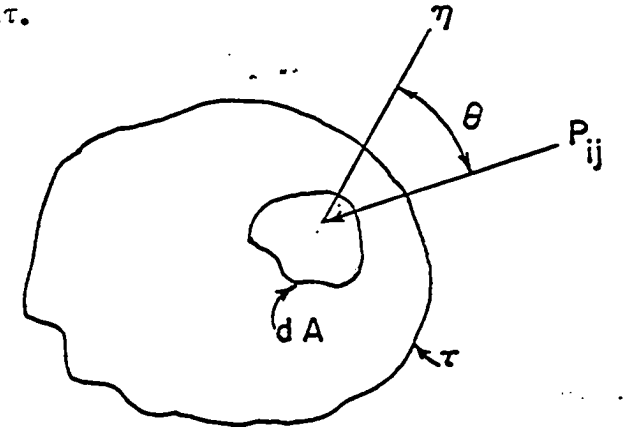

Figure 7. Reference for the pressure tensor P_{ij}

The net work done by the pressure tensor P_{ij} on the surface of the volume τ, per unit time is

$$\int_A P_{ij}\, v_j\, dA_i = \int_A [p\, \delta_{ij}\, v_j + \tau_{ij}\, v_j]\, \eta_i\, dA = \int_\tau [(p\, v_i)_{,i} + (\tau_{ij}\, v_j)_{,i}]\, d\tau. \tag{54}$$

Other forms of work such as net shaft work performed on the fluid within the voluem τ, per unit time, per unit volume, will be designated as

$$Ws/J. \tag{55}$$

The conservation of energy requires that the sum of all energy terms, Equations 42 through 55 inclusive, be equal to zero, hence

$$\int_\tau -(k\, T_{,i})_{,i}\, d\tau + \int_A [\alpha_i \sum_{k=1}^{s} q_{ok}\, F_{ki} - \epsilon_i\, \sigma\, T_i^4]\, \eta_i\, dA + \int_\tau [(\rho\, \bar{u}\, v)_i]_{,i}\, d\tau + \int_\tau \left(\frac{\rho v^2}{2Jg_c}\, v_i\right)_{,i} d\tau + \int_\tau \left(\rho\, g\, \frac{z_k}{Jg_c}\, v_i\right)_{,i} d\tau + \int_\tau [(pv_i)_{,i} + (\tau_{ij}\, v_j)_{,i}]\, \frac{d\tau}{J} + \int_\tau \frac{W_s}{J}\, d\tau + \int_\tau \frac{\partial}{\partial t}(E\rho)\, d\tau = 0. \tag{56}$$

Regroup the volume integrals in the following manner.

$$\int_\tau \left[-k\, T_{,i} + (\rho\, \bar{u}\, v)_i + \frac{\rho v^2}{2Jg_c}\, v_i + \frac{\rho\, g\, z_k\, v_i}{Jg_c} + \rho\, v_i + \tau_{ij}\, v_j\right]_{,i} \frac{d\tau}{J} + \int_\tau \frac{\partial}{\partial t}(E\rho)\, d\tau + \int_\tau [\alpha_i \sum_{k=1}^{s} q_{ok}\, F_{ki} - \epsilon_i\, \sigma\, T_i^4]_{,i}\, d\tau + \int_\tau \frac{W_s\, d\tau}{J} = 0. \tag{57}$$

Expand the following terms in Equation 57

$$(\rho\, \bar{u}\, v)_{i,i} + (p\, v_i)_{,i} + \frac{\partial}{\partial t}(\bar{u}\, \rho). \tag{58}$$

Equation 58 becomes

$$(\rho\, \bar{u})\, v_{i,i} + (\rho\, \bar{u})_{,i}\, v_i + \frac{\partial}{\partial t}(\bar{u}\, \rho) + p_{,i}\, v_i + p\, v_{i,i} = \frac{D}{Dt}(\rho\, \bar{u}), +$$

$$(p + \rho\, \bar{u})\, v_{i,i} + \frac{Dp}{Dt} - \frac{\partial p}{\partial t} = \frac{D}{Dt}(\rho\, h) + (h\, \rho)\, v_{i,i} - \frac{\partial p}{\partial t} = \rho\, \frac{D}{Dt}(h) +$$

$$h \frac{D}{Dt} (\rho) + (h \rho) v_{i,i} - \frac{\partial p}{\partial t} \tag{59}$$

but from Equation 41 and assuming $\psi = 0$

$$h \frac{D}{Dt} (\rho) = - (h \rho) v_{i,i} \tag{60}$$

hence, Equation 58 becomes, with the J factor added

$$\rho \frac{D}{Dt} (h) - \frac{\partial P}{J \partial t} . \tag{61}$$

Redefine the following terms in Equation 57 as follows

$$(-k T_{,i})_{,i} = q_{ic,i} \tag{62}$$

$$\int_{\tau} [\alpha_i \sum_{k=1}^{s} q_{ok} F_{ki} - \epsilon_i \sigma T_i^4]_{,i} \, d\tau = \int_{\tau} Q_{NRi,i} \, d\tau. \tag{63}$$

Expand the following terms in Equation 57

$$(\frac{\rho v^2}{2Jg_c} v_i)_{,i} + (\frac{\rho g z_k v_i}{Jg_c})_{,i} = (\frac{\rho v^2}{2Jg_c}) v_{i,i} + (\frac{\rho v^2}{2Jg_c})_{,i} v_i + (\frac{\rho g z_k}{Jg_c}) v_{i,i} +$$

$$(\frac{\rho g z_k}{Jg_c})_{,i} v_i = \frac{D}{Dt} (\frac{\rho v^2}{2Jg_c}) - \frac{\partial}{\partial t} (\frac{\rho v^2}{2Jg_c}) + [\frac{\rho v^2}{2Jg_c} + \frac{\rho g z_k}{Jg_c}] v_{i,i} + \frac{D}{Dt}$$

$$(\frac{\rho g z_k}{Jg_c}) - \frac{\partial}{\partial t} (\frac{\rho g z_k}{Jg_c}) = \rho \frac{D}{Dt} (\frac{v^2}{2Jg_c}) + \rho \frac{D}{Dt} (\frac{g z_k}{Jg_c}) - \frac{\partial}{\partial t} (\frac{\rho v^2}{2Jg_c}) - \frac{\partial}{\partial t} (\frac{\rho g z_k}{Jg_c}). \tag{64}$$

Substituting Equations 61 and 64 into Equation 57 yields

$$\int_{\tau} [q_{ic,i} + \rho \frac{D}{Dt} (h + \frac{v_i^2}{2Jg_c} + \frac{g z_k}{Jg_c}) + Q_{NRi,i} + (\frac{T_{ij} v_j}{J})_{,i} + \frac{W_s}{J} - \frac{\partial P}{J \partial t} +$$

$$\frac{\partial}{\partial t} (\frac{\rho v^2}{2Jg_c} + \frac{\rho g z_k}{Jg_c}) - \frac{\partial}{\partial t} (\frac{\rho v^2}{2Jg_c} + \frac{\rho g z_k}{Jg_c})] \, d\tau = 0. \tag{65}$$

Since $d\tau$ is an arbitrary volume and the integral is zero when evaluated over the volume, we have the general energy equation, as

$$\frac{\partial q_{ic}}{\partial x_i} + \rho \frac{D}{Dt} (h + \frac{v^2}{2Jg_c} + \frac{g z_k}{Jg_c}) + Q_{NRi,i} + \frac{\partial}{\partial x_i} (\frac{T_{ij} v_j}{J}) + \frac{W_s}{J} - \frac{\partial P}{J \partial t} = 0. \tag{66}$$

Equation 66 is the most general form of the conservation of energy. The terms in order represent,

a. The net heat energy conducted into the volume τ.

b. The net convective energy transported into the volume τ by virtue of mass transport.

c. The net radiant heat energy incident on the surface of the body τ.

d. The net work done by, in our particular problem, shear forces within and on the surface of the volume τ.

e. The net work done by external forces such as shaft or pump work.

f. The last term is a correction factor for the time variation in the hydrostatic component of the pressure tensor P_{ij}.

Equation 56 may be rewritten in terms of surface area integrals and integrated. When this is done, another useful computational form of the conservation of energy results,(32) i.e.,

$$Q_{net} + \sum \delta\, m_i \left(h_i + \frac{v_i^2}{2Jg_c} + \frac{z_i g}{Jg_c}\right) = \sum \delta\, m_e \left(h_e + \frac{v_e^2}{2Jg_c} + \frac{z_e g}{Jg_c}\right) +$$

$$\Delta \left[m \left(\bar{u} + \frac{v^2}{2Jg_c} + \frac{zg}{2\bar{g}_c}\right)\right]_\sigma + W_{net\ (shaft\ and\ frictional)}. \qquad (67)$$

DERIVATION OF THE MOMENT, LIFT AND DRAG FORCES ON A HYPOTHETICAL AIRFOIL IN A POTENTIAL FLOW FIELD

The moment, lift and drag forces acting on a thin supersonic airfoil will now be derived (26). It will be assumed that the angle of attack is small, and that due to the sharpness of the leading and trailing edges of the airfoil, the penalty in drag, due to detached shock, will be minimized.

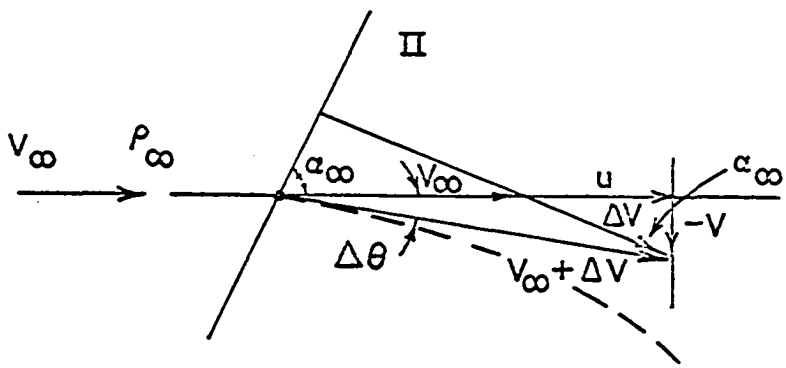

Figure 8. Streamline-Mach wave interaction

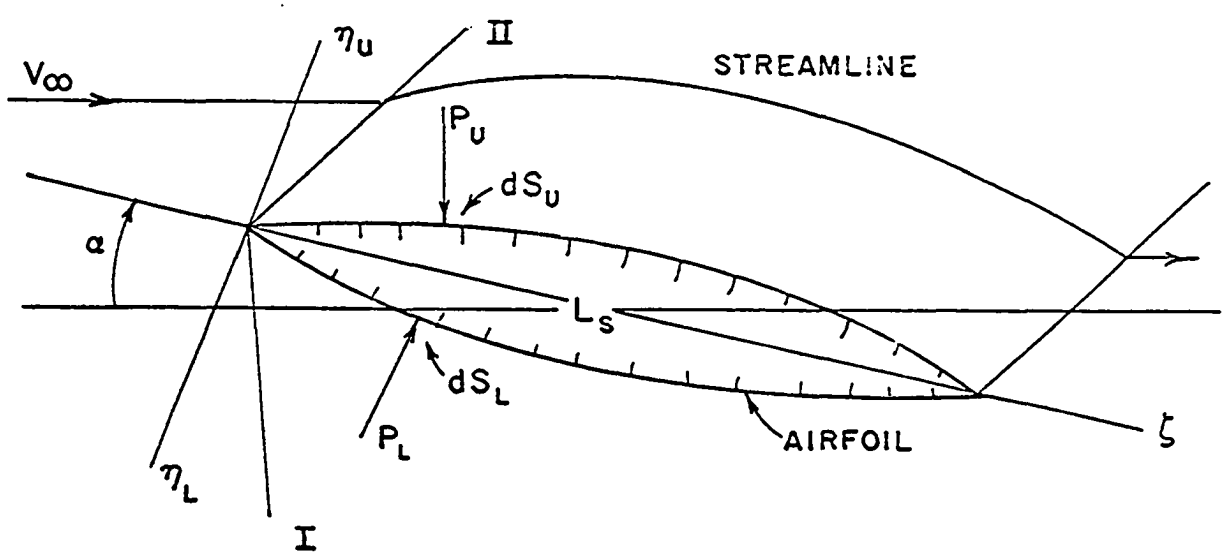

Figure 9. Hypersonic airfoil

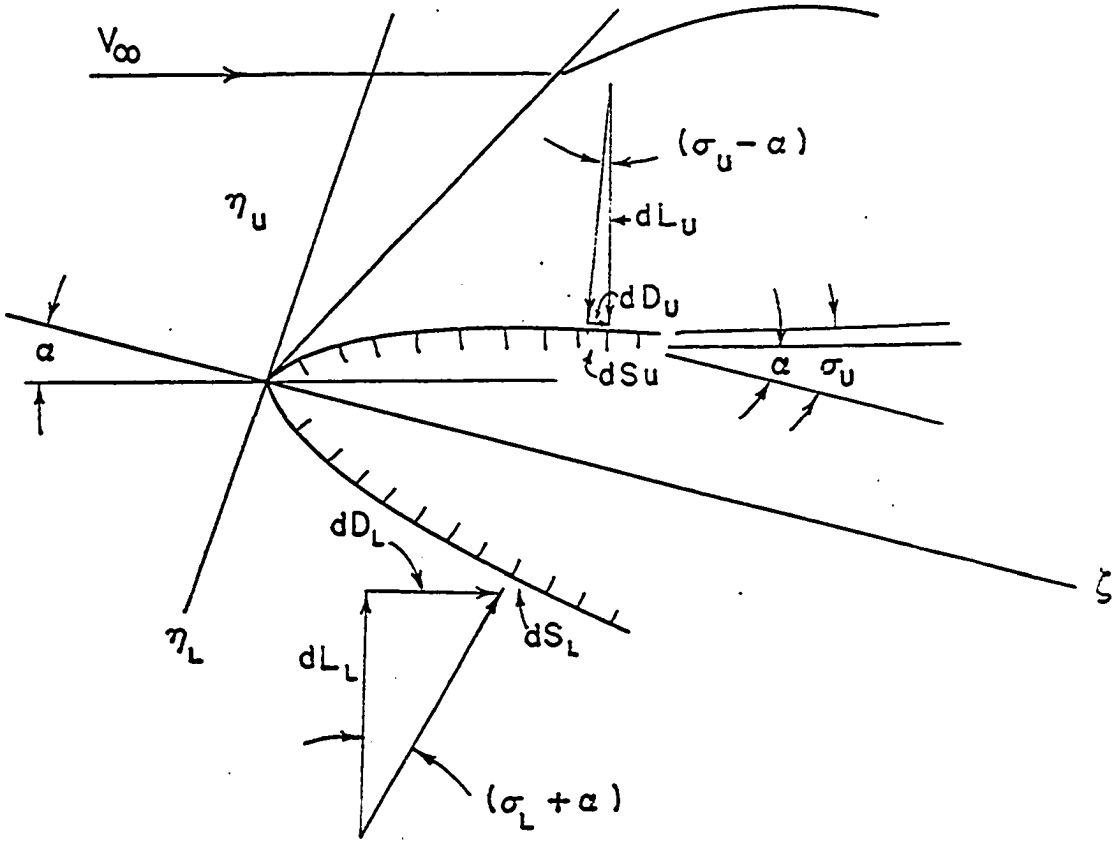

Figure 10. Section of hypersonic airfoil showing aerodynamic forces

The change in pressure when a streamline crosses a mach wave may be computed as, refer to Figure 8,

$$P - P_\infty = - \rho_\infty V_\infty u \tag{68}$$

but from Figure 8

$$\frac{u}{-V} = \text{Tan } \alpha_\infty \tag{69}$$

hence,

$$P - P_\infty = \rho_\infty V_\infty V \text{ Tan } \alpha_\infty. \tag{70}$$

If $\Delta\theta$ is the change in direction of the streamline and if $\Delta\theta$ is small, then

$$V = V_\infty \Delta\theta. \tag{71}$$

and Equation 70 becomes

$$P - P_\infty = \rho_\infty V_\infty^2 \text{ Tan } \alpha_\infty \Delta\theta \tag{72}$$

but

$$\text{Tan } \alpha_\infty = \frac{1}{\sqrt{M_\infty^2 - 1}} \tag{73}$$

hence, the required relation between the change in pressure and the change in direction of a streamline is

$$P - P_\infty = \frac{k P_\infty M_\infty^2}{\sqrt{M_\infty^2 - 1}} \Delta\theta. \tag{74}$$

Figure 9 represents a cross section of a thin airfoil. α is the angle of attack and η and ζ are airfoil axes. The pressures P_u and P_L act on the upper and lower surfaces respectively. The airfoil length is L_S and assume a span dimension of unity. The mach wave at the leading edge of the airfoil is designated by the line I and II.

Figure 10 is a more detailed view of a section of the airfoil and indicates the differential forces, lift dL and drag dD which act upon the differential surface dS. The subscripts refer to upper and lower surface. The inclination of the surface tangetn is indicated by σ. Note that the following relations for the local directions of the streamlines near the airfoil surface, relative to the undisturbed flow, are valid from the geometry of flow

$$\Delta\theta_u = \sigma_u - \alpha \tag{75}$$

$$\Delta\theta_L = -(\sigma_L + \alpha) \tag{76}$$

hence from Equations 74, 75, and 76 the local net surface pressures are

$$P_L - P_\infty = \frac{k P_\infty M_\infty^2}{\sqrt{M_\infty^2 - 1}} \quad (\sigma_L + \alpha), \tag{77}$$

$$P_u - P_\infty = \frac{k P_\infty M_\infty^2}{\sqrt{M_\infty^2 - 1}} (\sigma_u - \alpha). \tag{78}$$

Subtracting the second from the first, the pressure difference at any chordwise location is

$$P_L - P_u = \frac{k P_\infty M_\infty^2}{\sqrt{M_\infty^2 - 1}} (\sigma_L - \sigma_u + 2\alpha). \tag{79}$$

To obtain the aerodynamic counter clockwise moment per unit airfoil span about the leading edge, the expression for the differential moment is integrated over the length of the airfoil.

$$dM_{om} = (P_L - P_u)\, \zeta\, d\zeta \tag{80}$$

$$dM_{om} = \frac{k P_\infty M_\infty^2}{\sqrt{M_\infty^2 - 1}} (\sigma_L - \sigma_u + 2\alpha)\, \zeta\, d\zeta \tag{81}$$

now

$$\int_0^{L_S} \zeta\, d\zeta = L_S^2/2 \tag{82}$$

$$\int_0^{L_S} \zeta\, (\sigma_L - \sigma_u)\, d\zeta = S_u - S_L. \tag{83}$$

S_L is the area between the lower surface and the chord and S_u is the area above the upper surface and the chord. Assuming symmetry with respect to the chord

$$S_u = S_L \tag{84}$$

hence, Equation 81 integrated over the length of the airfoil yields

$$M_{om} = \frac{k P_\infty M_\infty^2}{\sqrt{M_\infty^2 - 1}} \alpha L_S^2 . \tag{85}$$

Let

$$k\, g_c\, R\, T_\infty = a^2 \tag{86}$$

also

$$P_\infty = \rho_\infty\, R\, T_\infty \tag{87}$$

hence, the moment per unit span is

$$M_{om} = \frac{a^2\, \rho_\infty\, M_\infty^2\, L_S^2\, \alpha}{g_c\, \sqrt{M_\infty^2 - 1}} \quad . \tag{88}$$

The differential lift on lower and upper surfaces are

$$dL_L = P_L\, dS_L \cos(\sigma_L + \alpha) = P_L\, d\zeta \tag{89}$$

$$dL_u = -\, P_u\, dS_u \cos(\sigma_u - \alpha) \cong -\, P_u\, d\zeta \tag{90}$$

hence the total lift per unit span is

$$L_i = \int_o^{L_S} (P_L - P_u)\, d\zeta = \frac{k\, P_\infty\, M_\infty^2}{\sqrt{M_\infty^2 - 1}}\; 2\, \alpha\, L_S \tag{91}$$

since

$$\int_o^{L_S} \sigma_L\, d\zeta \cong \int_o^{L} \frac{d\eta_L}{d\zeta}\; d\zeta = \int_o^{L} d\eta_L = 0 \tag{92}$$

and

$$\int_o^{L_S} \sigma_u\, d\zeta = 0. \tag{93}$$

The drag may now be computed. Referring to Figure 10 the differential drag on lower and upper surfaces is

$$dD_L = P_L\, dS_L\, \mathrm{Sin}\,(\sigma_L + \alpha) \cong P_L\, (\sigma_L + \alpha)\, d\zeta \tag{94}$$

$$dD_u = P_u\, dS_u\, \mathrm{Sin}\,(\sigma_u - \alpha) \cong P_u\, (\sigma_u - \alpha)\, d\zeta \tag{95}$$

hence the total drag per unit span is

$$D = \int_0^{L_S} \frac{k\, P_\infty\, M_\infty^2}{\sqrt{M_\infty^2 - 1}} \left[(\sigma_L + \alpha)^2 + (\sigma_u - \alpha)^2 + P_\infty\,(\sigma_L + \alpha) + P_\infty(\sigma_u - \alpha)\right] d\zeta \quad (96)$$

$$D = \frac{k_\infty P_\infty M_\infty^2\, L_S}{\sqrt{M_\infty^2 - 1}}\,(2\alpha^2 + \sigma_L^2 + \sigma_u^2) \quad (97)$$

since

$$\int_0^{L_S} \sigma_L\, d\zeta = \int_0^{L_S} \sigma_u\, d\zeta = 0 \quad (98)$$

and

$$\frac{1}{L_S}\int_0^{L_S} \sigma_L^2\, d\zeta = \bar{\sigma}_L^2 \quad (99)$$

$$\frac{1}{L_S}\int_0^{L_S} \sigma_u^2\, d\zeta = \bar{\sigma}_u^2\,. \quad (100)$$

Equation 97 may be considered the sum of two parts. The first part is independent of the profile shape and is dependent only on the angle of attack, hence the drag associated with this part is known as the induced drag, i.e.,

$$D_{ind} = \frac{2\,\alpha^2\, k\, P_\infty\, M_\infty^2\, L_S}{\sqrt{M_\infty^2 - 1}}\,. \quad (101)$$

The second part of the equation depends only on the profile shape and is known as the wave drag due to thickness, i.e.,

$$D_{th} = \frac{k\, P_\infty\, M_\infty^2\, L_S}{\sqrt{M_\infty^2 - 1}}\,(\bar{\sigma}_L^2 + \bar{\sigma}_u^2). \quad (102)$$

Thus far only the drag forces due to normal pressure stresses acting on the surface have been calculated. Another form of drag force exists due to the boundary layer shearing stresses. If there is no interaction

between the potential flow region and the boundary layer at the interface of the two, then the shearing stress drag may be calculated and added directly to the preceding Equation 97, thus yielding the total drag.

The derivation of the shearing stress drag will be the subject of investigation in the next chapter.

DERIVATION OF THE FRICTIONAL DRAG ON A HYPOTHETICAL AIRFOIL BASED ON A VISCID FLOW

The equation for the frictional drag will now be developed, however, before deriving the equation for frictional drag a discussion of the boundary layer behavior at supersonic and hypersonic conditions is in order (21).

The difference between laminar and turbulent flows is one of relative steadiness between the two types of flow. In a laminar flow the velocities and properties at each point in the flow field are constant with respect to time and the fluid flows in "lamina or sheets", also in a laminar flow the interaction between adjacent fluid layers consist of a so-called molecular shear stress. The shear stress is a function of a fluid property called viscosity and a kinematic relationship. In a turbulent flow, the local acceleration $\partial u_i/\partial t$ may be much larger than the convective acceleration $u_i \frac{\partial u_i}{\partial x_i}$, also in turbulent flow an additional interaction is involved which is due to the transfer of momentum from layer to layer owing to the velocity fluctuations. This momentum transport phenomenon represents an apparent shearing stress and is called the turbulent friction. The magnitude of the turbulent friction or apparent shearing stress is $-\overline{(\rho u_i)' u_j'}$, where the u_i' and u_j' are the fluctuations of the velocity in the i and j directions and the bar denotes the temporal mean value of the product. The negative sign is chosen so as to correspond to the definition of positive friction such that the apparent shear stress τ is considered positive if the fluid layer at the distance x_i from the wall is accelerated by the outside flow. This additional

apparent shear stress results in skin friction drags for a turbulent boundary layer that is several orders of magnitude higher than that value associated with the non-turbulent laminar layer.

The first assumption made for the derivation of the friction drag is that in the equations of fluid motion μ is independent of x_i, hence for a two dimensional flow field Equation 35 reduces to

x momentum.

$$\mu \left(\frac{\partial^2 u}{\partial x^2} + \frac{\partial^2 u}{\partial y^2}\right) + \frac{\mu}{3} \frac{\partial}{\partial x} \left(\frac{\partial u}{\partial x} + \frac{\partial v}{\partial y}\right) - \frac{\partial P}{\partial x} + \bar{X} = \rho \left(\frac{\partial u}{\partial t} + \frac{\partial u}{\partial x} u + \frac{\partial u}{\partial y} v\right) \quad (103)$$

y momentum.

$$\mu \left(\frac{\partial^2 v}{\partial x^2} + \frac{\partial^2 v}{\partial y^2}\right) + \frac{\mu}{3} \frac{\partial}{\partial y} \left(\frac{\partial u}{\partial x} + \frac{\partial v}{\partial y}\right) - \frac{\partial P}{\partial} + \bar{Y} = \rho \left(\frac{\partial v}{\partial t} + \frac{\partial v}{\partial x} u + \frac{\partial v}{\partial y} v\right). \quad (104)$$

The continuity Equation 41 reduces to

$$\frac{\partial}{\partial x} (\rho u) + \frac{\partial}{\partial y} (\rho v) + \psi (xy) + \frac{\partial \rho}{\partial t} = 0. \quad (105)$$

The following assumptions will be made,

a. The boundary layer is a high speed (hypersonic) laminar layer.

b. There is no interaction between the laminar layer and the external flow field, that is, considering Figure 11.

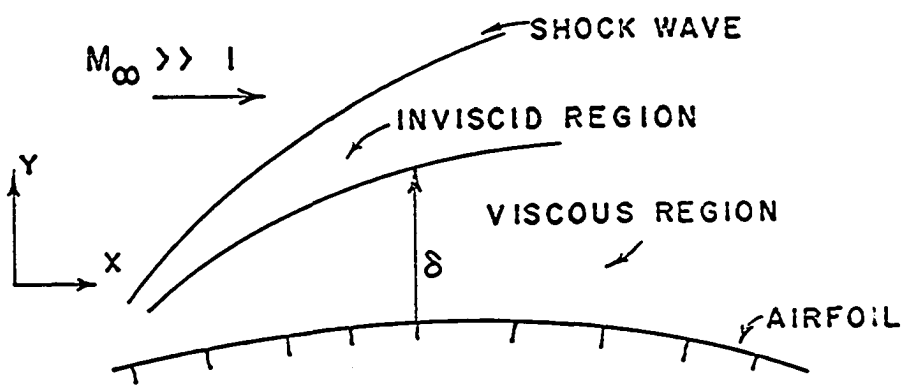

Figure 11. Hypersonic flow over an airfoil

A hypersonic laminar flow over a flat plate generates in the leading edge region a detached shock wave. In this region the shock constitutes the outer boundary of the viscous flow region. Between the shock and the leading edge, viscosity and heat conduction are dominant throughout and all terms in the momentum and energy equations are of the same order of magnitude. This region constitutes the stagnation point region and will be the subject of later investigation. The present analysis will be restricted to that portion of the flow downstream of the leading edge which can be treated as two distinct flow regimes as indicated in Figure 11.

At hypersonic speeds the laminar boundary layer is thicker than it is at supersonic speeds owing to the larger temperature gradient across the boundary layer. The growth of this thick boundary layer induces an outward deflection of the streamline which is sufficient to cause a change in the effective geometric shape of the body. This distortion of the body contours cause pressure variations to be propagated into the main (inviscid) stream along mach lines and this external pressure field in turn feeds back into the boundary layer and thus effects its rate of growth. This interaction between the boundary layer and the inviscid region can occur even at hypersonic speeds even though the flow is assumed uniform. Thus at hypersonic speeds, this viscous-compressible interaction can have important effects on the surface pressure distribution, skin friction, surface best transfer rates and also affect the laminar to turbulent transition. It is assumed that the change in the effective geometric shape due to laminar boundary layer growth is negligible, thus the assumption of no interaction.

c. It is assumed in the regions farther downstream (of the airfoil) that interactions between the mach waves generated by the growth of the laminar boundary layer and the shock wave from the leading edge are negligible. Thus the inviscid region can be treated as an isentropic flow across a single family of characteristics.

d. The assumption of a high speed hypersonic laminar boundary layer eliminates the apparent shearing stress or turbulent friction.

e. The flow is assumed to be steady, compressible and two dimensional flow relative to the airfoil surface.

f. The body forces are assumed to be zero.

g. The velocity (u) parallel to the airfoil surface is assumed to be a function of y only.

h. The partials of v are assumed to be negligible.

i. There are no mass sources or sinks.

If one assumes

$$u = \eta\ (y) \tag{106}$$

then Equation 103 becomes

$$\mu \frac{\partial^2 \eta}{\partial y^2} - \frac{\partial P}{\partial x} = \rho\ v \frac{\partial \eta}{\partial y}\ . \tag{107}$$

Equation 114 becomes

$$\frac{\partial P}{\partial y} = 0 \tag{108}$$

and Equation 105 becomes

$$\frac{\partial}{\partial x}\ (\rho \eta) = -\ \frac{\partial}{\partial y}\ (\rho v). \tag{109}$$

Integration of Equation 109 yields

$$- \int_0^y \frac{\partial(\rho\eta)}{\partial x} \, dy = + \rho v \tag{110}$$

so that Equation 107 becomes

$$\mu \frac{\partial^2 \eta}{\partial y^2} = \frac{\partial P}{\partial x} - \frac{\partial \eta}{\partial y} \int_0^y \frac{\partial(\rho\eta)}{\partial x} \, dy. \tag{111}$$

Outside of the boundary layer the velocity U is at most a function of x only, hence

$$\frac{dP}{dx} = - \rho \, U \frac{dU}{dx} \tag{112}$$

but $U \approx V_\infty$, hence

$$\frac{dP}{dx} = 0 \tag{113}$$

so that Equation 111 becomes

$$\mu \frac{\partial}{\partial y} \left(\frac{\partial \eta}{\partial y}\right) = - \frac{\partial \eta}{\partial y} \int_0^y \frac{\partial}{\partial x} (\rho\eta) \, dy. \tag{114}$$

Now

$$\mu \frac{\partial \eta}{\partial y} = \tau \tag{115}$$

so that Equation 114 becomes

$$\tau_w = \int_0^\delta \left[\frac{\partial \eta}{\partial y} \left(\int_0^\delta \frac{\partial}{\partial x} (\eta\rho) \, dy\right)\right] dy. \tag{116}$$

Equation 116 is integrated as follows

$$\tau_w = \left[\int_0^\delta \frac{\partial}{\partial x} (\eta\rho) \, dy \right] \eta \Big|_0^\delta - \int_0^\delta \eta \frac{\partial}{\partial x} (\eta\rho) \, dy \tag{117}$$

$$\tau_w = V_\infty \int_0^\delta \frac{\partial}{\partial x} (\eta\rho) \, dy - \int_0^\delta \eta \frac{\partial}{\partial x} (\eta\rho) \, dy \tag{118}$$

$$\tau_w = \int_0^\delta \frac{\partial}{\partial x} (V_\infty \eta\rho - \eta^2\rho) \, dy \tag{119}$$

$$\tau_w = \int_0^\delta \frac{\partial}{\partial x} [\rho\eta \, (V_\infty - \eta)] \, dy. \tag{120}$$

The preceding derivations have reduced the equations of momentum and continuity to the momentum integral of Von Karman's. The analysis for the frictional drag on the airfoil at this point is approximate only to the degree that the assumptions are themselves approximate.

It has been assumed that a hypersonic laminar boundary layer exists, however, if the flow should become turbulent, then a laminar sublayer will develop and the turbulent form of the equations of momentum and continuity will still reduce to Equation 120 in the laminar sublayer region under the assumptions stated up to this point. If one continues to assume that a hypersonic laminar boundary layer exists, the next assumption which seems to agree closely with experimental data is that the velocity in the boundary layer may be expressed as

$$\eta = \frac{V_\infty y}{\delta} \tag{121}$$

or, if one at this point assumes a turbulent boundary layer to exist the velocity in the turbulent boundary layer may be expressed as

$$\eta = V_\infty \left(\frac{y}{\delta}\right)^n \tag{122}$$

where n is some exponent often arrived at from experimental data taken within the buffer zone and turbulent core.

The substitution of Equation 121 into Equation 120 yields

$$\tau_w = \int_0^\delta \frac{\partial}{\partial x} \left[\rho V_\infty^2 \left(\frac{y}{\delta} - \frac{y^2}{\delta^2}\right)\right] dy. \tag{123}$$

ρ is not a constant in the preceding equation, therefore ρ must be determined as a function of y.

The perfect gas law and Equation 108 result in

$$\rho = \rho_\infty \frac{T_\infty}{T}. \tag{124}$$

The Prandtl number is assumed to be unity, hence, the total energy is constant throughout the boundary layer and the conservation of energy, following a streamline, requires that

$$\frac{u^2}{2Jg_c} + c_p T = \frac{V_\infty^2}{2Jg_c} + c_p T_\infty, \tag{125}$$

where u and T are the local velocity and temperature just inside the boundary layer and V_∞ and T_∞ are the free stream velocity and temperature, let

$$\frac{V_\infty^2}{2Jg_c} + c_p T_\infty = h_\infty^o \tag{126}$$

hence

$$T = \frac{h_\infty^o}{c_p} - \frac{u^2}{c_p 2Jg_c} . \tag{127}$$

Substituting Equations 106, 121, and 127 into Equation 124 yields

$$\rho = \frac{\rho_\infty T_\infty c_p / h_\infty^o}{1 - \frac{V_\infty^2}{2Jh_\infty^o g_c} (\frac{y}{\delta})^2}. \tag{128}$$

Substituting Equation 128 into Equation 123 yields

$$\tau_w = \frac{\partial}{\partial x} \int_0^\delta \frac{V_\infty^2 \rho_\infty T_\infty c_p}{h_\infty^o} \frac{(\frac{y}{\delta} - \frac{y^2}{\delta^2})}{(1 - \frac{V_\infty^2}{2h_\infty^o Jg_c} \frac{y^2}{\delta^2})} dy. \tag{129}$$

Define the following parameters

$$\frac{V_\infty^2 \rho_\infty T_\infty c_p}{h_\infty^o} = A \tag{130}$$

$$\frac{V_\infty^2}{2h_\infty^o Jg_c} = B \tag{131}$$

$$y/\delta = \eta \tag{132}$$

then

$$\tau_w = \frac{\partial}{\partial x}\int_0^1 A\delta \left(\frac{\eta - \eta^2}{1 - B\eta^2}\right) d\eta \tag{133}$$

$$\tau_w = \frac{\partial}{\partial x}\int_0^1 A\delta \frac{\eta\, d\eta}{1 - B\eta^2} - \frac{\partial}{\partial x}\int_0^1 \frac{A\delta\, \eta^2\, d\eta}{1 - B\eta^2}\,, \tag{134}$$

Integration of Equation 134 yields

$$\tau_w = \frac{\partial}{\partial x}\left[-\frac{A\delta}{2B} \ln (1-B\eta^2)\right]_0^1 - \frac{\partial}{\partial x}\left[A\delta \left(-\frac{\eta}{B} + \frac{1}{B}\left(\frac{1}{2\sqrt{B}} \ln \frac{1 + \eta\sqrt{B}}{1 - \eta\sqrt{B}}\right)\right)\right]_0^1 \tag{135}$$

or

$$\tau_w = \frac{\partial}{\partial x}\left[-\frac{A\delta}{2B} \ln (1 - B) + \frac{A\delta}{B} - \frac{A\delta}{2\, B\sqrt{B}} \ln \frac{1 + \sqrt{B}}{1 - \sqrt{B}}\right] \tag{136}$$

$$\tau_w = \left[\frac{A}{B} - \frac{A}{2B} \ln (1 - B) - \frac{A \ln}{2B\sqrt{B}} \frac{1 + \sqrt{B}}{1 - \sqrt{B}}\right] \frac{\partial \delta}{\partial x} \tag{137}$$

but, assuming a laminar boundary layer

$$\tau_w = \left(\mu \frac{\partial u}{\partial y}\right)_{y=o} = \frac{\mu V_\infty}{\delta}\,. \tag{138}$$

Let the bracket term in the Equation 137 be equal to $A\Gamma_1$, hence

$$\frac{\mu V_\infty}{\delta} = A\Gamma_1 \frac{\partial \delta}{\partial x} \tag{139}$$

integration of Equation 139 yields

$$\delta = \sqrt{\frac{2\mu V_\infty\, x}{A\Gamma_1}}\,. \tag{140}$$

In Equation 140 the viscosity μ is referenced to the airfoil surface while the other parameters are referenced to the free stream, hence it is advisable at this point to reference μ also to the free stream, now

$$\mu \simeq T \tag{141}$$

hence

$$\frac{\mu_w}{\mu_\infty} = \frac{T_w}{T_\infty} \tag{142}$$

or,

$$\mu_w = \frac{\mu_\infty T_w}{T_\infty} \tag{143}$$

also from Equation 127

$$T_w = \frac{h^o_\infty}{c_p} \tag{144}$$

hence

$$\delta = \sqrt{\frac{2\ V_\infty x}{\Gamma_1 A}\ \frac{\mu_\infty\ h^o_\infty}{T_\infty\ c_p}} \tag{145}$$

or

$$\delta = \sqrt{\frac{2\ \mu_\infty\ (h^o_\infty)^2\ x}{\Gamma_1\ T^2_\infty\ c^2_p\ \rho_\infty\ V_\infty}}\ . \tag{146}$$

Define

$$c_p\ T_{o_\infty} = h^o_\infty \tag{147}$$

then

$$(T_{o_\infty})^2 = (\frac{h^o_\infty}{c_p})^2 \tag{148}$$

hence

$$\delta = \sqrt{\frac{2\mu_\infty}{\Gamma_1 \rho_\infty V_\infty}\ (\frac{T_{o_\infty}}{T_\infty})^2\ x} \tag{149}$$

or

$$\frac{\delta}{x} = \sqrt{\frac{2}{\Gamma_1}\ (\frac{T_{o_\infty}}{T_\infty})^2\ \frac{1}{Re_x}}\ . \tag{150}$$

Equation 150 is of interest in that the function Γ_1 is a function of B but B is defined as.

$$\frac{V_\infty^2}{2Jh_\infty^o g_c} = B \tag{131}$$

from Equation 126 and 131, B may be expressed as

$$\frac{V_\infty^2}{2Jh_\infty^o g_c} = 1 - \frac{T_\infty}{T_{o_\infty}} = B. \tag{151}$$

If the ratio of the free stream temperature to the free stream stagnation temperature, relative to the airfoil, is expressed in terms of the mach number, B becomes,

since

$$\frac{T_\infty}{T_{o_\infty}} = \frac{1}{1 + (\frac{k-1}{2})\ M^2} \tag{152}$$

$$B = \frac{(\frac{k-1}{2})\ M^2}{1 + (\frac{k-1}{2})\ M^2} \cdot \tag{153}$$

The Reynolds number is

$$R_e = \frac{V_\infty\ \rho_\infty\ x}{\mu_\infty} \tag{154}$$

or

$$R_e = M \sqrt{k\ g_c\ R\ T_\infty}\ \frac{\rho_\infty}{\mu_\infty}\ x. \tag{155}$$

Substituting Equations 152 and 155 into Equation 150 yields the following equation for the <u>local</u> boundary layer thickness as a function of the mach number, distance along the airfoil surface, and free stream fluid properties.

$$\delta = [1 + \frac{(k - 1)}{2}\ M^2\ ] \sqrt{\frac{2\ \mu_\infty\ x}{\Gamma_1\ M\ \rho_\infty} \frac{1}{\sqrt{k\ g_c\ R\ T_\infty}}} \cdot \tag{156}$$

The preceding formula for δ includes the effects of compressibility, references all fluid properties within the boundary layer to the free stream fluid properties, accounts for the effect of altitude of the airfoil through the free stream fluid properties, accounts for the effect of velocity of the airfoil through the mach number and locates the position on the airfoil where δ is measured. Since the shear stress at the surface of the airfoil and the velocity within the boundary layer are functions of δ, it is obvious that the preceding effects are also accounted for in both. The shearing stress at the wall may be expressed as

$$\tau_w = \frac{\mu V_\infty}{\delta} \tag{138}$$

however, with Equations 143, 144, 147, and 156, Equation 138 may be rewritten as

$$\tau_w = \mu_\infty V_\infty \frac{T_w}{T_\infty} \frac{1}{\delta} \tag{157}$$

$$\tau_w = \frac{\mu_\infty V_\infty}{T_\infty} \frac{h^o_\infty}{c_p} \frac{1}{\delta} \tag{158}$$

$$\tau_w = \mu_\infty V_\infty \frac{T^o_\infty}{T_\infty} \frac{1}{\delta} \tag{159}$$

$$\tau_w = [k g_c R T_\infty]^{\frac{3}{4}} \sqrt{\frac{\Gamma_1 M^3 \rho_\infty \mu_\infty}{2x}} . \tag{160}$$

Equation 160 yields the shear stress on the airfoil surface at the distance x from the leading edge. It is obvious that the maximum shear stress exist near the leading edge. This is of course due to the velocity profile having its largest gradient near the leading edge.

Integrating Equation 160 over the length of the airfoil and multiplying by two to account for both surfaces yields the total friction

drag per unit airfoil span, i.e.,

$$D_f = \int_0^{L_S} [k\, g_c\, R\, T_\infty]^{\frac{3}{4}} \sqrt{\frac{\Gamma_1\, M^3\, \rho_\infty\, \mu_\infty}{2}}\; x^{-\frac{1}{2}}\, 2\, dx \tag{161}$$

$$D_f = [k\, g_c\, R\, T_\infty]^{\frac{3}{4}} \sqrt{8\, \Gamma_1\, M^3\, \rho_\infty\, \mu_\infty\, L_S}\ . \tag{162}$$

The total drag on the airfoil is now determined by the addition of Equation 162 and Equation 96

$$D_t = \frac{k\, P_\infty\, M_\infty^2\, L_S}{\sqrt{M_\infty^2 - 1}} \left[2\ \alpha^2 + \bar{\sigma}_L^{\,2} + \bar{\sigma}_u^{\,2}\right] + [k\, g_c\, R\, T_\infty]^{\frac{3}{4}} \sqrt{8\, \Gamma_1 M^3 \rho_\infty \mu_\infty L_S}\ . \tag{163}$$

Equation 163 will now be simplified by neglecting the square of the mean slope terms since the prior analyses have assumed the airfoil profile to approximate a flat plate, also since

$$k\, g_c\, R\, T_\infty = a^2 \tag{86}$$

and

$$P_\infty = \rho_\infty\, R\, T_\infty \tag{87}$$

Equation 163 becomes

$$D_T = \frac{2a^2\, \rho_\infty\, M_\infty^2\, L_S\ \alpha^2}{g_c\, \sqrt{M_\infty^2 - 1}} + a^{\frac{6}{4}} \sqrt{8\, \Gamma_1\, M^3\, \rho_\infty\, \mu_\infty\, L_S}. \tag{164}$$

DERIVATION OF THE SURFACE TEMPERATURE AND THE HEAT FLUX AT THE STAGNATION POINT

Missile, aircraft flight, or reentry flight at high speeds and any altitude introduces many technical problems. One of the most important problems which arises is the result of aerodynamic heating. Adiabatic wall temperatures under these high speed flight conditions can exceed the temperature limitations of most structural material commonly used for the skin of such vehicles.

With the high speed flights now possible, the problem of aerodynamic heating is not limited to flights at low altitudes but the problem also exists under the condition of high speed flight at high altitudes. The problem of aerodynamic heating must embody three major flow regimes; namely (25),

a. continuum or conventional gasdynamics,

b. slip flow, and

c. free-molecule flow.

The concept of the boundary layer proposed by Prandtl in 1903 has proved to be of the greatest practical utility, for it permits the field of flow to be treated in two parts:

a. the potential flow outside the boundary layer, where viscous stresses are negligible compared with inertia stresses, and

b. the thin boundary layer, where viscous stresses are of the same order of magnitude as inertia stresses.

The Navier-Stokes equations of motion for the flow over a body in a real fluid are extremely complicated and unsolvable. In the

realm of potential flow, however, these governing equations are subject to great simplification since the viscous and heat conduction terms may be assumed negligible compared with the remaining terms. On the other hand, in the region of the boundary layer, the velocity and temperature gradients are of necessity so large as not to be negligible.

In the realm of subsonic flow, the presence of a boundary layer on a body influences the potential flow by altering the effective boundaries of the potential flow by the amount of the boundary layer displacement thickness. The potential flow, in contrast, determines the longitudinal pressure distribution for the boundary layer and thus plays an important role in the behavior and formation of the boundary layer.

In the transonic and supersonic flow realm, shock waves may appear in the flow field so as to produce between the shock and the boundary layer an interaction which will have a pronounced effect on the potential flow. This interaction between the viscous and compressible forces also exerts profound influences on the boundary layer.

In order to understand the mechanism of aerodynamic heating, it is necessary to understand the role of viscous stresses acting simultaneously with heat transfer between fluid layers within the boundary layer. Viscous stresses within the boundary layer do shearing work on the fluid particles. This work alters the temperature of the fluid particles, i.e., the internal energy and temperature of the fluid in the inner layers increase. The variation in temperature leads to heat conduction and changes in density and viscosity. The velocity distribution in the boundary layer depends on the shear distribution as well as on the viscosity and density distribution, hence the skin friction is controlled in part by heat

transfer within the boundary layer. The effect of heating or cooling on the temperature distribution is shown schematically in Figure 12.

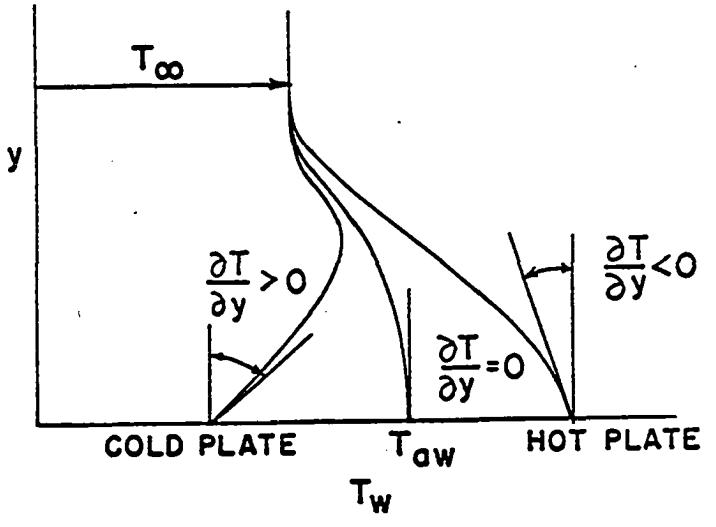

Figure 12. Effect of heating and cooling on temperature distribution

The preceding solution technique, in which the flow region has been assumed to be divided into two regions, i.e., the thin boundary layer and the potential flow region, usually suffices for solving most of the flow field problems around a body. There are, however, cases for which the preceding solution technique does not yield a satisfactory solution. At high flight speed and at high altitude the viscous region, i.e., boundary layer, may become thick enough to fill the entire flow field behind the shock wave. In such a case the concept of a thin boundary layer is no longer valid. Effects such as large pressure gradients along the surface, skin roughness, flow separation, oblique shocks, and the effect of vorticity generated by curved shocks are all present areas of controversy.

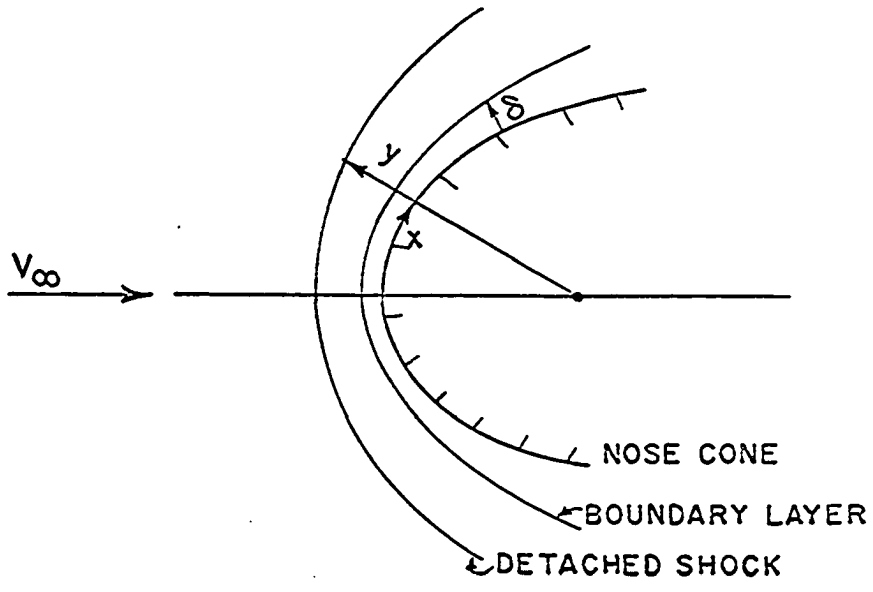

Figure 13. Leading edge of nose cone

Referring to Figure 13, in the case of a high speed flow a shock wave stands in front of the body and forms a region of subsonic flow around the stagnation point. In this region of subsonic flow the flow is nearly incompressible.(13, 31).

Very near the forward stagnation point in a two-dimensional flow past a body, the velocity U just outside the boundary layer is proportional to the distance x from the stagnation point so that

$$U = \bar{B}x. \tag{165}$$

where $\bar{B}$ is a constant corresponding to the velocity gradient at the stagnation point. Euler's equation of motion is valid just outside the boundary layer, hence,

$$U \frac{\partial U}{\partial x} = - \frac{1}{\rho} \frac{\partial P}{\partial x} \tag{166}$$

but from Equation 165

$$U \frac{\partial U}{\partial x} = \bar{B}^2 x \tag{167}$$

At this point an order of magnitude analysis applied to the boundary layer equations is necessary. Repeating the momentum equations, continuity and the general energy equation here for reference, we have

x momentum;

$$\mu \left(\frac{\partial^2 u}{\partial x^2} + \frac{\partial^2 v}{\partial y^2}\right) + \frac{\mu}{3} \frac{\partial}{\partial x} \left(\frac{\partial u}{\partial x} + \frac{\partial v}{\partial y}\right) - \frac{\partial P}{\partial x} + \bar{X} = \rho \left(\frac{\partial u}{\partial t} + u \frac{\partial u}{\partial x} + v \frac{\partial u}{\partial y}\right) \quad (103)$$

y momentum

$$\mu \left(\frac{\partial^2 v}{\partial x^2} + \frac{\partial^2 v}{\partial y^2}\right) + \frac{\mu}{3} \frac{\partial}{\partial y} \left(\frac{\partial u}{\partial x} + \frac{\partial v}{\partial y}\right) - \frac{\partial P}{\partial y} + \bar{Y} = \rho \left(\frac{\partial v}{\partial t} + u \frac{\partial v}{\partial x} + v \frac{\partial v}{\partial y}\right) \quad (104)$$

continuity

$$\frac{\partial}{\partial x} (\rho u) + \frac{\partial}{\partial y} (\rho v) + \psi (x, y) + \frac{\partial \rho}{\partial t} = 0. \quad (105)$$

The general energy Equation 66 becomes

$$\frac{\partial q_{xc}}{\partial x} + \frac{\partial q_{yc}}{\partial y} + \rho \frac{D}{Dt} \left(h + \frac{v^2}{2Jg_c} + \frac{gz_h}{Jg_c}\right) + Q_{NRx} + Q_{NRy} + \frac{\partial}{\partial x} \left(\frac{\tau_{xy} v_y}{J}\right) +$$

$$\frac{\partial}{\partial y} \left(\frac{\tau_{yx} v_x}{J}\right) + \frac{W_s}{J} - \frac{1}{J} \frac{\partial P}{\partial t} = 0. \quad (168)$$

If δ is the thickness of the boundary layer, u changes from zero to its maximum value U in the main stream in a length δ and if U is taken as a magnitude of standard order and δ as small then

item	order
$\frac{\partial u}{\partial y}$	$\frac{1}{\delta}$
$\frac{\partial^2 u}{\partial y^2}$	$\frac{1}{\delta^2}$
u	1
$\frac{\partial u}{\partial t}$	1

item	order
$\frac{\partial u}{\partial x}$	1
$\frac{\partial^2 u}{\partial x^2}$	1

(169)

If all sources or sinks ψ are assumed zero and the flow is assumed incompressible then the continuity equation reduces to:

$$\frac{\partial u}{\partial x} + \frac{\partial v}{\partial y} = 0. \tag{170}$$

but since the order of $\frac{\partial u}{\partial x}$ is 1 then $\frac{\partial v}{\partial y}$ is of order 1 but since v is zero when y is zero, then v will be of order δ, hence

item	order
$\frac{\partial v}{\partial t}$	δ
$\frac{\partial v}{\partial x}$	δ
$\frac{\partial^2 v}{\partial x^2}$	δ
$\frac{\partial^2 v}{\partial y^2}$	$\frac{1}{\delta}$

(171)

An order of magnitude analysis is applied to the energy equation as follows. The velocity u changes from zero to its maximum value in the main stream while the temperature T changes from T_w to T_δ, hence if T and u are taken as quantities of standard order and v is of order δ then.

item	order
$\frac{\partial^2 T}{\partial x^2}$	1
$\frac{\partial^2 T}{\partial y^2}$	$\frac{1}{\delta^2}$

item	order
$u \frac{\partial T}{\partial x}$	1
$v \frac{\partial T}{\partial y}$	1
$u \frac{\partial P}{\partial x}$	1
$v \frac{\partial P}{\partial y}$	δ

(172)

The energy equation is further simplified by assuming: q_{xc} is zero, steady state conditions exist, Q_{NRx} and Q_{NRy} are zero, W_s is zero, the potential energy term is zero, and the derivatives of the shear work may be neglected in comparison with the other remaining terms. Hence, the general energy Equation 168, for regions within the boundary layer near the stagnation point, becomes

$$u \frac{\partial T}{\partial x} + v \frac{\partial T}{\partial y} = \frac{k_c}{c_p \rho} \frac{\partial^2 T}{\partial y^2} \quad . \tag{173}$$

The continuity Equation 170 remains as

$$\frac{\partial u}{\partial x} + \frac{\partial v}{\partial y} = 0. \tag{170}$$

The x momentum Equation 103 becomes

$$u \frac{\partial u}{\partial x} + v \frac{\partial u}{\partial y} = \bar{B}^2 x + \frac{\mu}{\rho} \frac{\partial^2 u}{\partial y^2} \quad . \tag{174}$$

The y momentum Equation 104 becomes

$$\frac{\partial P}{\partial y} = 0 \tag{175}$$

since $\mu \frac{\partial^2 v}{\partial y^2}$ is of order δ. Define a stream function such that

$$\psi = (\bar{\gamma}\, \bar{B})^{\frac{1}{2}} x F(\eta) \tag{176}$$

where

$$\eta = \left(\frac{\bar{B}}{\bar{\gamma}} \right)^{\frac{1}{2}} y \quad . \tag{177}$$

Then the velocity components may be expressed as

$$u = \bar{B} \, x \, F' \tag{178}$$

$$v = - (\bar{\gamma} \, \bar{B})^{\frac{1}{2}} F. \tag{179}$$

where the primes indicate differentiation with respect to y.

The continuity Equation 170 is thus seen to be satisfied. Performing the required differentiation and substitution into Equation 174 yields

$$F'^2 - F \, F'' = 1 + F''' \, . \tag{180}$$

The numerical integration of Equation 180 has been carried out and the results given in Reference 31.

Now assume the boundary layer temperature profile to be of the form.

$$T = T_w - (T_w - T_\infty) \, \theta \, (\eta). \tag{181}$$

Substituting Equations 178, 179, and 181 into the general energy Equation 173 yields for $\theta \, (\eta)$

$$\theta'' + Pr \, F \, \theta' = 0. \tag{182}$$

where Pr is the Prandtl number. The boundary conditions on θ are

$$\begin{aligned} \theta \, (o) &= 0 \\ \theta \, (\infty) &= 1 \end{aligned} \tag{183}$$

the solution of Equation 182 may be written as.

$$\theta \, (\eta) = \alpha \, (Pr) \int_o^\eta \left[e^{-Pr \int_o^\eta F \, d\eta} \right] d\eta \tag{184}$$

and from Equation 183

$$\frac{1}{\alpha \, (Pr)} = \int_o^\infty e^{-Pr \int_o^\eta F \, d\eta} \, d\eta. \tag{185}$$

The parameter α (Pr) has been found to be closely approximated by(31)

$$\alpha \text{ (Pr)} = .570 \text{ Pr}_{\infty}^{0.4} . \tag{186}$$

It should be noted at this point that the solutions obtained are approximate for an axisymmetric flow over a spherical nose cone but for a flat nose cone the solutions are actually those of the equations of motion, continuity and energy. An interpretation of the Equation 185 is also in order. The first derivative of Equation 181 with respect to y, yields

$$\frac{dT}{dy} = - (T_w - T_\infty) \frac{d\theta}{d\eta} \frac{d\eta}{dy} \tag{187}$$

but from Equation 184,

$$\frac{d\theta}{d\eta} = \alpha \text{ (Pr) } e^{-\text{Pr} \int_o^\eta d\eta} \tag{188}$$

so that

$$\frac{dT}{dy} = - (T_w - T_\infty) \frac{d\eta}{dy} \alpha \text{ (Pr) } e^{-\text{Pr} \int_o^\eta F \, d\eta} \tag{189}$$

but the heat conducted from the boundary layer to the wall is

$$q_w = - k_c \frac{dT}{dy} \Big|_{\eta = 0} \tag{190}$$

so that from Equation 189

$$q_w = k_c \frac{d\eta}{dy} \alpha \text{ P(r) } (T_w - T_\infty). \tag{191}$$

The heat conducted to the wall may also be expressed in terms of a film coefficient as

$$q_w = h \text{ } (T_w - T_\infty) \tag{192}$$

so that

$$h = k_c \frac{d\eta}{dy} \alpha \text{ P(r)}. \tag{193}$$

Multiplying Equation 193 through by x and dividing by k_c yields the Nusselt number based on free stream properties, also from Equations 177 and 186,

$$\frac{d\eta}{dy} = \sqrt{\frac{\bar{B}}{\bar{\gamma}}} \tag{194}$$

so that,

$$Nu_\infty = \left(\frac{hx}{k_c}\right)_\infty = .570\ Pr_\infty^{0.4} \sqrt{\frac{\bar{B}x^2}{\bar{\gamma}}} \ . \tag{195}$$

Equation 186 thus establishes the first constant of integration of θ, and this constant is required in the definition of the free-stream Nusselt number at the stagnation point as indicated in Equation 195.

In the preceding analysis for the free stream Nusselt number, the reference temperature was the free stream temperature T_∞. In an earlier discussion, it was stated that the heat flux at the surface does not depend on the difference between the wall temperature T_w and the free stream temperature T_∞, but on the difference between the wall temperature T_w and the adiabatic wall temperature T_{aw}, see Figure 12. Thus the appropriate definition of a flim coefficient of heat transfer is one based on the adiabatic wall temperature as a reference, i.e.,

$$h = \frac{q_w}{T_w - T_{aw}} \ . \tag{196}$$

In order to derive the stagnation heat flux it is now necessary to derive the heat flux along the surface of a flat plate such that the heat flux is independent of the distance measured along the surface of the plate (29). If one assumes a zero pressure gradient along the surface of the plate, incompressible flow and a constant viscosity μ, Equation

103 becomes

$$u \frac{\partial u}{\partial x} + v \frac{\partial u}{\partial y} = \frac{\mu}{\rho} \frac{\partial^2 u}{\partial y^2} \quad . \tag{197}$$

Expanding the general energy Equation 66, using $h = c_p T$, and assuming that the velocity and temperature gradients in the x-direction are much less than in the y direction and that the corresponding viscous shear stresses and heat conduction terms in the x-direction are negligible results in

$$\rho u \left[c_\rho \frac{\partial T}{\partial x} + \frac{\partial}{\partial x} \left(\frac{u^2 + v^2}{2Jg_c} \right) \right] + \rho v \left[c_P \frac{\partial T}{\partial y} + \frac{\partial}{\partial y} \left(\frac{u^2 + v^2}{2Jg_c} \right) \right] =$$

$$\frac{\partial}{\partial y} \left(k \frac{\partial T}{\partial y} \right) + \frac{\partial}{\partial y} \left(\frac{\mu u}{J} \frac{\partial u}{\partial y} \right) \tag{198}$$

now.

$$v/u \ll 1 \tag{199}$$

and the stagnation temperature may be written as

$$T_o = T + \left(\frac{u^2 + v^2}{2c_p Jg_c} \right) \approx T + \frac{u^2}{2c_p Jg_c} . \tag{200}$$

Assuming that the specific heat, c_p, and viscosity, μ, are constant, then from Equation 200

$$\frac{1}{2c_p Jg_c} \frac{\partial}{\partial y} (u^2) = \frac{\partial T_o}{\partial y} - \frac{\partial T}{\partial y} \tag{201}$$

and

$$\frac{1}{2c_p Jg_c} \frac{\partial}{\partial x} (u^2) = \frac{\partial T_o}{\partial x} - \frac{\partial T}{\partial x} . \tag{202}$$

The Prandtl number is

$$Pr = \frac{c_p \mu}{k_c} \tag{203}$$

and substituting Equations 201 and 202 into Equation 198 yields

$$u \frac{\partial T_o}{\partial x} + v \frac{\partial T_o}{\partial y} = \frac{\mu}{\rho} \frac{\partial^2 T_o}{\partial y^2} + \frac{\mu}{\rho} \frac{\partial}{\partial y} \left[\left(\frac{1}{Pr} - 1 \right) \frac{\partial T}{\partial y} \right]. \tag{204}$$

An important simplification will now be made by assuming that the Pr is approximately one. Fortunately, this assumption is valid since for air the Pr number is close to one. With this assumption Equation 204 yields

$$u \frac{\partial T_o}{\partial x} + v \frac{\partial T_o}{\partial y} = \frac{\mu}{\rho} \frac{\partial^2 T_o}{\partial y^2} . \tag{205}$$

Equation 197 and 205 are seen to be similar, i.e., the temperature profile and velocity profile are similar for all values of x, hence, at every point with the same velocity u and v, the temperature will be the same, therefore, for a uniform flow along the surface of the plate, a point on the surface will remain at a constant temperature. Another important result arising from the similarity is that the viscous boundary layer and the thermal boundary layer have the same thickness. This last important result permits the assumption that the stagnation temperature T_o is of the form

$$T_o = A\, u + B. \tag{206}$$

The assumption for T_o does not include a length dimension and both Equation 197 and 205 are satisfied. The boundary conditions on T_o are

$$T_o = T_{o_\infty}$$

$$u = V_\infty$$

$$T_o = T_w$$

$$u = 0. \tag{207}$$

hence, Equation 206 becomes

$$\frac{u}{V_\infty} = \frac{T_o - T_w}{T_{o_\infty} - T_w} . \tag{208}$$

From thermodynamics

$$c_p = \frac{k\,R}{(k-1)J} \tag{209}$$

the free-stream speed of sound is

$$a^2 = k\,g_c\,R\,T_\infty \tag{210}$$

or

$$\frac{1}{c_p} = \frac{(k-1)\,T_\infty\,g_c J}{a^2} \tag{211}$$

so that

$$\frac{1}{c_p} = M_\infty^2\,T_\infty\,\frac{(k-1)g_c J}{V_\infty^2} . \tag{212}$$

From Equation 200, the stagnation temperature T_o is

$$T_o = T + \frac{u^2}{2c_p J g_c} \tag{200}$$

or

$$T = T_o - \frac{u^2}{2c_p\,J g_c} \tag{213}$$

from Equation 208

$$\frac{u}{V_\infty}\,(T_{o_\infty} - T_w) + T_w = T_o \tag{214}$$

hence, from Equations 212 and 214, Equation 213 becomes

$$T = \frac{u}{V_\infty}\,(T_{o_\infty} - T_w) - \left(\frac{k-1}{2}\right)\,M_\infty^2\,T_\infty\,\left(\frac{u}{V_\infty}\right)^2 + T_w \tag{215}$$

or

$$T - T_w = \frac{u}{V_\infty}\,(T_{o_\infty} - T_w) - \left(\frac{k-1}{2}\right)\,M_\infty^2\,T_\infty\,\left(\frac{u}{V_\infty}\right)^2 . \tag{216}$$

The heat flux at the surface of the plate is

$$q_w = - k_c \left(\frac{\partial T}{\partial y}\right)_w \tag{217}$$

from Equations 215 and 217:

$$q_w = + \frac{k_c}{V_\infty} \left(T_w - T_{o_\infty}\right) \left(\frac{\partial u}{\partial y}\right)_w \tag{218}$$

assuming a laminar boundary layer

$$\tau_w = \mu \left(\partial u/\partial y\right)_w,$$

hence, Equation 218 becomes

$$q_w = c_p \frac{\tau_w}{V_\infty} \left(T_w - T_{o_\infty}\right) \tag{219}$$

referring to Equation 198

$$q_w = h \left(T_w - T_{aw}\right) \tag{198}$$

and noting that when the Pr number is equal to one, that $T_{aw} = T_{o_\infty}$, then.

$$q_w = h \left(T_w - T_{o_\infty}\right). \tag{220}$$

The local skin-friction coefficient may be defined as

$$c_{f_\infty} = \frac{\tau_w}{\frac{1}{2}\rho_\infty V_\infty^2}, \tag{221}$$

hence, from Equations 219, 220, and Equation 221

$$\frac{c_p \tau_w}{V_\infty} = h = \frac{c_{f_\infty} \rho_\infty V_\infty^2 c_p}{2 V_\infty}. \tag{222}$$

Now the Stanton number is defined as

$$C_{h_\infty} = \frac{h}{c_p \rho_\infty V_\infty} = \frac{C_{f_\infty}}{2} \tag{223}$$

but the Stanton number may also be written as

$$C_{h_\infty} = \frac{h}{c_p \rho_\infty V_\infty} = \left(\frac{hx}{k_c}\right) \left(\frac{k_c}{c_p \mu_{o_\infty}}\right) \left(\frac{\mu_{o_\infty}}{x \rho_\infty V_\infty}\right) = \frac{Nu_\infty}{Pr_\infty \, Rey_\infty} \, . \tag{224}$$

Thus the general expression for the heat flux based upon free-stream properties and independent of a length dimension is, from Equations 220, 222, 223, and 224 equal to

$$q_w = \frac{Nu_\infty}{Pr_\infty \, Rey_\infty} \rho_\infty V_\infty c_p (T_w - T_{o_\infty}). \tag{225}$$

For a Pr number of one,

$$q_w = \frac{Nu_\infty}{Rey_\infty} \rho_\infty V_\infty c_p (T_w - T_{o_\infty}). \tag{226}$$

Equation 195 yields the equation for the free stream Nusselt number in the vicinity of the stagnation region while Equation 226 yields the heat flux at the surface of a plate based on a defined free stream Nusselt number. If the Nusselt number defined in Equation 195 is substituted into Equation 226, then the heat flux at the surface of the plate in the stagnation region will be defined, thus substituting Equation 195 into Equation 226 yields

$$q_{w_{stag}} = .570 \, c_p \sqrt{\bar{B} \, \rho_{o_\infty} \, \mu_{o_\infty}} \, (T_w - T_{o_\infty}). \tag{227}$$

The velocity gradient $\bar{B}$ will now be established, thus completing the formulation for the stagnation heat flux.

The velocity gradient $\bar{B}$ is defined by Formula 165. Consider the translation of a sphere in an infinite inviscid fluid. The velocity potential must satisfy the following conditions:

1. The Laplace equation $\nabla^2 \phi = 0$ everywhere except singular points.
2. The fluid remains at rest at infinity; i.e., the space derivates

of ϕ must vanish at infinity.

3. The boundary conditions at the surface of the solid must be satisfied; i.e., $\frac{DF}{Dt} = 0$, where F is a general boundary equation.

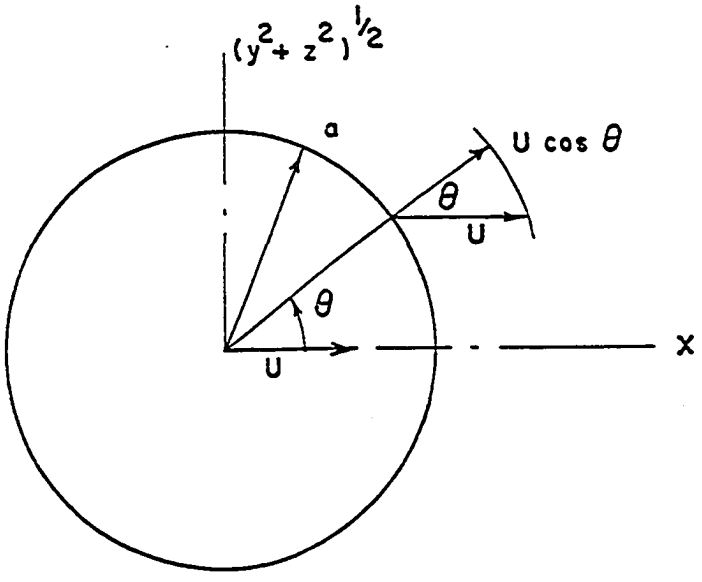

Figure 14a. Translating sphere

The fluid velocity normal to the surface is,

$$u_r = - \frac{\partial \phi}{\partial r} \tag{228}$$

hence, the boundary condition is

$$- \frac{\partial \phi}{\partial r} = U \cos \theta \tag{229}$$

for r = a.

Let.

$$y^2 + z^2 = \omega^2 \tag{230}$$

then the general boundary equation may be written as.

$$F = (x - U t)^2 + \omega^2 - a^2 = 0 \tag{231}$$

so that

$$\frac{DF}{Dt} = u \frac{\partial F}{\partial x} + v' \frac{\partial F}{\partial \omega} + \frac{\partial F}{\partial t} = 0 \tag{232}$$

but for t = 0.

$$u = - \frac{\partial \phi}{\partial x}$$

$$v' = - \frac{\partial \phi}{\partial \omega} \tag{233}$$

so that Equation 232 becomes

$$x \frac{\partial \phi}{\partial x} + \omega \frac{\partial \phi}{\partial \omega} + U x = 0 \tag{234}$$

for r = a, dividing Equation 234 through by a and realizing that

$$\frac{x}{a} = \cos \theta \tag{235}$$

$$\frac{\omega}{a} = \sin \theta \tag{236}$$

results in

$$\cos \theta \frac{\partial \phi}{\partial x} + \sin \theta \frac{\partial \phi}{\partial \omega} = - U \cos \theta \tag{237}$$

but the left hand side of Equation 237 is $\frac{\partial \phi}{\partial r}$ so that the boundary condition, Equation 229, is satisfied.

The fluid flow around the sphere, Figure 14, will have axial symmetry with respect to the x-axis, hence, the LaPlace equation becomes.

$$\frac{\partial}{\partial r} \left(r^2 \frac{\partial \phi}{\partial r} \right) + \frac{1}{\sin \theta} \frac{\partial}{\partial \theta} \left(\sin \theta \frac{\partial \phi}{\partial \theta} \right) = 0 \tag{238}$$

where ϕ is the velocity potential.

The velocity potential for a doublet is.

$$\phi = \frac{\bar{\mu} \cos \theta}{r^2} \tag{239}$$

where ϕ satisfies Equation 238, $\bar{\mu}$ is any constant, hence substituting Equation 239 into Equation 229 yields.

$$-\frac{\partial\phi}{\partial r} = \frac{2\bar{\mu}}{r^3}\cos\theta = U\cos\theta. \tag{240}$$

which is satisfied for r = a if

$$\bar{\mu} = U\,a^3/2 \tag{241}$$

hence, for a translating sphere in an infinite fluid

$$\phi = \frac{Ua^3}{2r^2}\cos\theta \tag{242}$$

and for a steady flow of an infinite fluid around a sphere.

$$\phi = \frac{Ua^3}{2r^2}\cos\theta + Ur\cos\theta \tag{243}$$

now,

$$v_\theta = -\frac{1}{r}\frac{\partial\phi}{\partial\theta}, \tag{244}$$

hence

$$v_\theta = \frac{Ua^3}{2r^3}\sin\theta\cdot\frac{\theta}{\theta} + U\sin\theta\cdot\frac{\theta}{\theta}. \tag{245}$$

Refer now to Figure 13 and noting that in Figure 13 x is equal to $a\theta$, Equation 245 thus modified to the coordinate system of Figure 13 becomes

$$U_x = \frac{Ua^2}{2r^3}\frac{\sin\theta}{\theta}x + \frac{U\,x}{a}\frac{\sin\theta}{\theta} \tag{246}$$

but by definition $\bar{B}$ is equal to $\frac{U_x}{x}$ in the neighborhood of the stagnation point, hence from Equation 246 at r = a and as θ 0

$$\bar{B}_{sphere} = \frac{3U}{D} = \frac{3V_\infty}{D} \tag{247}$$

$$V_\infty = (k\,g\,R\,T_\infty)^{\frac{1}{2}}M_\infty \tag{248}$$

hence

$$\bar{B}_{sphere} = \frac{3\,a\,M_\infty}{D}. \tag{249}$$

The stagnation point heat flux Equation 229 becomes

$$q_{w_{stag}} = .99 c_p \sqrt{\frac{M_\infty \, a \, \rho_{o_\infty} \, \mu_{o_\infty}}{D}} \; (T_{o_\infty} - T_w) \; . \tag{250}$$

The stagnation point heat flux due to radiation is

$$q_R = - \sigma \, \epsilon_s \, T_w^4 \; . \tag{251}$$

The net heat flux at the stagnation point is

$$q_{w_{stag}} - q_R = q_{net_{stag}} \tag{252}$$

hence, the governing differential equation for the skin temperature at the stagnation point is

$$\frac{dT_w}{dt} = \frac{.99 c_p}{G} \sqrt{\frac{M_\infty \, a \, \rho_{o_\infty} \, \mu_{o_\infty}}{D}} \; (T_{o_\infty} - T_w) - \frac{\sigma \, \epsilon_s}{G} T_w^4 \tag{253}$$

where G is the heat absorption capacity of the nose cone.

Assuming that the net heat flux at the stagnation point is zero, Equations 250, 251, and 252 yield for the steady state temperature T_w

$$\sigma \, \epsilon_s \, T_w^4 = .99 c_p \sqrt{\frac{M_\infty \, a \, \rho_{o_\infty} \, \mu_{o_\infty}}{D}} \; (T_{o_\infty} - T_w) \tag{254}$$

or

$$T_w^4 = \frac{.99 c_p}{\sigma \, \epsilon_s} \sqrt{\frac{M_\infty \, a \, \rho_{o_\infty} \, \mu_{o_\infty}}{D}} \; (T_{o_\infty} - T_w) \tag{255}$$

Equation 255 may be solved by trial and error to yield the stagnation, point temperature (steady state) and then Equation 251 may be used for determining the stagnation heat flux (steady state).

DERIVATION OF THE EQUATIONS OF MOTION AND THE INEQUALITY HEATING CONSTRAINT EQUATION

Defining the generalized coordinates as

$$q_1 = x \tag{256}$$

$$q_2 = h \tag{257}$$

$$q_3 = \gamma \tag{258}$$

Equation 23 becomes, for the x coordinate

$$\frac{d}{dt}\left(\frac{\partial L}{\partial \dot{x}}\right) - \frac{\partial L}{\partial x} = Q_x \tag{259}$$

$$m\ddot{x} + m g_c \frac{R_o^2}{R^2}\frac{\partial R}{\partial x} = Q_x \tag{260}$$

but from Equation 20.

$$\frac{\partial R}{\partial x} = \frac{x}{R}$$

hence, Equation 260 becomes

$$m\ddot{x} + \frac{m g_c R_o^2 x}{[(R_o + h)^2 + x^2]^{\frac{3}{2}}} = Q_x \tag{261}$$

for the h coordinate

$$\frac{d}{dt}\left(\frac{\partial L}{\partial \dot{h}}\right) - \frac{\partial L}{\partial h} = Q_h \tag{262}$$

$$m\ddot{h} + m g_c \frac{R_o^2}{R^2}\frac{\partial R}{\partial h} = Q_h \tag{263}$$

but from Equation 20

$$\frac{\partial R}{\partial h} = \frac{R_o + h}{R}\,.$$

Hence Equation 263 becomes.

$$m\ddot{h} + \frac{m\, g_c R_o^2 (R_o + h)}{[(R_o + h)^2 + x^2]^{\frac{3}{2}}} = Q_h \tag{264}$$

for the γ coordinate,

$$I\ddot{\gamma} = Q_\gamma \,. \tag{265}$$

The generalized forces Q_i will now be defined. Referring to Figure 14b.

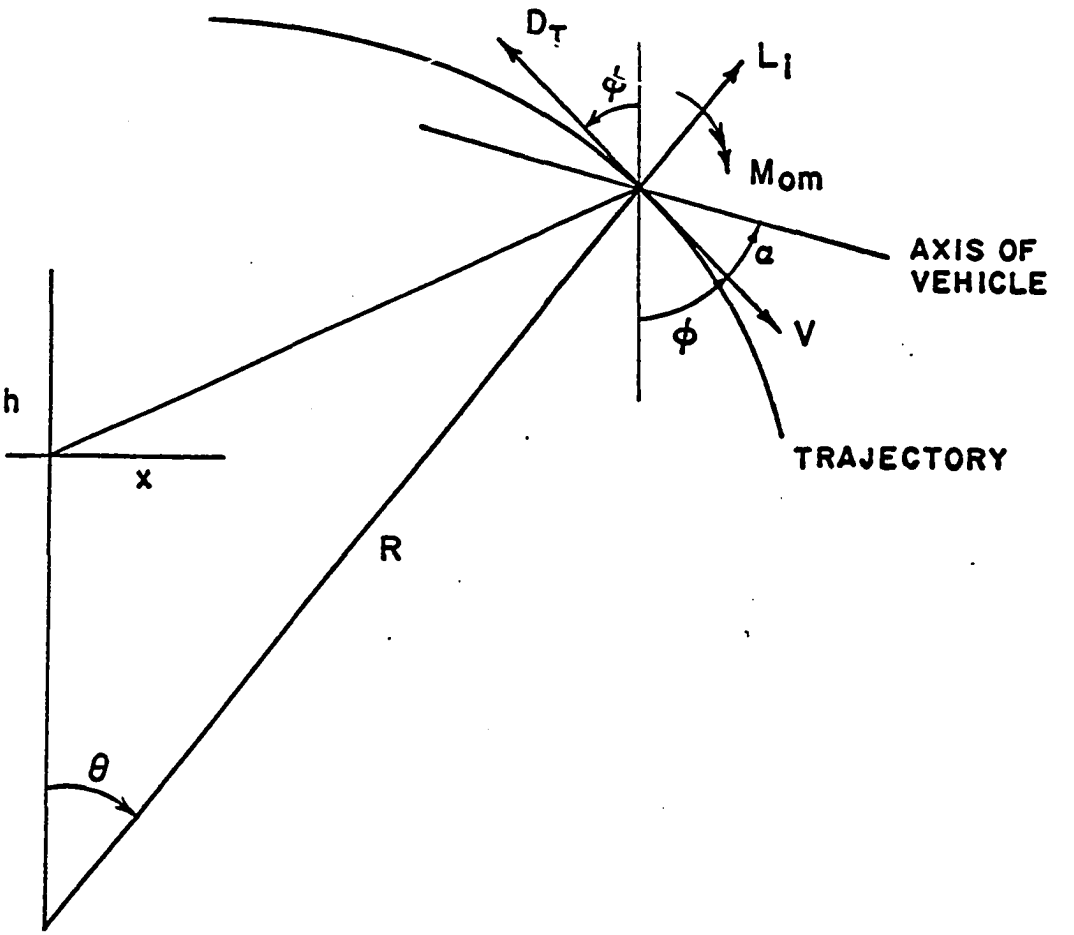

Figure 14b. Generalized forces

The generalized forces are:

$$Q_x = L_i \cos \phi - D_t \sin \phi \tag{266}$$

$$Q_h = L_i \sin \phi + D_t \cos \phi \tag{267}$$

$$Q_\gamma = M_{om}. \tag{268}$$

The equations of motion thus become, for the x coordinate

$$m\ddot{x} + \frac{m g_c R_o^2 x}{[(R_o + h)^2 + x^2]^{\frac{3}{2}}} = L_i \cos \phi - D_t \sin \phi \tag{269}$$

for the h coordinate

$$m\ddot{h} + \frac{m g_c R_o^2 (R_o + h)}{[(R_o + h)^2 + x^2]^{\frac{3}{2}}} = L_i \sin \phi + D_t \cos \phi \tag{270}$$

for the γ coordinate

$$I\ddot{\gamma} = - M_{om} \tag{271}$$

where L_i, D_t, and M_{om} are defined as per Equations 91, 164, and 88, respectively.

Equation 269 may be ximplified by noting that

$$\frac{R_o^2 x}{[(R_o + h)^2 + x^2]^{\frac{3}{2}}} \ll 1. \tag{272}$$

Equation 270 may also be simplified by noting that

$$\frac{R_o^2 (R_o + h)}{[(R_o + h)^2 + x^2]^{\frac{3}{2}}} \approx 1. \tag{273}$$

The preceding simplifications are the results of a sample calculation which indicates that for a reentry vehicle traveling 15,000 ft/sec, reentering at an altitude of 100 miles, the maximum value for x is

approximately 500 miles, assuming no drag or lift forces acting on the vehicle, and assuming an earth radius of 4,000 miles.

Substituting Equations 3, 88, 91, 164, 272, and 273, into the equations of motion 269, 270, and 271 yield, for the x coordinate

$$m \dot{v}_x = - \frac{2 a \rho_\infty L_S (v_x^2 + v_h^2)^{\frac{1}{2}} \alpha}{g_c \sqrt{(v_x^2 + v_h^2) - a^2}} v_h - \frac{2 a \rho_\infty L_S (v_x^2 + v_h^2)^{\frac{1}{2}} \alpha^2}{g_c \sqrt{(v_x^2 + v_h^2) - a^2}} + \sqrt{8 \Gamma_1 \rho_\infty \mu_\infty L_S (v_x^2 + v_h^2)^{\frac{1}{2}}} v_x \qquad (274)$$

for the h coordinate,

$$m \dot{v}_h = \frac{2 a \rho_\infty L_S (v_x^2 + v_h^2)^{\frac{1}{2}} \alpha}{g_c \sqrt{(v_x^2 + v_h^2) - a^2}} v_x - \frac{2 a \rho_\infty L_S (v_x^2 + v_h^2)^{\frac{1}{2}} \alpha^2}{g_c \sqrt{(v_x^2 + v_h^2) - a^2}} + \sqrt{8 \Gamma_1 \rho_\infty \mu_\infty L_S (v_x^2 + v_h^2)^{\frac{1}{2}}} v_h - mg_c, \qquad (275)$$

also

$$\dot{x} = v_x \qquad (276)$$

$$\dot{h} = v_h \qquad (277)$$

Designate the maximum allowable temperature at the stagnation point by T_{wo}. Note that at the stagnation point there exists the inequality

$$0 < T_w < T_{wo}. \qquad (278)$$

Equation 253 may be integrated to yield the temperature at the stagnation point at any time t. At the instant that the stagnation temperature becomes equal to the maximum allowed, the condition

$$\left(\frac{dT_w}{dt}\right)_{T_w = T_{wo}} = 0 \qquad (279)$$

must be imposed on Equation 253. Under this condition and at that instant Equation 253 may be written as

$$\sigma \epsilon_s T_{wo}^4 = .99 c_p \sqrt{\frac{\rho_{o_\infty} \mu_{o_\infty} a M_\infty}{D}} (T_{o_\infty} - T_{wo}). \tag{280}$$

Now the right hand side of Equation 280 is the stagnation heat flux and the left hand side is a constant for a given surface and a given temperature T_{wo}. Equation 280 thus establishes the upper bound for the stagnation heat flux and this upper bound has the magnitude

$$\sigma \epsilon_s T_{wo}^4 = q_{wo}. \tag{281}$$

Note that at the stagnation point there exists an inequality of the form.

$$0 < q_w < q_{wo} \tag{282}$$

which will hereafter be considered as the inequality heating constraint.

Equation 271 may be rewritten as

$$I (\dot{\omega}_1 + \dot{\omega}_2) = - \frac{\rho_\infty L_s^2 (v_x^2 + v_h^2) a \alpha}{g_c \sqrt{(v_x^2 + v_h^2) - a^2}} \tag{283}$$

where

$$\omega_1 = \dot{\phi} \tag{284}$$

$$\omega_2 = \dot{\alpha} \tag{285}$$

$$\dot{\phi} = \frac{v_x \dot{v}_h - v_h \dot{v}_x}{v_h^2 + v_x^2} \tag{286}$$

$$\ddot{\phi} = \frac{(v_h^2 + v_x^2)[v_x \ddot{v}_h - \ddot{v}_x v_h]}{(v_h^2 + v_x^2)^2} - \frac{(v_x \dot{v}_h - v_h \dot{v}_x)(2)(v_h \dot{v}_h + v_x \dot{v}_x)}{(v_h^2 + v_x^2)^2}. \tag{287}$$

A GENERAL VARIATIONAL FORMULATION

The methods of the variational calculus have been extensively used since World War II in the realm of space dynamics. With the advent of jet engines as aircraft propulsion systems and the increase in flight velocities a new wealth of important and unsolved problems of flight mechanics have arisen which can best be formulated and interpreted by variational methods (12).

The variational approach is useful in investigations

a. which formulate the optimum conditions of flight in a general fashion, valid (among other factors) for an arbitrary dependence of the characteristics of the airframe and of the engine on the Mach number,

b. which unify all the optimum conditions of flight in a vertical plane into one single equation; this equation contains, as a particular case, the answer to a variety of problems such as ceiling, best range, best endurance, maximum level speed, steepest ascent, best rate of climb, flattest descent, etc.,

c. which unify all the optimum conditions of flight in a horizontal plane into one single equation such as in (b),

d. which seek answers to design problems such as best airfoil shape, best airfoil contour, etc.

A general variational formulation of a three degree of freedom reentry vehicle will now be derived based on an inequality constraint of the form.

$$0 < q_w < q_{wo} \tag{282}$$

and subject to the condition that

$$\int_t dG = \Delta G \Big|_{t_1}^{t_2} = \text{extremal.} \tag{288}$$

Where G is some function to be specified later.

The kinematic constraints are:

$$\dot{x} - v_x = 0 \tag{289}$$

$$\dot{h} - v_h = 0 \tag{290}$$

$$\dot{\alpha} - \omega_2 = 0. \tag{291}$$

The kinetic constraints are:

$$m \dot{v}_x - F_x (v_x\ v_h\ \alpha) = 0 \tag{292}$$

$$m \dot{v}_h - F_h (v_x\ v_h\ \alpha) = 0 \tag{293}$$

$$I (\dot{\omega}_1 + \dot{\omega}_2) + g (v_x\ v_h\ \alpha) = 0 \tag{294}$$

where F_x, F_h, and g are the right hand side of Equations 274, 275, and 283. q_w in the inequality constraint Equation 282 is subject to

$$[q_w - q_w (v_x\ v_h)] = 0 \tag{295}$$

where $q_w (v_x\ v_h)$ is given by Equation 250.

The problem as presented to this point is a Bolza problem, however, if the Bolza technique is applied, Equation 295 will drop out of the resulting formulation. In order to adjoin Equation 295 to the resulting formulation, it is necessary to define a new variable z such that

$$z^2 - q_w (q_{wo} - q_w) = 0. \tag{296}$$

z is known as the Valentine variable. The addition of Equation 296 serves not only to adjoin Equation 295 to the system of equations but also effectively replaces the inequality heating constraint, Equation 282.

q_w is always greater than zero and subject to the inequality constraint, Equation 282. With these conditions on q_w, it is obvious that z is real in Equation 296.

To formulate the general variational problem, multiply Equations 289 through 296 by λ_1, λ_2, . . . λ_8 respectively and add. This yields a new function

$$F = \lambda_1 (\dot{x} - v_x) + \lambda_2 (\dot{h} - v_h) + \lambda_3 (\alpha - \omega_2) + \lambda_4 [m \dot{v}_x - F_x(v_x v_h \alpha)] +$$

$$\lambda_5 [m \dot{v}_h - F_h (v_x v_h \alpha)] + \lambda_6 [I (\dot{\omega}_1 + \dot{\omega}_2) + g (v_x v_h \alpha)] +$$

$$\lambda_7 [q_w - q_w (v_x v_h)] + \lambda_8 [z^2 - q_w (q_{wo} - q_w)] \qquad (297)$$

or

$$F = (x, h, \alpha, v_x, v_h, \omega_2, q_w, z). \qquad (298)$$

The time (t) is considered the independent variable and F must satisfy the Euler-Lagrange equations.

$$\frac{d}{dt} \left(\frac{\partial F}{\partial \dot{q}_i}\right) - \frac{\partial F}{\partial q_i} = 0 \qquad (299)$$

with respect to x, h, α, v_x, v_h, ω_2, q_w, and z

for x.

$$\frac{d}{dt} \left(\frac{\partial F}{\partial \dot{x}}\right) - \frac{\partial F}{\partial x} = \dot{\lambda}_1 = 0 \qquad (300)$$

for h.

$$\frac{d}{dt} \left(\frac{\partial F}{\partial \dot{h}}\right) - \frac{\partial F}{\partial h} = \dot{\lambda}_2 = 0 \qquad (301)$$

for α.

$$\frac{d}{dt} \left(\frac{\partial F}{\partial \dot{\alpha}}\right) - \frac{\partial F}{\partial \alpha} = \dot{\lambda}_3 + \left[\lambda_4 \frac{\partial F_x}{\partial \alpha} + \lambda_5 \frac{\partial F_h}{\partial \alpha} - \lambda_6 \frac{\partial g}{\partial \alpha} \right] = 0 \qquad (302)$$

for v_x.

$$\frac{d}{dt} \left(\frac{\partial F}{\partial \dot{v}_x}\right) - \frac{\partial F}{\partial v_x} = m \dot{\lambda}_4 + I \frac{d}{dt} \left(\lambda_6 \frac{\partial \dot{\omega}_1}{\partial \dot{v}_x}\right) + \left[\lambda_1 + \lambda_4 \frac{\partial F_x}{\partial v_x} + \lambda_5 \frac{\partial F_h}{\partial v_x} - \right.$$

$$\left. \lambda_6 I \frac{\partial \dot{\omega}_1}{\partial v_x} - \lambda_6 \frac{\partial g}{\partial v_x} + \lambda_7 \frac{\partial q_w}{\partial v_x} \right] = 0 \qquad (303)$$

for v_h:

$$\frac{d}{dt}\left(\frac{\partial F}{\partial \dot{v}_h}\right) - \frac{\partial F}{\partial v_h} = m\,\dot{\lambda}_5 + I\,\frac{d}{dt}\left(\lambda_6\,\frac{\partial \dot{\omega}_1}{\partial \dot{v}_h}\right) + \left[\lambda_2 + \lambda_4\,\frac{\partial F_x}{\partial v_h} + \lambda_5\,\frac{\partial F_h}{\partial v_h} - \right.$$

$$\left.\lambda_6\,I\,\frac{\partial \dot{\omega}_1}{\partial v_h} - \lambda_6\,\frac{\partial g}{\partial v_h} + \lambda_7\,\frac{\partial q_w}{\partial v_h}\right] = 0 \tag{304}$$

for ω_2:

$$\frac{d}{dt}\left(\frac{\partial F}{\partial \dot{\omega}_2}\right) - \frac{\partial F}{\partial \omega_2} = I\,\dot{\lambda}_6 + \lambda_3 = 0 \tag{305}$$

for q_w:

$$\frac{d}{dt}\left(\frac{\partial F}{\partial \dot{q}_w}\right) - \frac{\partial F}{\partial q_w} = -\left[\lambda_7 - \lambda_8\,(q_{wo} - 2q_w)\right] = 0 \tag{306}$$

for z:

$$\frac{d}{dt}\left(\frac{\partial F}{\partial \dot{z}}\right) - \frac{\partial F}{\partial z} = -\,2\lambda_8\,z = 0. \tag{307}$$

F must satisfy Equations 289 through 296 and 300 through 307 and also the following boundary condition

$$dG + \sum_{L=1}^{8} \frac{\partial F}{\partial \dot{q}_i}\,\delta\,q_i \Bigg|_{t_1}^{t_2} = 0. \tag{308}$$

Equation 308 is often referred to as the transversality condition.

Equation 308 becomes:

$$dG + \lambda_1\,\delta x + \lambda_2\,\delta h + \lambda_3\,\delta\alpha + \left(m\,\lambda_4 + I\,\lambda_6\,\frac{\partial \dot{\omega}_1}{\partial \dot{v}_x}\right)\delta v_x +$$

$$\left(m\,\lambda_5 + I\,\lambda_6\,\frac{\partial \dot{\omega}_1}{\partial \dot{v}_h}\right)\delta v_h + I\,\lambda_6\,\delta\omega_2 \Bigg|_{t_1}^{t_2} = 0 \tag{309}$$

since:

$$\frac{\partial F}{\partial \dot{q}_w} = 0 \tag{310}$$

and

$$\frac{\partial F}{\partial \dot{z}} = 0.$$

There are 16 variables composed of the six state variables, x, h, α, v_x, v_h, ω_2, the constraint variables, q_w, the Valentine variable, z, and the eight Lagrange multipliers λ_i (i=1 . .8). There are eight constraint equations, 289 through 296, and eight Euler-Lagrange first-order differential equations, 300 through 307. There are the same number of equations as there are variables. There are 12 first-order differential equations in this system which give rise to 12 constants of integration. These constants may be evaluated in the following manner.

There are six initial boundary conditions on x, h, α, v_x, v_h, and ω_2, and for the initial phase of the flight λ_7 and λ_8 are set equal to zero. There are six first-order non-linear differential equations for the λ_1 through λ_6 and only the transversality condition remains as a boundary condition. Thus it appears there are five remaining unknown constants of integration for which there is no available information. An examination of the equations of motion, Equations 274, 275, and 283, reveal that these equations are sufficient for completely defining the initial phase of the flight. This implies the non-existence of a variational problem, with regards to v_x, v_h, and α, during the initial phase of flight, hence, all λ_i may be equal to zero during the initial phase of flight since the trajectory is completely defined by the three equations of motion. During the heating constrained phase of flight, the stagnation heat flux equation becomes effective and from Equation 280, it is obvious that there is only one unknown in the equation which is the mach number,

hence, Equation 280, when effective, forms a constraining relation between v_x and v_h and the system reduces to a two degree of freedom system. The third equation of motion, Equation 283, can no longer be admitted since the angle of attack must now be generated in such a manner that a heating constraint trajectory results until impact occurs.

The vehicle must now be considered as a two degree of freedom system whose two equations of motion, Equations 274 and 275, contain the unknown parameter α. This implies the existence of a variational problem and the possibility that the λ_i might serve as generating functions for determining an α which would yield a trajectory subjected to the heating constraint inequality, Equation 282, and the conditions imposed by Equation 288. Since the λ_i, which are functions of time, become effective at the instant of maximum heating, the initial value for the λ_i (t_H) will be taken as zero, this may allow some "overshoot" on the preassigned maximum value of q_{wo}, however, this can be corrected with data from "computer runs". The remaining λ_i which may turn out to be constants will be determined with the aid of the transversality condition. Thus there are sufficient boundary conditions for all λ_i.

The initial condition for the stagnation point temperature is

$$T_w (t_1) = T_{w1}. \tag{312}$$

A control theory analysis of this system of equations is now in order. An inspection of Equations 303 and 304 indicate that λ_3 and λ_4 are dependent upon λ_7 provided λ_7 is not zero.

In Equation 307 either λ_8 or z must be equal to zero, assuming $z = 0$ and $\lambda_8 \neq 0$, Equation 306 is seen to reduce to

$$\lambda_7 = \lambda_8 (q_{wo} - 2q_w) \tag{313}$$

but when z equals zero, from Equation 296, q_w must equal q_{wo} or zero, but q_w is never zero, hence Equation 313 becomes

$$\lambda_7 = - \lambda_8 q_{wo}. \tag{314}$$

Equations 303, 304, and 314 reveal the important fact that when the equality sign in Equation 282 holds, that the heating constraint effect can be applied continuously over a trajectory. The possibility that λ_8 may alternately switch from z non-zero value to a zero value may exist, if so, the vehicle would be flying an on-off constraint trajectory. Assume that λ_8 does switch from a non-zero value to a zero value; at the instant of switching, λ_7 must also "switch" to zero to satisfy Equation 314, but if $q_w = q_{wo}$, then z must also be equal to zero to satisfy Equation 296. The value of zero for λ_8 and z simultaneously cannot be permitted for if it could there would be no meaning in the definition of the inequality constraint Equation 282 and the adjoining Equation 296. Thus the important result which the preceding analysis yields is that the heating constraint, once continuously effective, is applied continuously over the trajectory and that the total flight trajectory would consist at most of a off-on constraint trajectory with no switching allowed during the latter phase. The preceding analysis indicates that switching of λ_8 from zero is permitted when the heating constraint becomes continuously effective. It is obvious from Equations 280 and 281, that one of the parameters which governs the "range" is the value of T_{wo}, which is dependent on the allowable nose cone surface temperature, and that the preceding system of equations will yield a unique solution for a

preassigned T_{wo}. To speak of a near-constraint type of trajectory has no meaning since any trajectory slightly above and similar to that for a preassigned T_{wo} is a near-constraint trajectory and the angle of attack can be arbitrarily chosen at any instance to yield any near-constraint trajectory, for which there will correspond a near value to the preassigned T_{wo}. This near constraint trajectory will thus involve variations such that the necessary condition for an extremal for Equation 288 will exist, i.e.,

$$E > 0 \tag{315}$$

where.

$$E = F\left(q_i^* \dot{q}_i^*\right) - F\left(q_i \dot{q}_i\right) - \sum_{i=1}^{6} \left(\dot{q}_i^* - \dot{q}_i\right) \frac{\partial F}{\partial \dot{q}_i} \tag{316}$$

where * denotes functions subjected to finite, admissible variations. The q_i, the derivatives of which occur in F, (here x, h, α, v_x, v_h, q_w), must be continuous, i.e., $q_i^* = q_i$. ΔG in Equation 288 will be the extremal value corresponding to the prescribed T_{wo}.

The preceding general variational formulation has been shown to be mathematically compatiable under the conditions and constraints imposed and the uniqueness of a solution has been tacitly established by the preceding argument.

Due to the complexity of the system of equations obtained in the general variational formulation, the following assumptions will be made with no loss in generality.

It will be assumed that the center of pressure of the airfoil coincides with the mass center of the vehicle, thus no aerodynamic moment is generated. It will also be assumed that the mass inertia of the

vehicle with respect to the pitch axis through the center of mass is negligible.

α, which appears in the force equations, will be set equal to zero during the initial phase of the reentry flight. The λ_i must be set equal to zero, since for a preassigned α, the two equations of motion are sufficient for specifying the trajectory and under this condition the λ_i have no meaning. Hence, the initial phase of flight consist of a minimum drag free ballistic trajectory.

At the instant that the stagnation surface temperature reaches a preassigned T_{wo}, the imposed condition of zero on the λ_i and will be relaxed and the λ_i will then serve as generating functions generating an equivalent angle of attack so as to fly the vehicle on an aerodynamic heating constraint trajectory, subjected to the conditions of Equation 288.

The preceding assumptions thus reduce the vehicle to a two degree of freedom system with equivalent lift and drag. They also eliminate the equation of motion, Equation 283. Since the inequality heating constraint, Equation 282, is also equivalent to an inequality velocity constraint, Equation 282, will be replaced by the following inequality velocity constraint.

$$0 < V < V_m \tag{317}$$

where V_m will be determined later.

The formulation for this simplified version of the general variational formulation will now be presented.

The kinematic constraints are:

$$\dot{x} - v_x = 0 \tag{318}$$

$$\dot{h} - v_h = 0. \tag{319}$$

The kinetic constraints are:

$$m \dot{v}_x - F_x (v_x\ v_h\ \alpha) = 0 \tag{320}$$

$$m \dot{v}_h - F_h (v_x\ v_h\ \alpha) = 0 \tag{321}$$

also,

$$V - \sqrt{v_x^2 + v_h^2} = 0 \tag{322}$$

and the Valentine variable is

$$z^2 - V (V_m - V) = 0. \tag{323}$$

The function F becomes

$$F = \lambda_1 (\dot{x} - v_x) + \lambda_2 (\dot{h} - v_h) + \lambda_3 (m \dot{v}_x - F_x) + \lambda_4 (m \dot{v}_h - F_h) +$$

$$\lambda_5 (V - \sqrt{v_x^2 + v_h^2}) + \lambda_6 (z^2 - V (V_m - V)) \tag{324}$$

where,

$$F = (x\ h\alpha\ v_x\ v_h\ V\ z). \tag{325}$$

The Euler-Lagrange equations are

$$\frac{d}{dt} \left(\frac{\partial F}{\partial \dot{q}_i}\right) - \frac{\partial F}{\partial q_i} = 0 \tag{326}$$

for x.

$$\dot{\lambda}_1 = 0 \qquad \lambda_1 = a_1 \tag{327}$$

for h.

$$\dot{\lambda}_2 = 0 \qquad \lambda_2 = a_2 \tag{328}$$

for α.

$$\lambda_3 \frac{\partial F_x}{\partial \alpha} + \lambda_4 \frac{\partial F_h}{\partial \alpha} = 0 \tag{329}$$

for v_x

$$m \dot{\lambda}_3 = + a_1 + \lambda_3 \frac{\partial F_x}{\partial v_x} + \lambda_4 \frac{\partial F_h}{\partial v_x} + \lambda_5 \frac{v_x}{\sqrt{v_x^2 + v_h^2}} \tag{330}$$

for v_h

$$m \dot{\lambda}_4 = + a_2 + \lambda_3 \frac{\partial F_x}{\partial v_h} + \lambda_4 \frac{\partial F_h}{\partial v_h} + \lambda_5 \frac{v_h}{\sqrt{v_x^2 + v_h^2}} \tag{331}$$

for V

$$\lambda_5 = \lambda_6 (V_m - 2V) \tag{332}$$

for z

$$2z \lambda_6 = 0 \tag{333}$$

There are seven variables of state and six unknown Lagrange multipliers. There are 13 equations which relate these variables and the Lagrange multipliers. There are eight first-order non-linear differential equations. The boundary conditions are:

Initial conditions for the initial phase.

$$x (t_1) = 0 \qquad v_x(t_1) = V_{ix}$$

$$h (t_1) = h_1 \qquad v_h (t_1) = 0$$

$$\lambda_i = 0 \qquad \alpha = 0 \tag{334}$$

The terminal conditions for this phase of flight is:

$$V_m = \sqrt{v_x^2 + v_h^2}\ , \text{ when } T_w = T_{wo} \tag{335}$$

where V_m is the velocity which corresponds to the root of Equation 280.

Initial conditions for the second phase.

$$x (t_1') = x \qquad v_x(t_1') = v_x$$

$$h (t_1') = h \qquad v_h(t_1') = v_h$$

$$z = 0 \qquad \alpha \neq 0$$

$$\lambda_5 = - \lambda_6 V_m \qquad \lambda_i (t_1') = 0. \tag{336}$$

The transversality condition is

$$dG + a_1 \delta x + a_2 \delta h + m \lambda_3 \delta v_x + m \lambda_4 \delta v_h \Big|_{t_1'}^{t_2} = 0 \tag{337}$$

and the impact condition which terminates the problem is

$$h = - R_o + \sqrt{R_o^2 - x^2} \quad . \tag{338}$$

A flow sheet for the computer computation is shown on Figure 15. The problem is designated as P 1.

SUMMARY OF EQUATIONS REQUIRED FOR THE COMPUTATION

OF A TRAJECTORY FOR PROBLEM P 1

$$a = \sqrt{k\, g_c\, R\, T_\infty} \tag{86}$$

$$T_{o_\infty} = T_\infty \left(1 + \frac{k-1}{2} M_\infty^2\right) \tag{152}$$

$$\mu_{o_\infty} = \mu_\infty \left(1 + \frac{k-1}{2} M_\infty^2\right) \tag{339}$$

$$\rho_{o_\infty} = \rho_\infty \left(1 + \frac{k-1}{2} M_\infty^2\right)^{\frac{1}{k-1}} \tag{340}$$

$$M_\infty = \frac{\sqrt{v_x^2 + v_h^2}}{a} \tag{341}$$

$$\beta = \frac{\left(\frac{k-1}{2}\right) M_\infty^2}{1 + \left(\frac{k-1}{2}\right) M_\infty^2} \tag{153}$$

$$q_w = .99 c_\rho \sqrt{\frac{M_\infty\, a\, \rho_{o_\infty}\, \mu_{o_\infty}}{D}}\, (T_{o_\infty} - T_w) \tag{250}$$

$$\dot{T}_w = \frac{.99 c_p}{G} \sqrt{\frac{M_\infty\, a\, \rho_{o_\infty}\, \mu_{o_\infty}}{D}}\, (T_{o_\infty} - T_w) - \frac{\sigma\, \epsilon_s\, T_w^4}{G} \tag{253}$$

$$q_{wo} = .99 c_p \sqrt{\frac{M_\infty\, a\, \rho_{o_\infty}\, \mu_{o_\infty}}{D}}\, (T_{o_\infty} - T_{wo}) \tag{280}$$

$$q_{wo} = \sigma\, \epsilon_s\, T_{wo}^4 \tag{281}$$

$$\dot{v}_x = \frac{F_x}{m} \tag{274}$$

$$\dot{v}_h = \frac{F_h}{m} \tag{275}$$

$$v_x = \dot{x} \tag{276}$$

$$v_h = \dot{h} \tag{277}$$

$$F_x = - \frac{2\, a\, \rho_\infty\, L_S\, (v_x^2 + v_h^2)^{\frac{1}{2}}\, v_h\, \alpha}{g_c \sqrt{v_x^2 + v_h^2 - a^2}} - \frac{2a\, \rho_\infty\, L_S\, (v_x^2 + v_h^2)^{\frac{1}{2}}\, v_x\, \alpha^2}{g_c \sqrt{v_x^2 + v_h^2 - a^2}} -$$

$$v_x \sqrt{8\, \Gamma_1\, \rho_\infty\, \mu_\infty\, L_S\, (v_x^2 + v_h^2)^{\frac{1}{2}}} \tag{342}$$

$$F_h = \frac{2\, a\, \rho_\infty\, L_S\, (v_x^2 + v_h^2)^{\frac{1}{2}}\, v_x\, \alpha}{g_c \sqrt{v_x^2 + v_h^2 - a^2}} - \frac{2\, a\, \rho_\infty\, L_S\, (v_x^2 + v_h^2)^{\frac{1}{2}}\, v_h\, \alpha^2}{g_c \sqrt{v_x^2 + v_h^2 - a^2}} -$$

$$v_h \sqrt{8\, \Gamma_1\, \rho_\infty\, \mu_\infty\, L_S\, (v_x^2 + v_h^2)^{\frac{1}{2}}} - m\, g_c \tag{343}$$

$$\Gamma_1 = \frac{1}{B} - \frac{1}{2B} \ln (1 - B) - \frac{1}{2B^{\frac{3}{2}}} \ln (1 + \sqrt{B}) + \frac{1}{2B^{\frac{3}{2}}} \ln (1 - \sqrt{B}) \tag{344}$$

$$V_m^6 - 5\, a^2 \frac{T_{wo}}{T_\infty} V_m^4 - \frac{8\, 4\, a^6\, q_{wo}}{c_p\, T_\infty \dfrac{a \mu_\infty \rho_\infty}{D}} = 0 \tag{345}$$

V_m is the velocity corresponding to the maximum surface temperature T_{wo}.

$$V = \sqrt{v_x^2 + v_h^2} \tag{322}$$

$$z^2 = V\, (V_m - V) \tag{323}$$

$$\lambda_3 \frac{\partial F_x}{\partial \alpha} + \lambda_4 \frac{\partial F_h}{\partial \alpha} = 0 \tag{329}$$

$$\dot{\lambda}_3 = \frac{a_1}{m} + \frac{\lambda_3}{m} \frac{\partial F_x}{\partial v_x} + \frac{\lambda_4}{m} \frac{\partial F_h}{\partial v_x} + \frac{\lambda_5}{m} \frac{v_x}{V} \tag{330}$$

$$\dot{\lambda}_4 = \frac{a_2}{m} + \frac{\lambda_3}{m} \frac{\partial F_x}{\partial v_h} + \frac{\lambda_4}{m} \frac{\partial F_h}{\partial v_h} + \frac{\lambda_5}{m} \frac{v_h}{V} \tag{331}$$

$$\lambda_5 = \lambda_6\, (V_m - 2V) \tag{332}$$

$$0 = 2\, z\, \lambda_6 \tag{333}$$

Equations 329, 330, and 331 may be combined to yield

$$\dot{\lambda}_3 = \frac{a_1}{m} + \frac{\lambda_3}{m} F_1 + \frac{\lambda_5 v_x}{m V} \tag{346}$$

$$\dot{\lambda}_4 = + \frac{a_2}{m} + \frac{\lambda_4}{m} F_2 + \frac{\lambda_5 v_h}{m V} \tag{347}$$

$$\lambda_5 \left(v_h + v_x \frac{\partial F_x}{\partial \alpha} \Big/ \frac{\partial F_h}{\partial \alpha}\right) + a_1 \frac{\partial F_x}{\partial \alpha} \Big/ \frac{\partial F_h}{\partial \alpha} + a_2 = \lambda_3 \left[(F_2 - F_1) \frac{\partial F_x}{\partial \alpha} \Big/ \frac{\partial F_h}{\partial \alpha} - m \dot{\left(\frac{\partial F_x}{\partial \alpha} \Big/ \frac{\partial F_h}{\partial \alpha}\right)}\right]. \tag{348}$$

Equation 348 defines a relationship between λ_3 and a_1, a_2, and λ_5, where

$$F_1 = \frac{\frac{\partial F_x}{\partial v_x}\frac{\partial F_h}{\partial \alpha} - \frac{\partial F_x}{\partial \alpha}\frac{\partial F_h}{\partial v_x}}{\frac{\partial F_h}{\partial \alpha}} \tag{349}$$

$$F_2 = \frac{\frac{\partial F_h}{\partial v_h}\frac{\partial F_x}{\partial \alpha} - \frac{\partial F_h}{\partial \alpha}\frac{\partial F_x}{\partial v_h}}{\frac{\partial F_x}{\partial \alpha}} . \tag{350}$$

The initial conditions for the initial phase of flight are

$$x(t_1) = 0 \qquad v_x(t_1) = V_{1x}$$

$$h(t_1) = h_1 \qquad v_h(t_2) = 0.$$

$$t_w(t_1) = T_{w1} \tag{351}$$

See Figure 15 for the other conditions, the terminal conditions for the initial phase are

$$V = V_m, \text{ when } T_w = T_{wo}. \tag{352}$$

The initial conditions for the second phase are the terminal conditions for the first phase. The problem is terminated when impact occurs, i.e.,

$$h = -R_o + \sqrt{R_o^2 - x^2} \tag{338}$$

The initial conditions for all λ_i (t) may be taken as zero.

At this point it is necessary to define the function G which appears in Equation 288 and in the transversality equation. Repeating the transversality equation,

$$dG + a_1 \delta x + a_2 \delta h + \lambda_3 m \delta v_x + \lambda_4 m \delta v_h \Big|_{t_1'}^{t_2} = 0,$$

and since

$$dq_i = \delta q_i + \dot{q}_i \, dt \tag{353}$$

then Equation 309 may be written as

$$dG + a_1 dx + a_2 dh + \lambda_3 m \dot{v}_x + \lambda_4 m d v_h - C \, dt \Big|_{t_1'}^{t_2} = 0 \tag{354}$$

where

$$C = a_1 v_x + a_2 v_h + \lambda_3 m \dot{v}_x + \lambda_4 m \dot{v}_h \, . \tag{355}$$

If G is equal to t, where t is time, then the condition imposed on the system by Equation 288 is that of minimum time of descent, Under this condition C = 1, and since x and h are not explicit in Equation 297 for F and both are free at t_2, then a_1 and a_2 may be set equal to zero. The transversality condition then becomes.

$$1 = \lambda_3 m \dot{v}_x + \lambda_4 m \dot{v}_h \tag{356}$$

If G is equal to x or h, then the condition imposed on the system by Equation 288 is that of maximum range or altitude. Under this condition either a_1 or a_2 is equal to - 1 while the other is set equal to zero. C is also equal to zero under this condition.

If G is set equal to zero, then the system is subjected only to the inequality velocity constraint expressed by Equation 317. Under this

condition the transversality equation becomes

$$0 = \lambda_3 \, m \, \dot{v}_x + \lambda_4 \, m \, \dot{v}_h \Big|_{t_1}^{t_2} \tag{357}$$

This last condition for G will be the one admitted in this investigation. Prior analysis has indicated that for a prescribed T_{wo}, there exist a unique trajectory and time of descent, hence the reason for relaxing any condition imposed by Equation 288.

The remaining equations are

$$\frac{\partial F_x}{\partial v_x} = \frac{2 \, a \, \rho_\infty \, L_S \, \alpha \, v_h \, v_x}{g_c} \left[\frac{\sqrt{v_x^2 + v_h^2}}{3\sqrt{v_x^2 + v_h^2 - a^2}} - \frac{1}{\sqrt{v_x^2 + v_h^2 - a^2}\sqrt{v_x^2 + v_h^2}} \right]$$

$$- \left[\sqrt{8\Gamma_1 \, \rho_\infty \, \mu_\infty \, L_S (v_x^2 + v_h^2)^{\frac{1}{2}}} + \frac{v_x^2 \sqrt{8 \, \Gamma_1 \, \rho_\infty \, \mu_\infty \, L_S}}{2 \, (v_x^2 + v_h^2)^{\frac{3}{4}}} \right] \tag{358}$$

$$\frac{\partial F_h}{\partial v_h} = \frac{2 \, a \, \rho_\infty \, L_S \, \alpha \, v_x \, v_h}{g_c} \left[\frac{1}{\sqrt{v_x^2 + v_h^2 - a^2}\sqrt{v_x^2 + v_h^2}} - \frac{\sqrt{v_x^2 + v_h^2}}{3\sqrt{v_x^2 + v_h^2 - a^2}} \right]$$

$$- \left[\sqrt{8\Gamma_1 \, \rho_\infty \, \mu_\infty \, L_S \, (v_x^2 + v_h^2)^{\frac{1}{2}}} \; \frac{- v_h^2 \sqrt{8 \, \Gamma_1 \, \rho_\infty \, \mu_\infty \, L_S}}{2 \, (v_x^2 + v_h^2)^{\frac{3}{4}}} \right] \tag{359}$$

$$\frac{\partial F_x}{\partial v_h} = \frac{2 \, a \, \rho_\infty \, L_S \, \alpha}{g_c} \left[\frac{v_h^2 \sqrt{v_x^2 + v_h^2}}{3\sqrt{v_x^2 + v_h^2 - a^2}} \frac{- v_h^2}{\sqrt{v_x^2 + v_h^2 - a^2}\sqrt{v_x^2 + v_h^2}} - \right.$$

$$\left. \frac{\sqrt{v_x^2 + v_h^2}}{\sqrt{v_x^2 + v_h^2 - a^2}} \right] - \left[\sqrt{8\Gamma_1 \, \rho_\infty \, \mu_\infty \, L_S} \; \frac{v_h \, v_x}{2 \, (v_x^2 + v_h^2)^{\frac{3}{4}}} \right] \tag{360}$$

$$\frac{\partial F_h}{\partial v_x} = \frac{2a\rho_\infty \, L_S \alpha}{g_c} \left[\frac{\sqrt{v_x^2 + v_h^2}}{\sqrt{v_x^2 + v_h^2 - a^2}} + \frac{v_x^2}{\sqrt{v_x^2 + v_h^2 - a^2}\sqrt{v_x^2 + v_h^2}} - \frac{v_x^2\sqrt{v_x^2 + v_h^2}}{3\sqrt{v_x^2 + v_h^2 - a^2}} \right]$$

$$- \frac{v_x\, v_h \sqrt{8\, \Gamma_1\, \rho_\infty\, \mu_\infty\, L_S}}{2\,(v_x^2 + v_h^2)^{\frac{3}{4}}} \tag{361}$$

$$\frac{\partial F_x}{\partial \alpha} = - \frac{2\, a\, \rho_\infty\, L_S\, (v_x^2 + v_h^2)^{\frac{1}{2}}\, v_h}{g_c \sqrt{v_x^2 + v_h^2 - a^2}} - \frac{4a\, \rho_\infty\, L_S\, (v_x^2 + v_h^2)^{\frac{1}{2}}\, v_x\, \alpha}{g_c \sqrt{v_x^2 + v_h^2 - a^2}} \tag{362}$$

$$\frac{\partial F_h}{\partial \alpha} = \frac{+ 2a\, \rho_\infty\, L_S\, (v_x^2 + v_h^2)^{\frac{1}{2}}\, v_x}{g_c \sqrt{v_x^2 + v_h^2 - a^2}} - \frac{4a\, \rho_\infty\, L_S\, (v_x^2 + v_h^2)^{\frac{1}{2}}\, v_h\, \alpha}{g_c \sqrt{v_x^2 + v_h^2 - a^2}} . \tag{363}$$

$$\alpha_1 = \frac{m\, g_c\, v_x}{A\, V_m^2} \pm \sqrt{\frac{m^2 g_c^2\, v_x^2}{A^2\, V_m^4} + \left(\frac{V_m^2\, D + v_h\, m\, g_c}{A\, V_m^2}\right)} \tag{364}$$

$$A = \frac{2\, a\, \rho_\infty\, L_S\, V_m}{g_c \sqrt{V_m^2 - a^2}} \tag{365}$$

A flow diagram which indicates the sequence of computed data is shown on Figure 15 which follows. The principal equations are indicated by numbered blocks. The numbers shown correspond to the number of the equation listed in this chapter. All supporting data calculations are indicated in the block labeled subroutine calculations. All given data is indicated in the block labeled given data.

The given data for this flow diagram is

$c_\rho = 0.24$ $\quad \frac{BTo}{lb\text{-}^oR}$

$L_S = 3.00$ ft.

$g_c = 32.2$ $\quad \frac{lb\text{-}ft}{lb_F\ sec^2}$

$\mu_\infty = \mu_\infty\,(T_\infty)$ $\quad$ lb/ft-sec

$D = 2.00$ ft.

T_{wo} = (preassigned)

ϵ = 0.80

σ = 4.80×10^{-13} $\frac{BTU}{sec\text{-}Ft^2\text{-}{}^{o}R^4}$

k = 1.40

R = 53.3 $\frac{ft\text{-}lb_F}{lb\text{-}{}^{o}R}$

m = 8.00 slugs

R_o = 21×10^6 ft.

G = 2.00 $\frac{BTU}{ft^2\text{-}{}^{o}R}$

The final phase of this analytical study is the solving of the system of equations listed in this chapter and in the sequence as indicated on Figure 15 with the aid of a digital computer.

Figure 15. Flow sheet- P 1

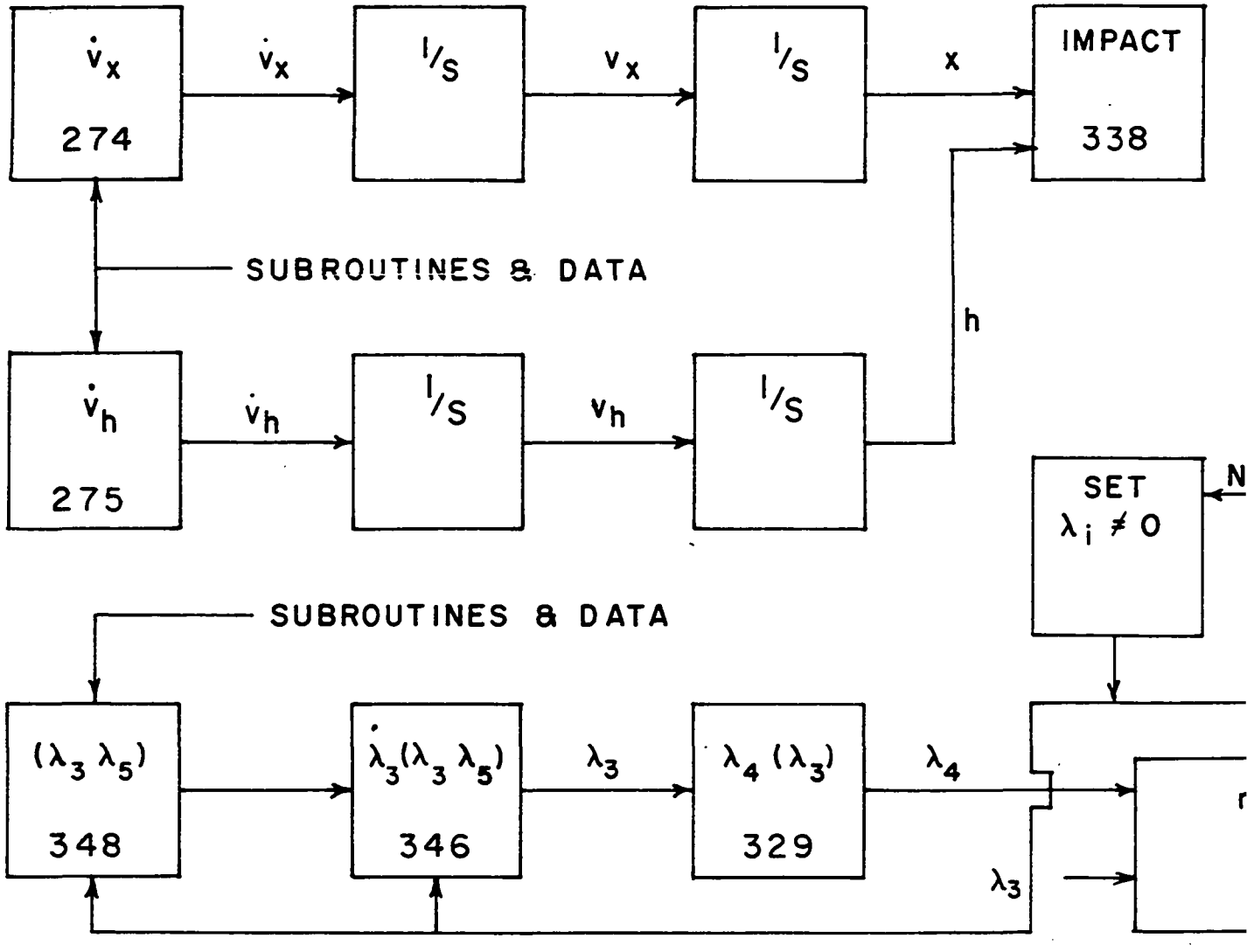
$\dot{v}_x$
274
$\dot{v}_x$
1/S
v_x
1/S
x
IMPACT
338
SUBROUTINES & DATA
h
$\dot{v}_h$
275
$\dot{v}_h$
1/S
v_h
1/S
SET
$\lambda_i \neq 0$
N
SUBROUTINES & DATA
$(\lambda_3\ \lambda_5)$
348
$\dot{\lambda}_3(\lambda_3\ \lambda_5)$
346
λ_3
$\lambda_4\ (\lambda_3)$
329
λ_4
λ_3

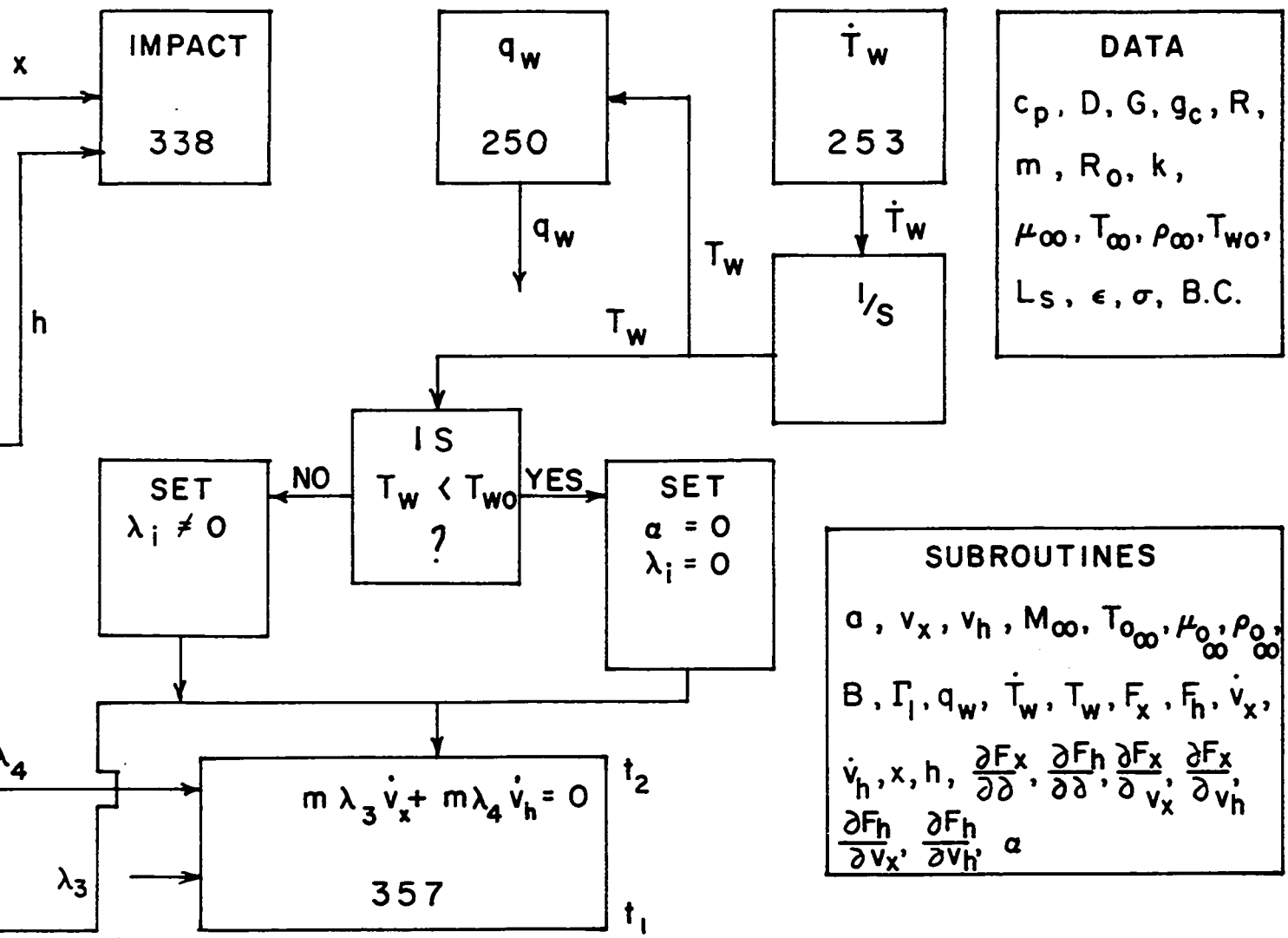
x
IMPACT
338
h
q_w
250
q_w
T_w
$\dot{T}_w$
253
$\dot{T}_w$
T_w
1/S
DATA
c_p, D, G, g_c, R,
m, R_o, k,
μ_∞, T_∞, ρ_∞, T_{wo},
L_s, ϵ, σ, B.C.
IS
$T_w < T_{wo}$
?
NO
YES
SET
$\lambda_i \neq 0$
SET
$\alpha = 0$
$\lambda_i = 0$
SUBROUTINES
a, v_x, v_h, M_∞, T_{o_∞}, μ_{o_∞}, ρ_{o_∞},
B, Γ_1, q_w, $\dot{T}_w$, T_w, F_x, F_h, $\dot{v}_x$,
$\dot{v}_h$, x, h, $\frac{\partial F_x}{\partial \delta}$, $\frac{\partial F_h}{\partial \delta}$, $\frac{\partial F_x}{\partial v_x}$, $\frac{\partial F_x}{\partial v_h}$,
$\frac{\partial F_h}{\partial v_x}$, $\frac{\partial F_h}{\partial v_h}$, α
λ_4
λ_3
$m\lambda_3\dot{v}_x + m\lambda_4\dot{v}_h = 0$
357
t_2
t_1

CONCLUSIONS

Figures 16 through 26, which follow this chapter, represent the results obtained from the solving of the system of equations listed in the preceding chapter and in the sequence indicated by the flow sheet, Figure 15. These equations were solved with the aid of an IBM-7074 digital computer.

A qualitative analysis of the results obtained is now in order. Figure 16 is a plot of the calculated data in which the angle of attack, α, which serves as an equivalent lift or reverse thrust parameter, was held at zero. Holding the angle of attack, α, equal to zero results in a ballistic trajectory. The initial conditions for this reentry flight were reentry at an altitude of 300,000 feet with a horizontal reentry velocity of 10,000 feet per second and a nose cone surface temperature of $300^{\circ}R$. The maximum temperature which the nose cone surface attained was $6626^{\circ}R$ and the maximum down range was approximately 240 miles. The time of descent was 199 seconds.

Figures 17 through 21 are plots of the calculated data for reentry flights in which the reentry altitude was 300,000 feet, the reentry velocity was 10,000 feet per second, the initial nose cone surface temperature was $300^{\circ}R$ and the trajectory was subjected to a heating constraint. During the initial phase of these reentry flights the angle of attack, α, was set equal to zero. At the instant that the nose cone surface temperature reached a preassigned value, T_{wo}, the Lagrange multipliers served to generate an angle of attack, α, such that a heating constrained trajectory resulted. The preassigned values for T_{wo} are indicated on the

figures as well as the maximum value of the angle of attack at the instant of constraint. After constraint bec›me effective there was an overshoot of approximately 400°R for all preassigned values of T_{wo}. The variation in the value of the angle of attack is indicated after the system stabilized at the indicated T_{wo} (max). The time of descent is also indicated for each reentry flight. Note that the maximum angle of attack and steepest descent are associated with the smaller values of the preassigned nose cone surface temperature, T_{wo}. Figure 21 is a plot of the maximum value of α versus the preassigned value of T_{wo}.

Figures 22 through 26 are plots of the calculated data for reentry flight in which the reentry altitude was 300,000 feet, the reentry velocity was 7500 feet per second, the initial nose cone temperature was 300°R and the trajectory was subjected to a heating constraint. These figures list the same data as the figures for the reentry velocity trajectories of 10,000 feet per second, however, the trajectories are considerably different as the figures indicate. The reentry velocity trajectories of 7500 feet per second do not indicate a steep descent at the instant that the heating constraint becomes effective, the maximum angle of attack at the instant of heating constraint is much less and the down range is greater as compared with the reentry velocity of 10,000 feet per second. After constraint bec›me effective there was an overshoot of approximately 400°R for all preassigned values of T_{wo} as was the case for the reentry velocity of 10,000 feet per second. Figure 26 is a plot of the maximum value of α versus the preassigned value of T_{wo}.

Figures 21 and 26 are important in that the angle of attack, α, is also indicative of the violent braking action or deceleration required at

the instant that the heating constraint becomes effective.

An explanation of the overshoot of approximately 400°R for all preassigned values of T_{wo} and for both values of reentry velocity is in order. The overshoot is due to a traceable error which was introduced in the formulation of Equation 345 for V_m. V_m is the velocity which corresponds to the equivalent Mach number which satisfies Equation 250 when $T_w = T_{wo}$. The stagnation viscosity, stagnation density, and stagnation temperature in this equation are also functions of the Mach number. All of these functions have the form of Equations 152, 339, and 340. In order to derive a "working" expression for the velocity V_m, the one (1) in all the expressions of the form of Equations 152, 339, and 340 was dropped. This is not unrealistic since all the reentry velocities correspond to high Mach numbers, i.e., hypersonic speeds.

An explanation of the difference between the shape of the trajectories for the reentry velocities of 10,000 feet per second and 7500 feet per second is in order. A steeper descent is indicated during the initial constraint period in the case of the reentry velocity runs for 10000 feet per second as compared with the 7500 feet per second runs for all preassigned values of T_{wo}. Figures 21 and 26 are plots of the equivalent angle of attack at the instant of constraint versus the preassigned values of T_{wo} for the velocities indicated. The trajectory plots and Figures 21 and 26 indicate that, for a given reentry velocity, as the preassigned value for T_{wo} increases that the equivalent braking action, which is required at the instant of constraint, decreases. This is due to the fact that the vehicle's speed must be reduced if heating constraint at the preassigned value of T_{wo} is to be accomplished. The trajectory plots also

indicate that the more severe the equivalent braking action at the instant of constraint, the smaller the down range even though the reentry velocity may be higher than those case with less severe equivalent braking action.

The results of this study, which the calculated data and the plotted data confirm, are:

a. The Lagrange multipliers do generate an equivalent lift or reverse thrust program which will "fly" and "hold" the reentry vehicle on a heating constrained trajectory.

b. It is obvious that the calculated and plotted data that the factors which control down range, for a given reentry height are the initial values for the reentry velocity, nose cone surface temperature, and the preassigned value of T_{wo}.

c. The "overshoot" on the preassigned value for T_{wo} can be eliminated by reducing the error in the equation for V_m.

d. The severe braking action required at the instant of heating constraint can be reduced by reducing the space vehicle's velocity prior to reentry by the use of retrograde rockets. The strain on the space vehicle would be less during retrograde firing than during heating constraint braking.

e. Any reduction in the severity of the equivalent braking action at the instant that the heating constraint becomes effective improves the down range for a preassigned T_{wo}.

The further extension of this investigation is now limited to reducing the "overshoot" mentioned in (c) and the severity of the equivalent braking action mentioned in (e). This can be done by generating a numerical technique for solving the exact equation for V_m with the

aid of a computer, and the severity of the equivalent braking action can be reduced by additional computer runs with more compatiable pre-assigned values for the reentry velocity and T_{wo}.

Figure 16. Altitude and nose cone surface temperature versus range

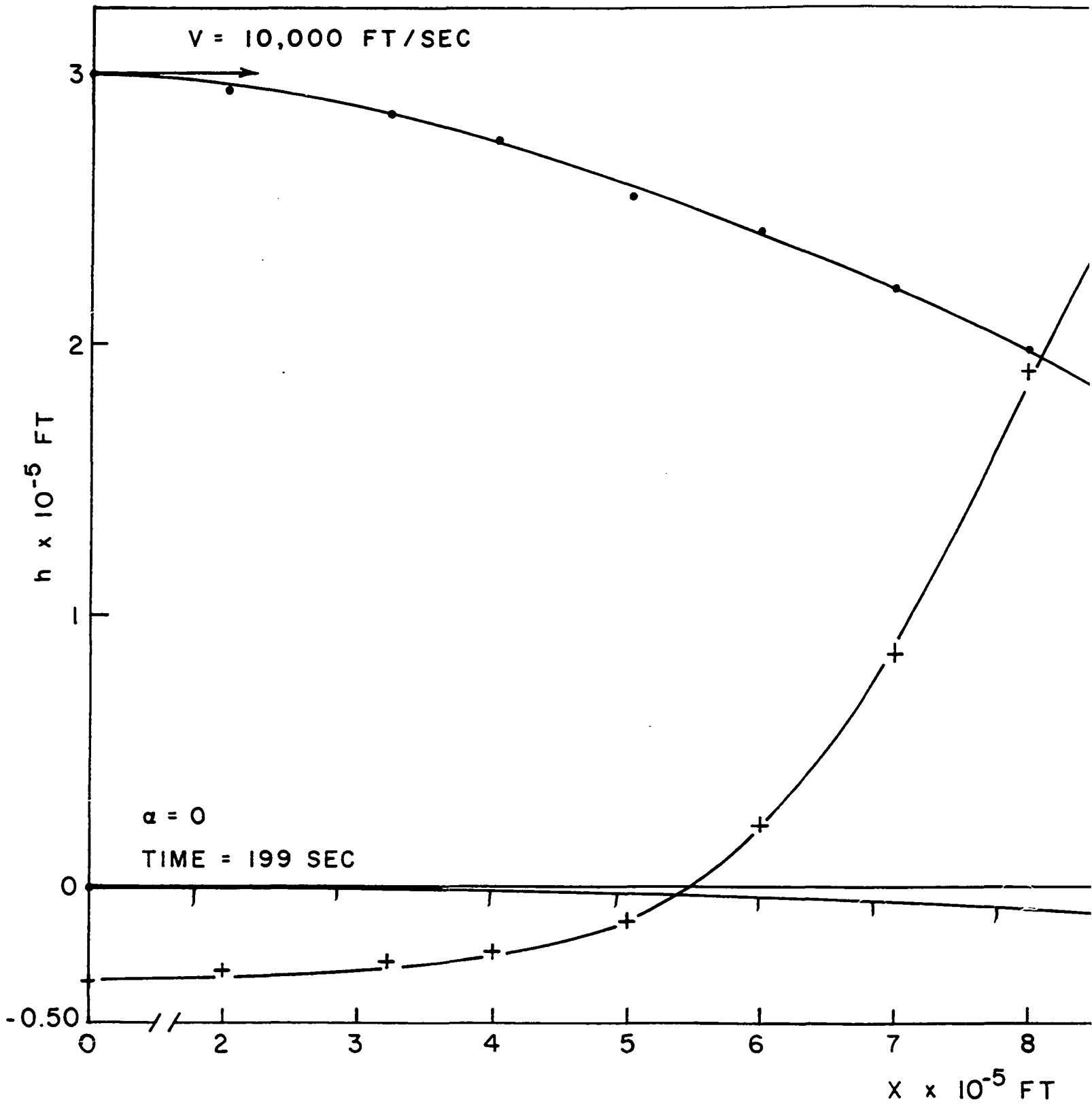
V = 10,000 FT/SEC
3
2
1
0
-0.50
h x 10^-5 FT
α = 0
TIME = 199 SEC
0
2
3
4
5
6
7
8
X x 10^-5 FT

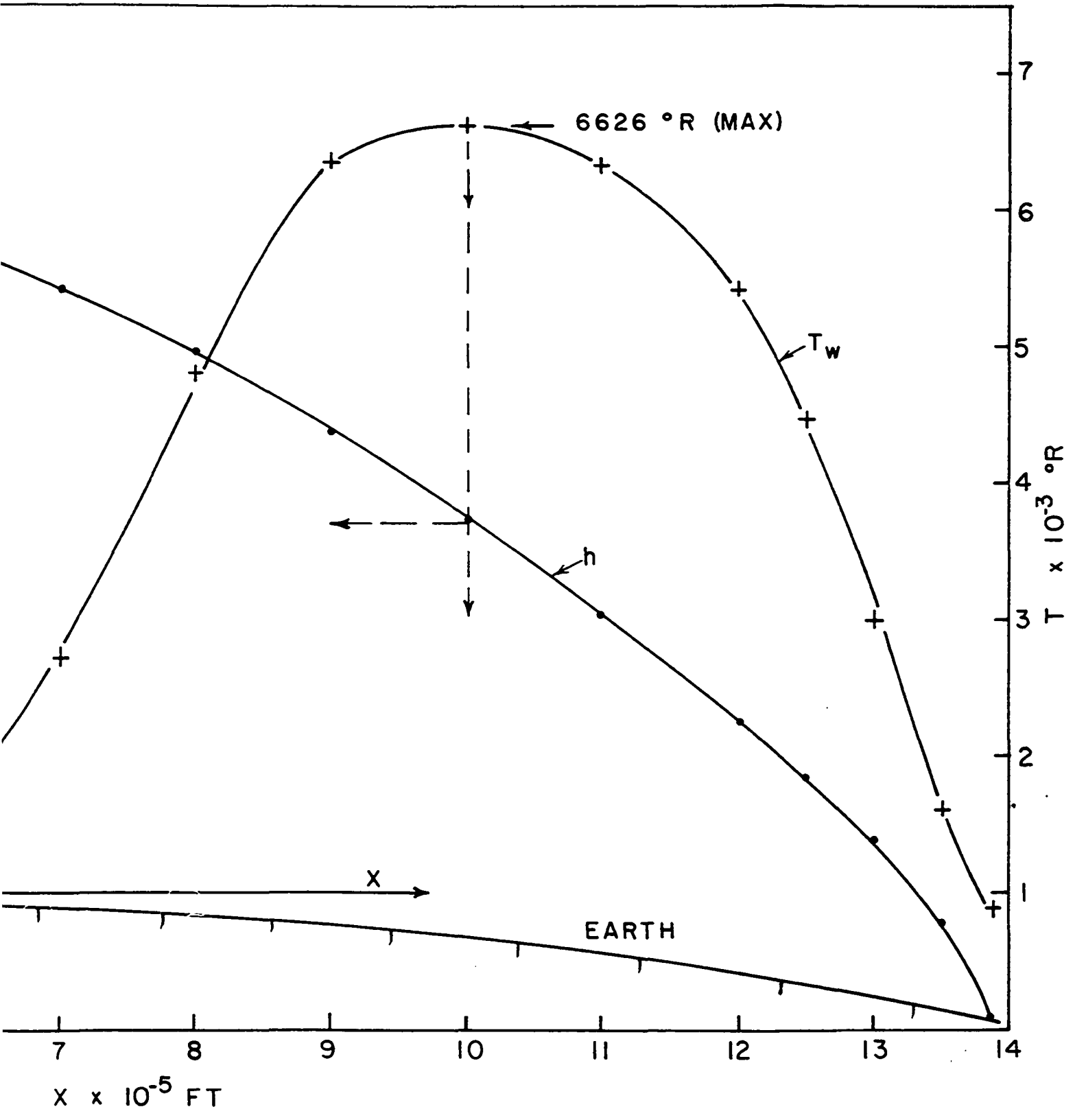
6626 °R (MAX)
T_w
h
X
EARTH
7
8
9
10
11
12
13
14
X x 10^{-5} FT
1
2
3
4
5
6
7
T x 10^{-3} °R

Figure 17. Altitude and nose cone surface temperature versus range

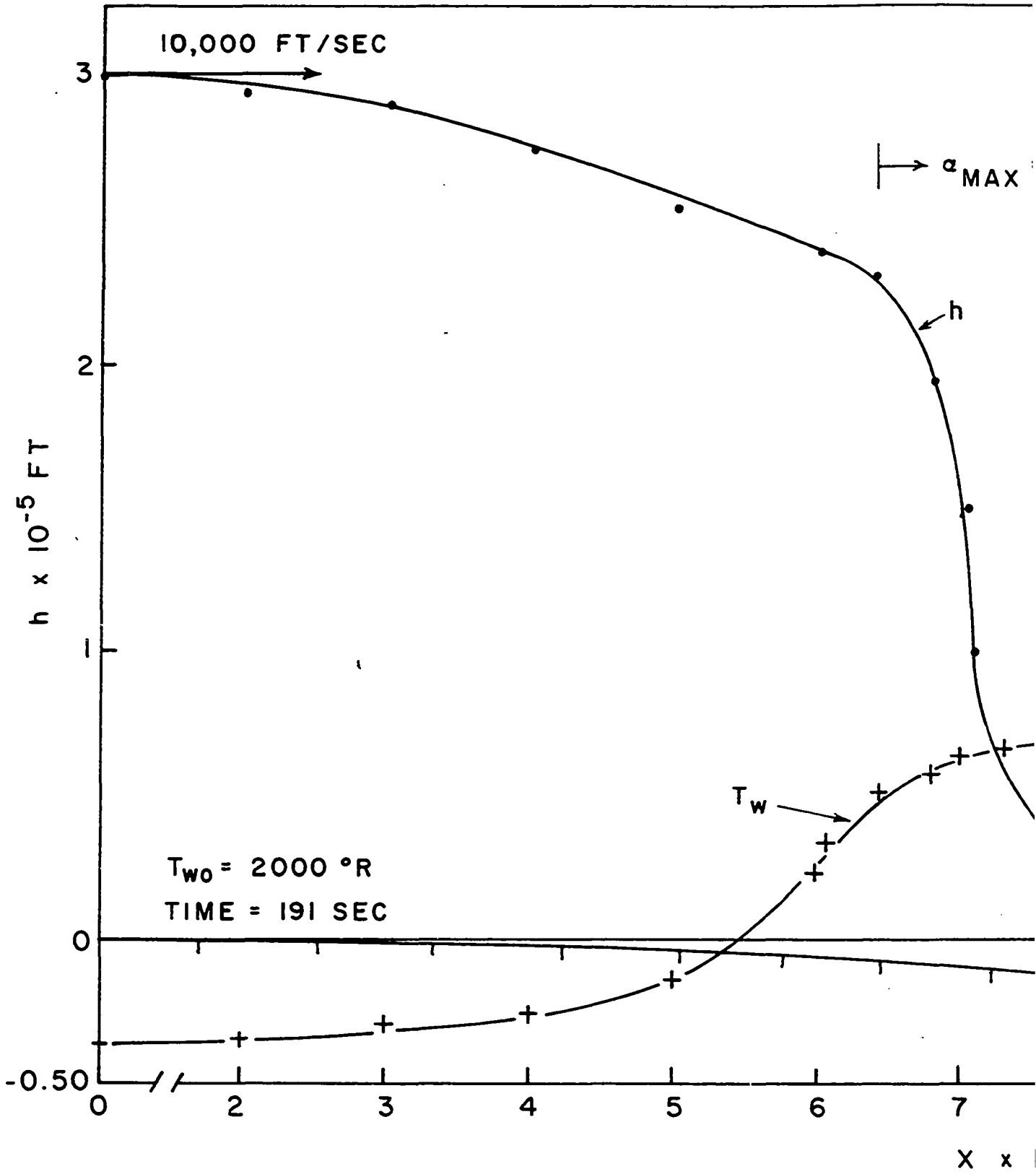
10,000 FT/SEC
α_{MAX}
h
T_W
T_{WO} = 2000 °R
TIME = 191 SEC
h x 10^{-5} FT
3
2
1
0
-0.50
0
2
3
4
5
6
7
X x

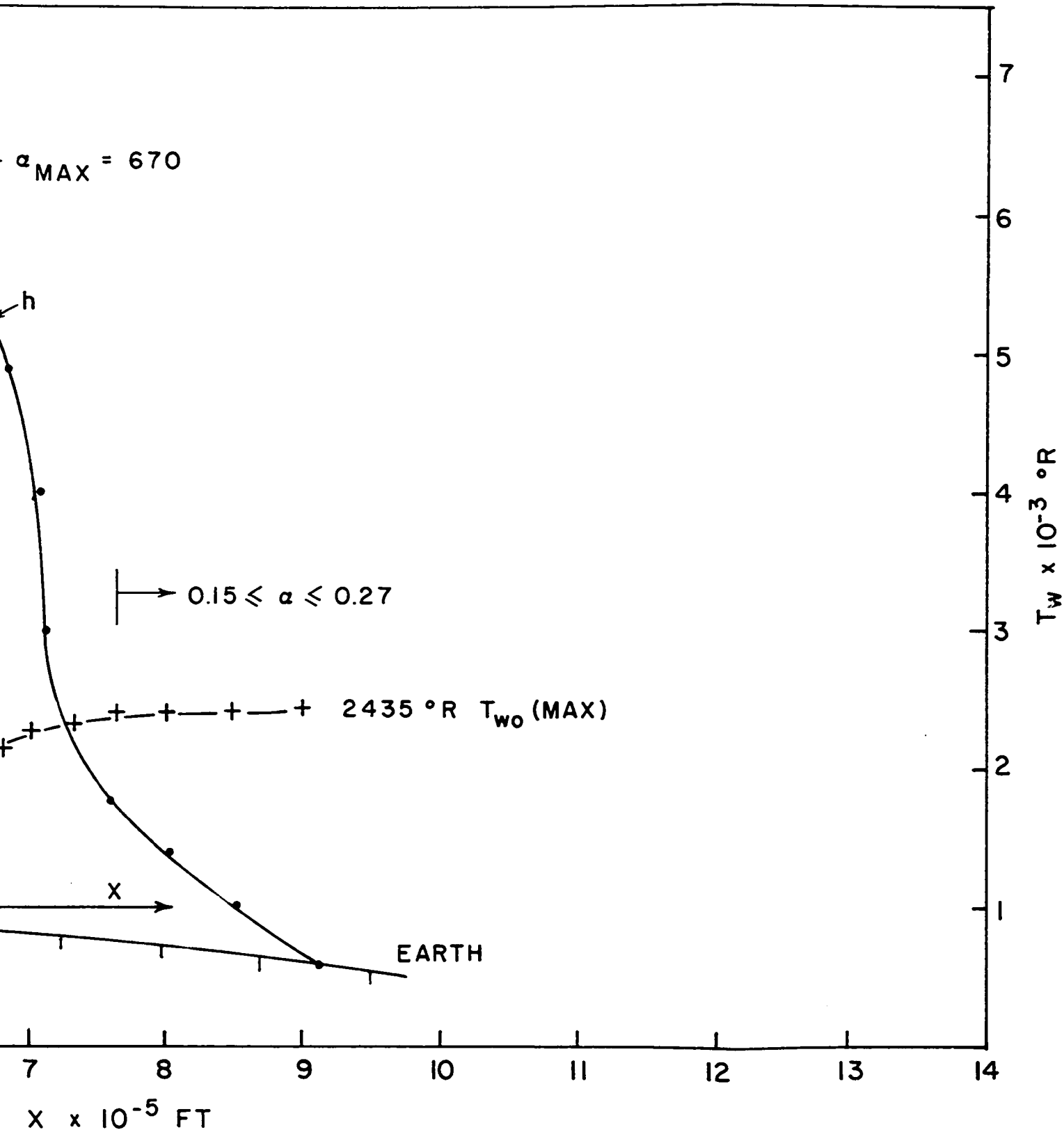
α_{MAX} = 670
h
0.15 ≤ α ≤ 0.27
2435 °R T_{wo} (MAX)
X
EARTH
7
8
9
10
11
12
13
14
X x 10^{-5} FT
1
2
3
4
5
6
7
T_w x 10^{-3} °R

Figure 18. Altitude and nose cone surface temperature versus range

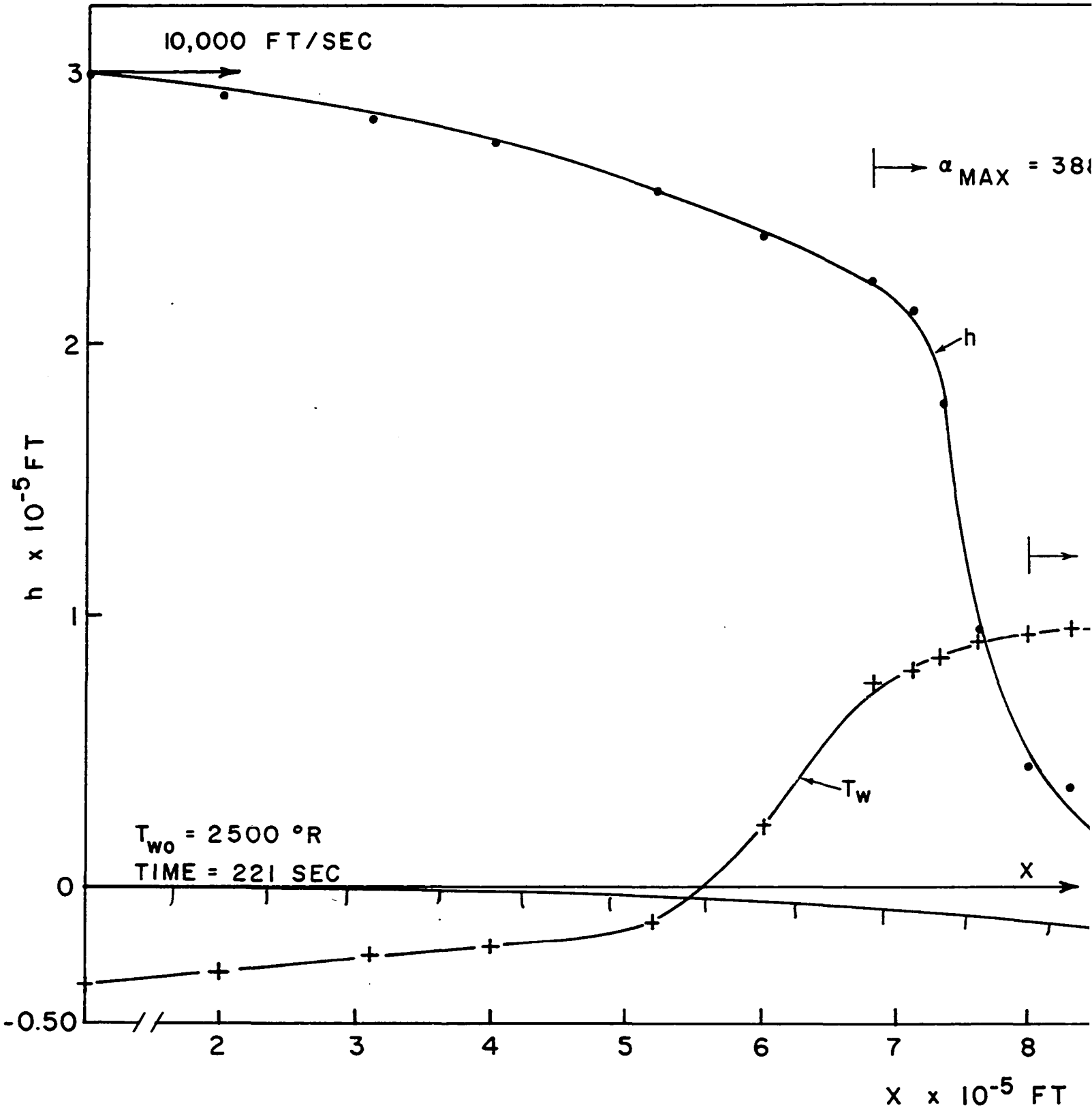
10,000 FT/SEC
α_{MAX} = 38
h
T_w
T_{wo} = 2500 °R
TIME = 221 SEC
X
h x 10^{-5} FT
X x 10^{-5} FT
3
2
1
0
-0.50
2
3
4
5
6
7
8

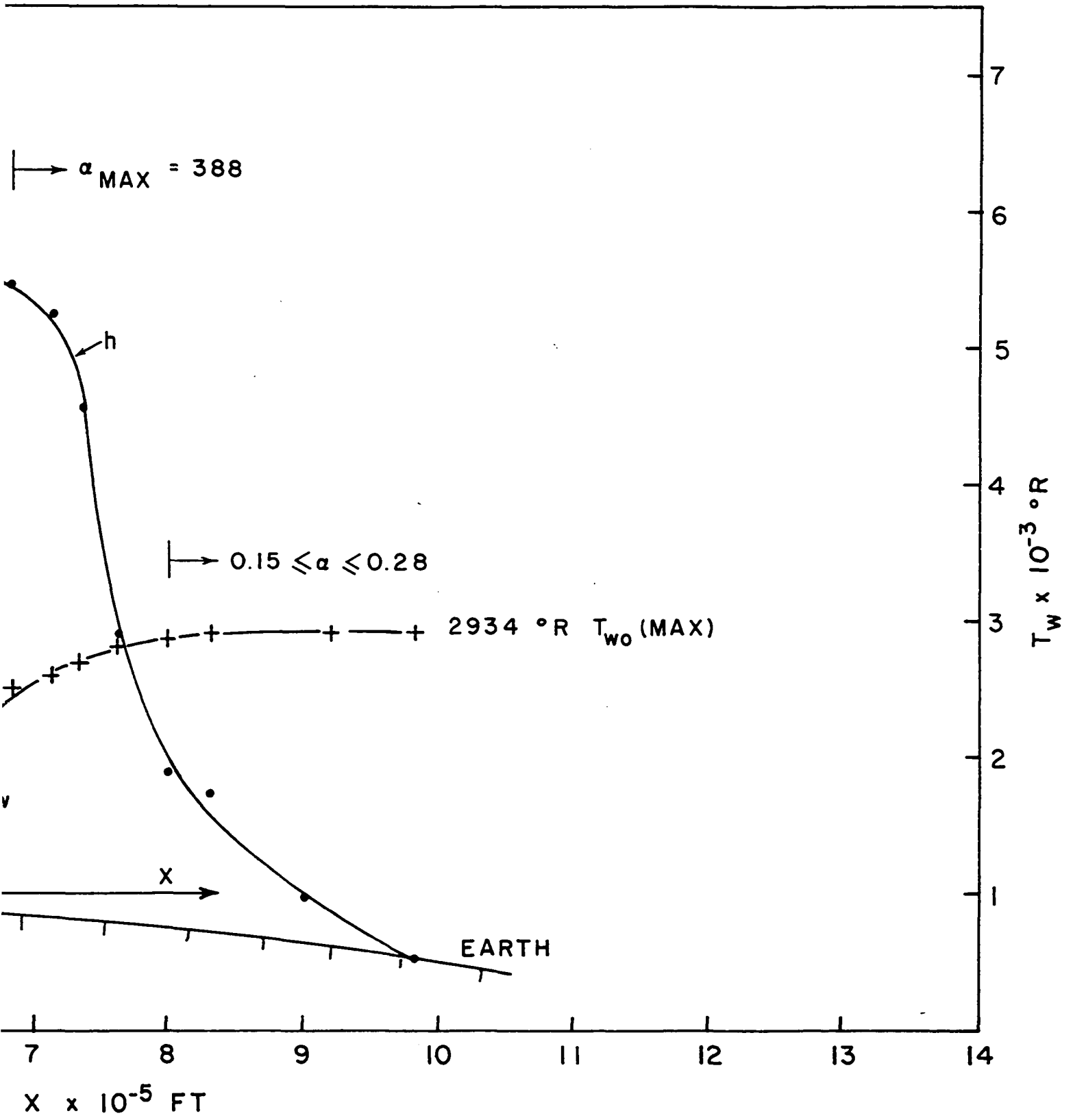
α MAX = 388
h
0.15 ≤ α ≤ 0.28
2934 °R Two (MAX)
X
EARTH
7
8
9
10
11
12
13
14
X x 10-5 FT
1
2
3
4
5
6
7
Tw x 10-3 °R

Figure 19. Altitude and nose cone surface temperature versus range

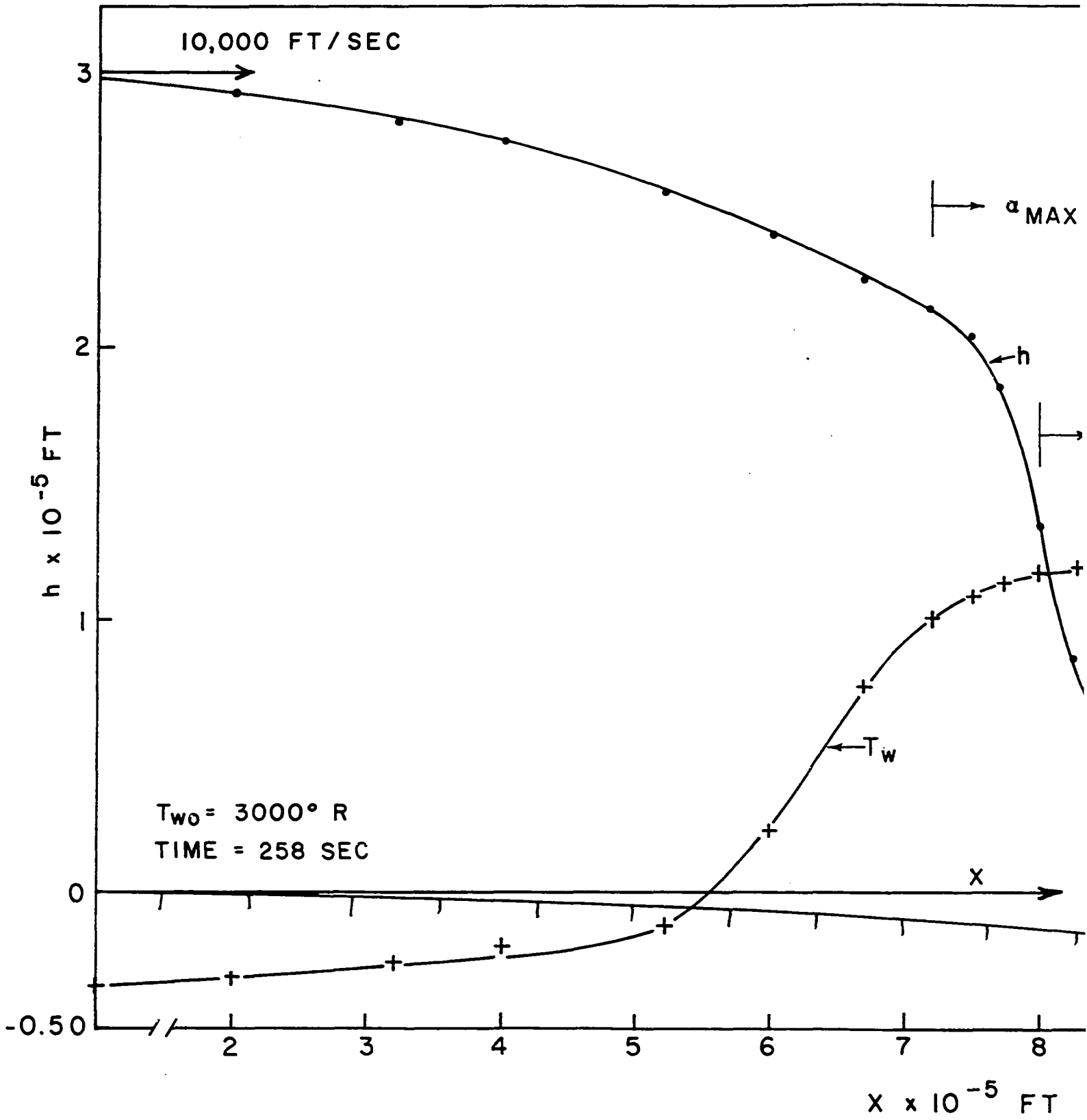
10,000 FT/SEC
α_{MAX}
h
T_w
T_{wo} = 3000° R
TIME = 258 SEC
X
h x 10^{-5} FT
X x 10^{-5} FT
3
2
1
0
-0.50
2
3
4
5
6
7
8

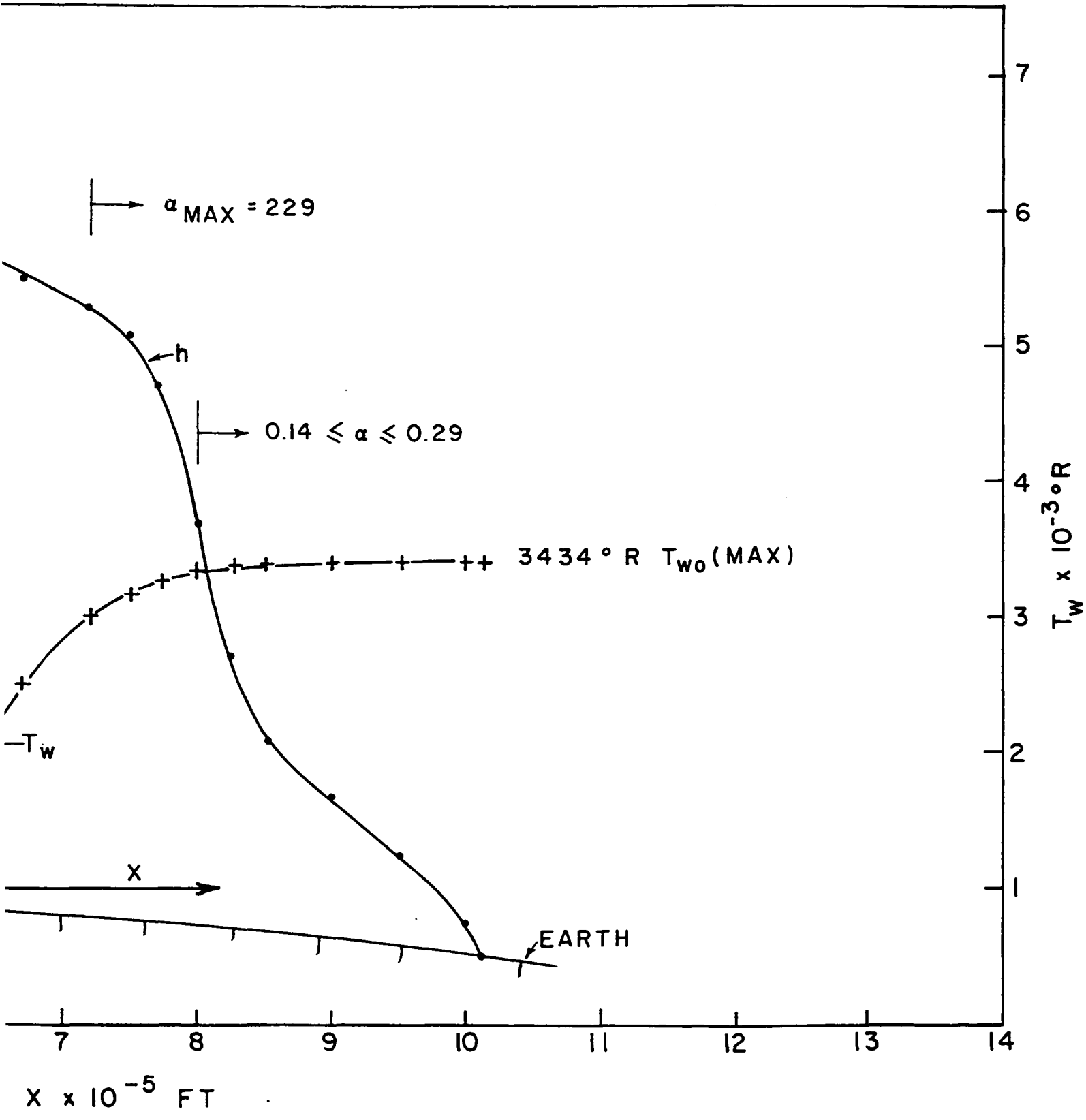
$\alpha_{MAX} = 229$
h
$0.14 \leqslant \alpha \leqslant 0.29$
3434° R T_{wo}(MAX)
T_w
X
EARTH
7
8
9
10
11
12
13
14
X x 10^{-5} FT
7
6
5
4
3
2
1
T_w x 10^{-3}°R

Figure 20. Altitude and nose cone surface temperature versus range

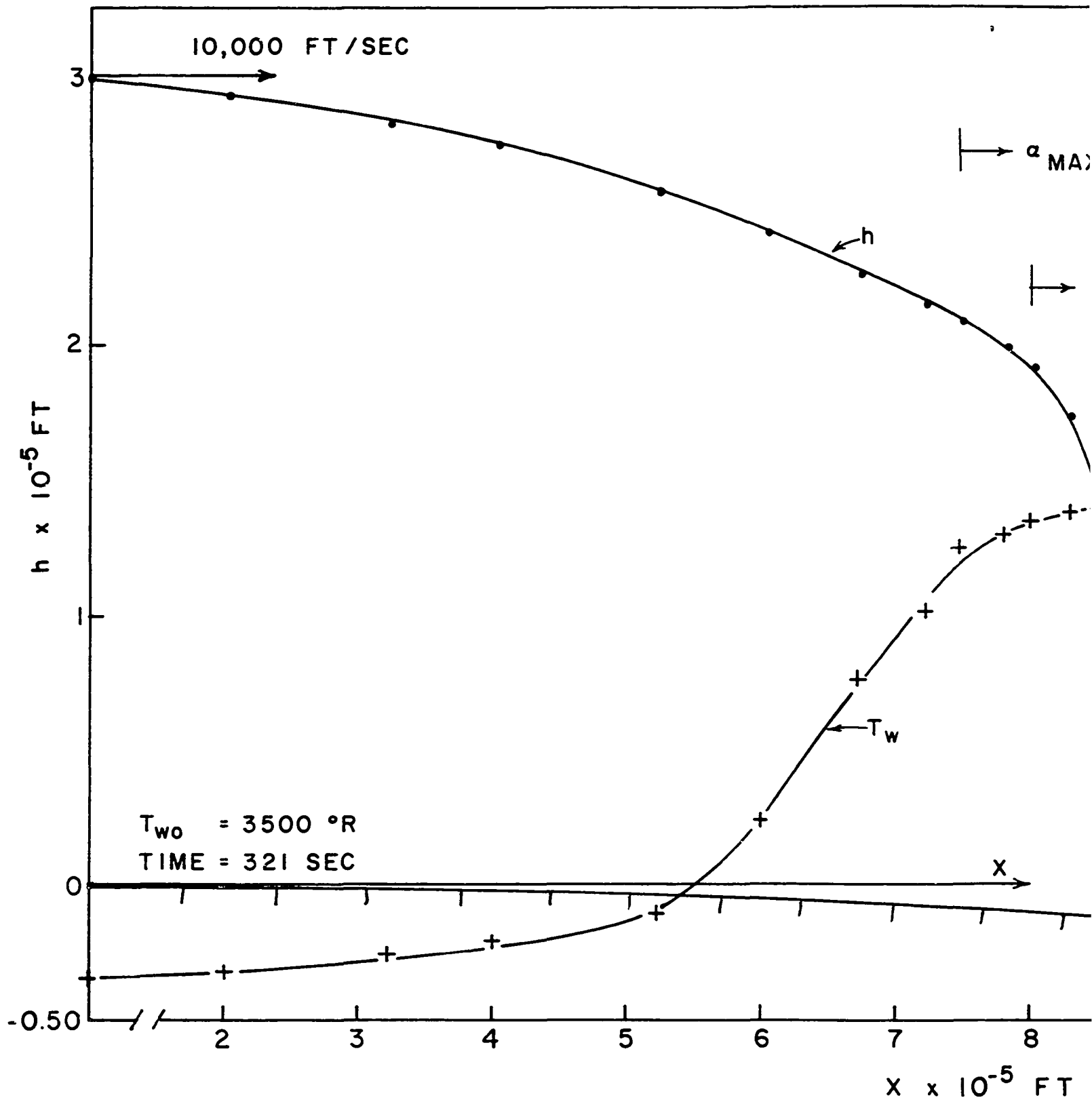
10,000 FT/SEC
α MAX
h
T_w
T_{wo} = 3500 °R
TIME = 321 SEC
X
h x 10^{-5} FT
X x 10^{-5} FT
3
2
1
0
-0.50
2
3
4
5
6
7
8

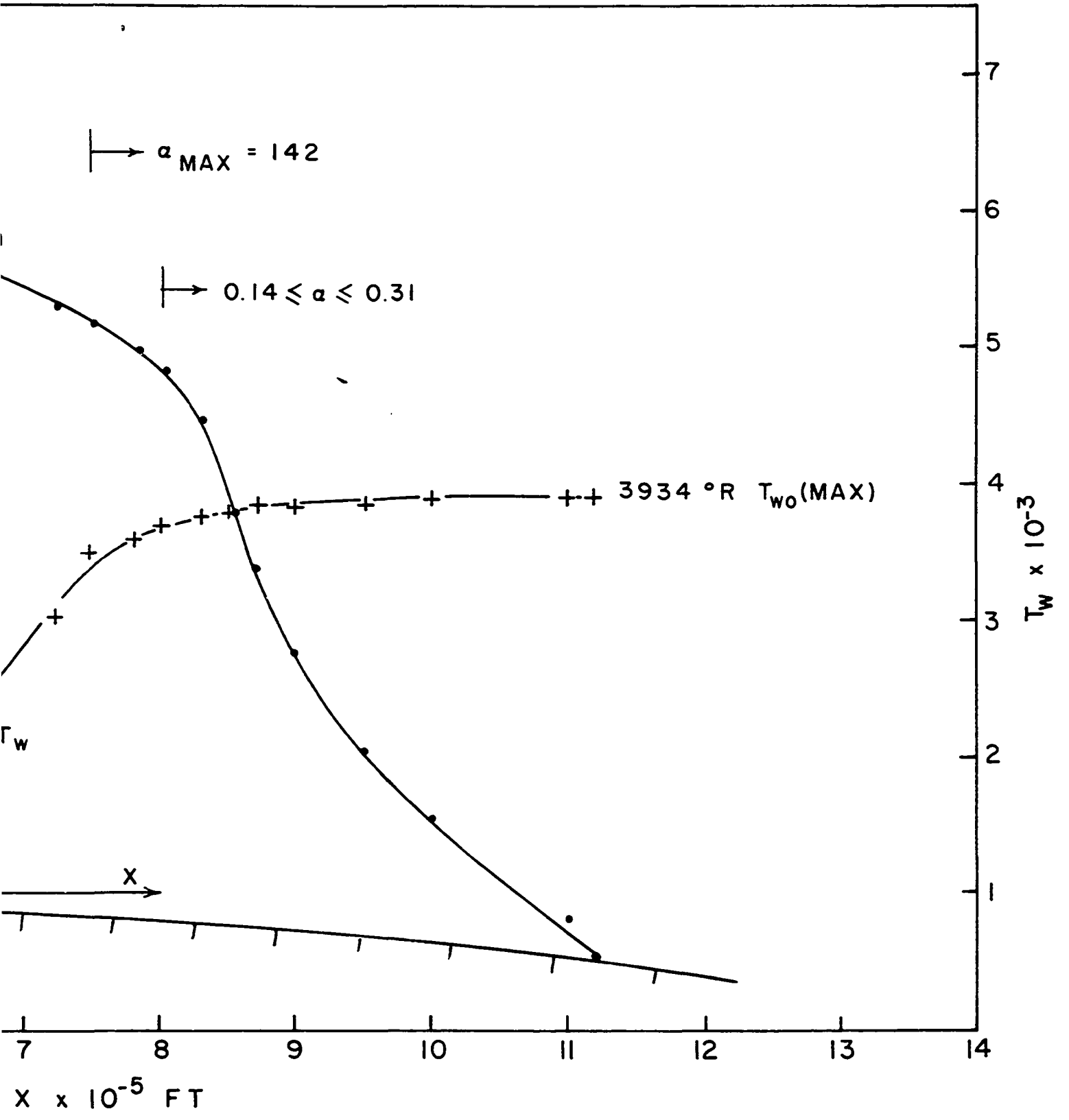
$\alpha_{MAX} = 142$
$0.14 \leq \alpha \leq 0.31$
3934 °R $T_{WO}(MAX)$
T_W
X
7
8
9
10
11
12
13
14
X x 10^{-5} FT
1
2
3
4
5
6
7
T_W x 10^{-3}

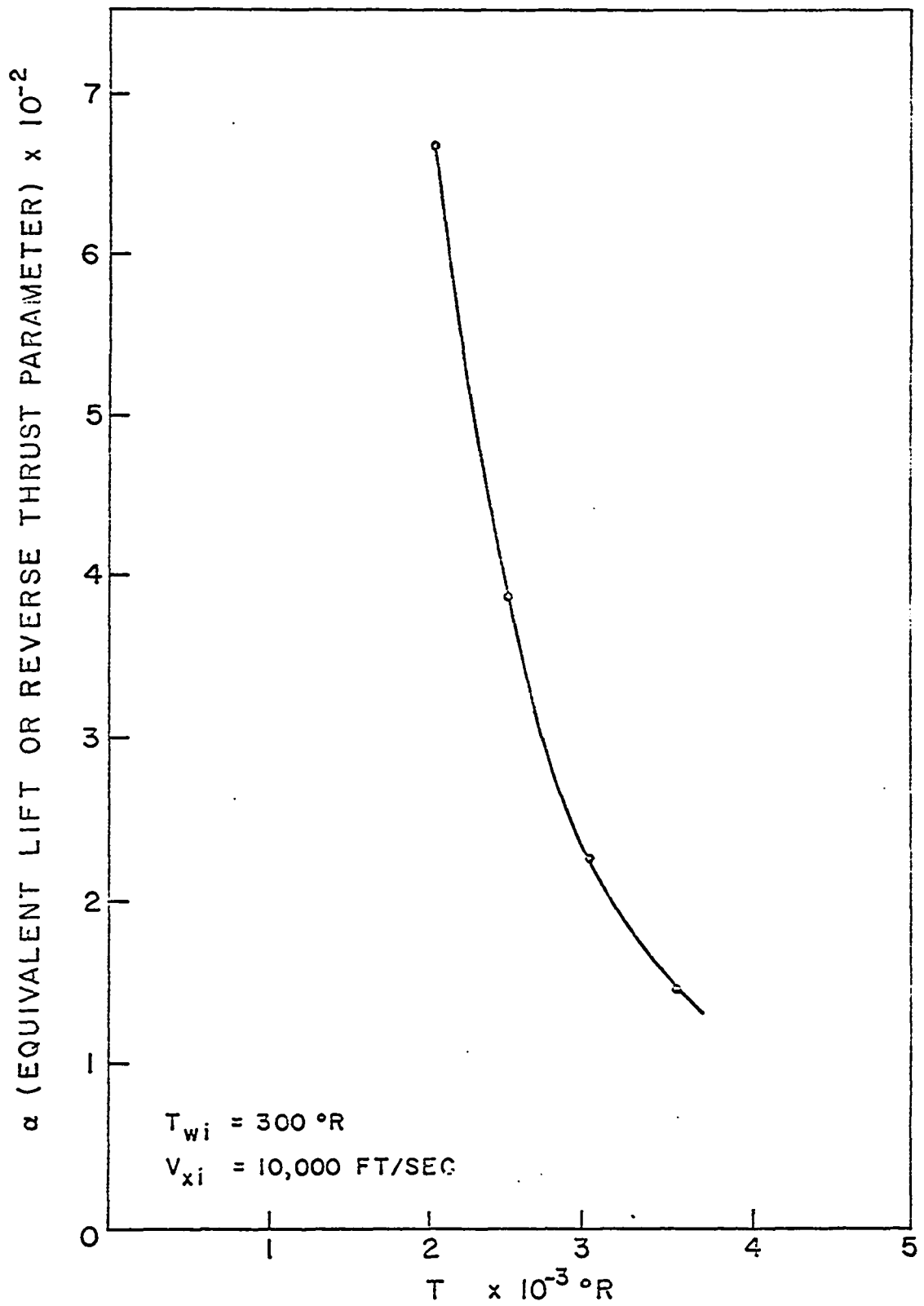

Figure 21. α versus preassigned T_{wo}

Figure 22. Altitude and nose cone surface temperature versus range

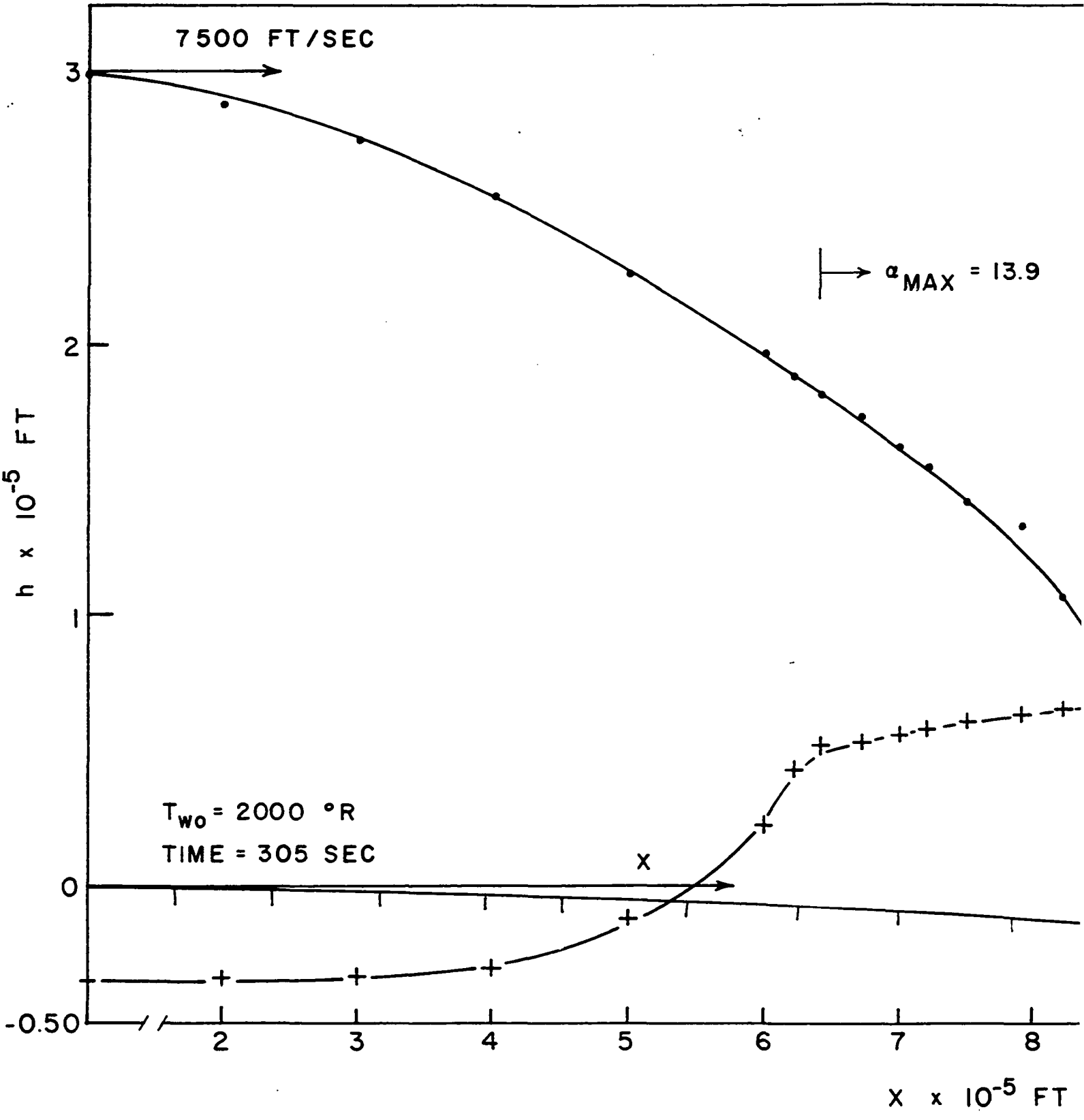
7500 FT/SEC
α_{MAX} = 13.9
T_{wo} = 2000 °R
TIME = 305 SEC
X
h x 10^{-5} FT
X x 10^{-5} FT
3
2
1
0
-0.50
2
3
4
5
6
7
8

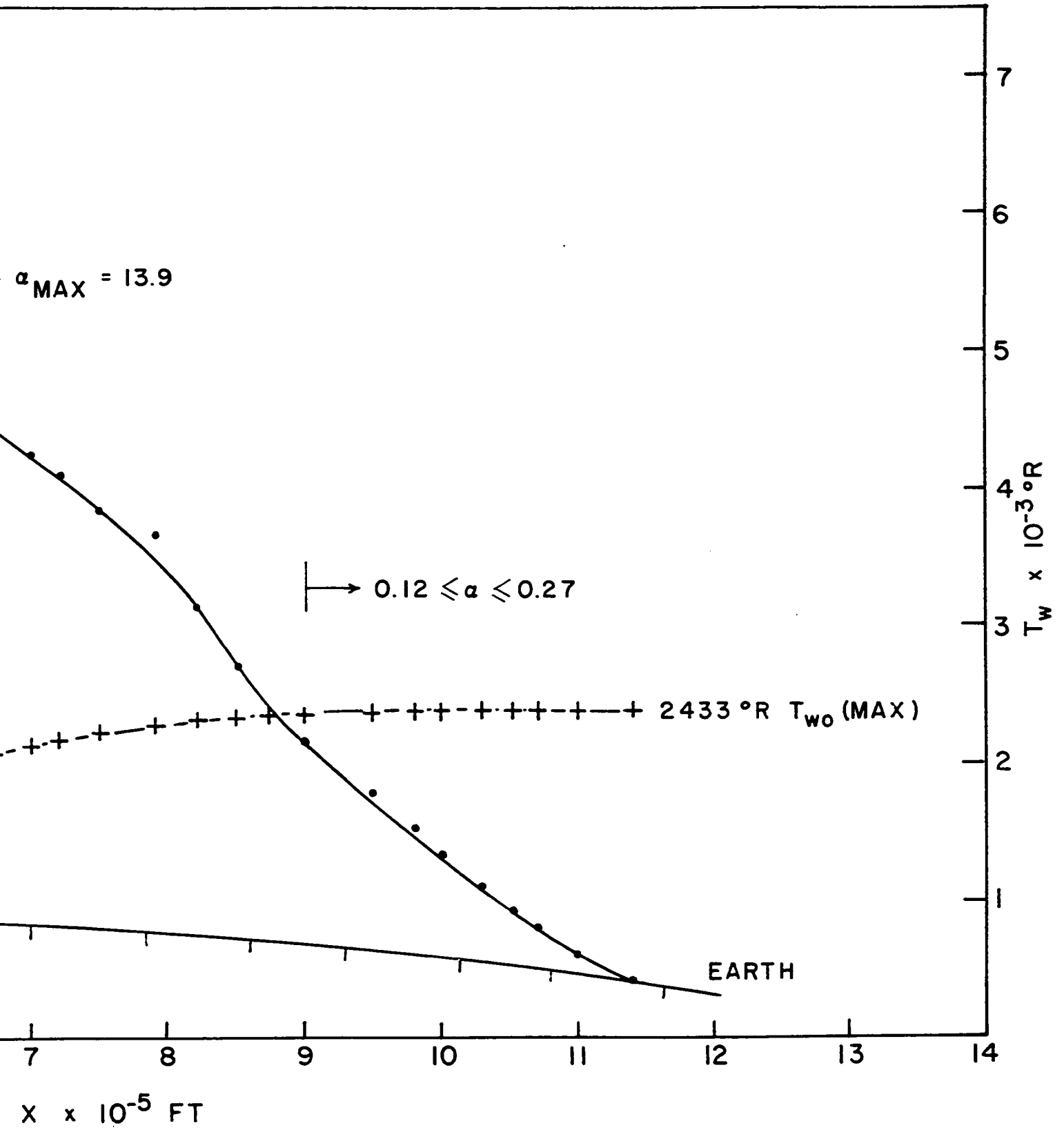
α_{MAX} = 13.9
0.12 ≤ α ≤ 0.27
2433 °R T_{wo} (MAX)
EARTH
7
8
9
10
11
12
13
14
X x 10^{-5} FT
1
2
3
4
5
6
7
T_w x 10^{-3} °R

Figure 23. Altitude and nose cone surface temperature versus range

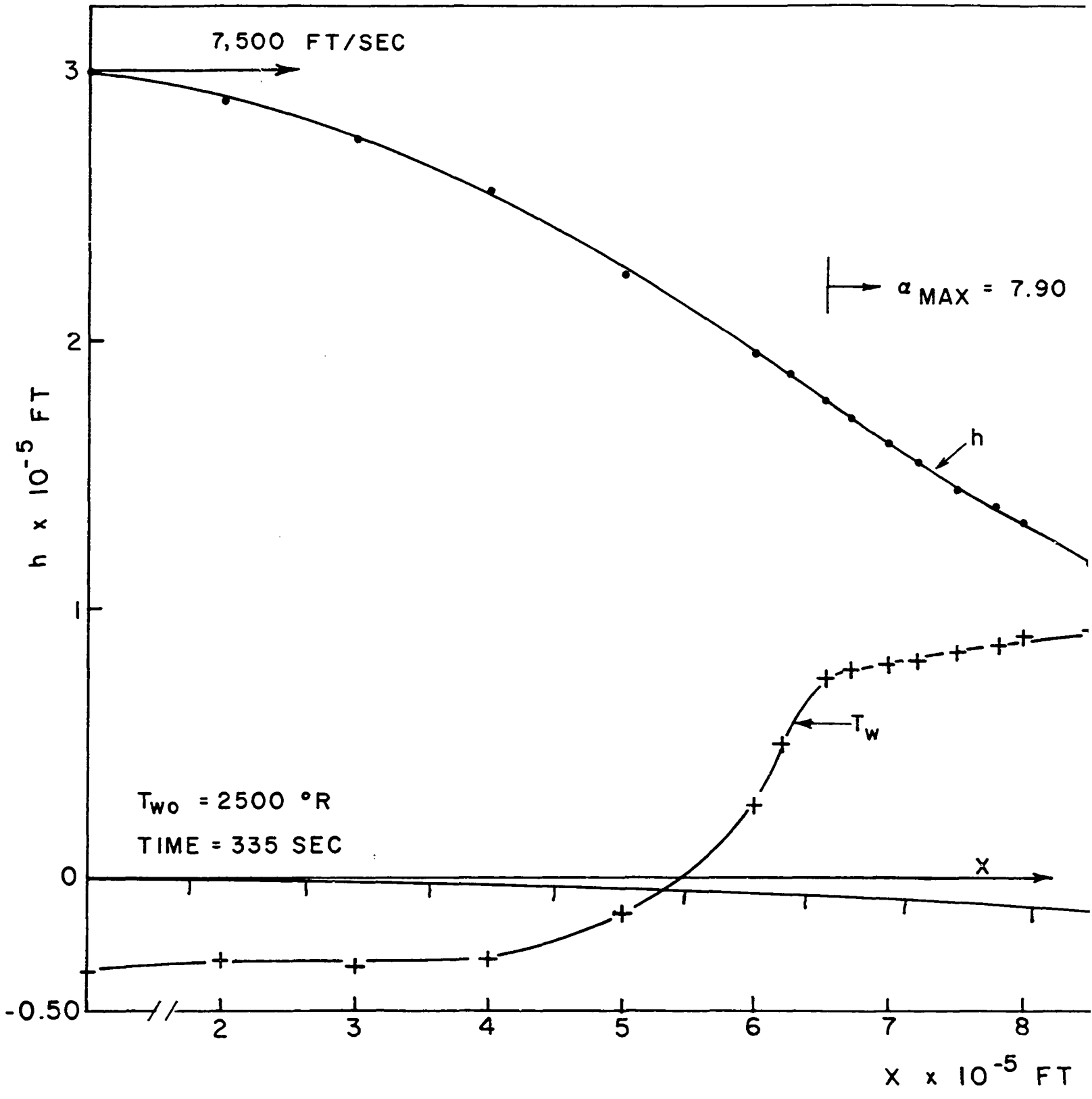
7,500 FT/SEC
α_{MAX} = 7.90
h
T_w
T_{wo} = 2500 °R
TIME = 335 SEC
X
h x 10^{-5} FT
X x 10^{-5} FT
3
2
1
0
-0.50
2
3
4
5
6
7
8

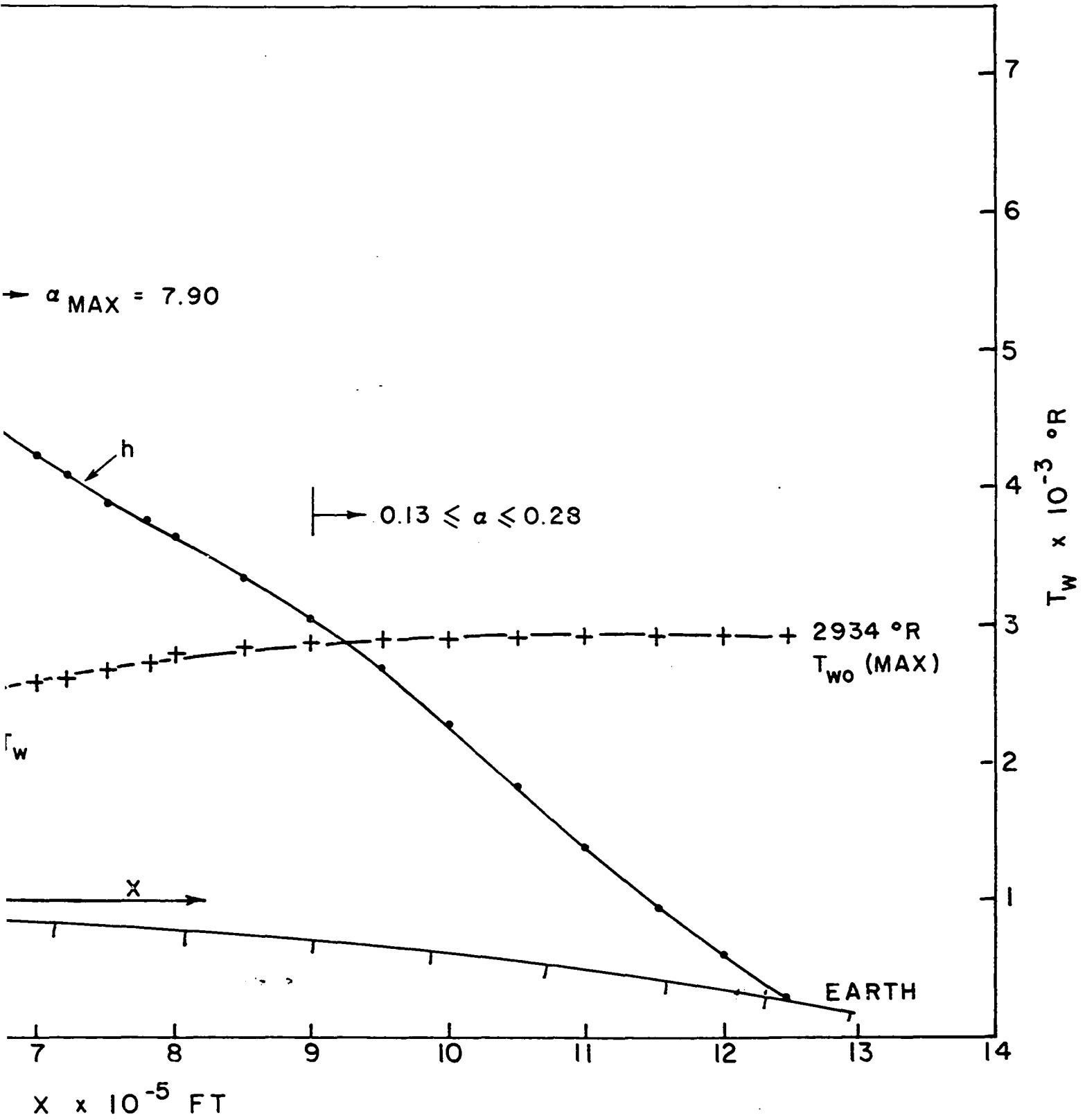
α MAX = 7.90
h
0.13 ≤ α ≤ 0.28
2934 °R
Tw0 (MAX)
Tw
X
EARTH
7
8
9
10
11
12
13
14
X x 10-5 FT
1
2
3
4
5
6
7
Tw x 10-3 °R

Figure 24. Altitude and nose cone surface temperature versus range

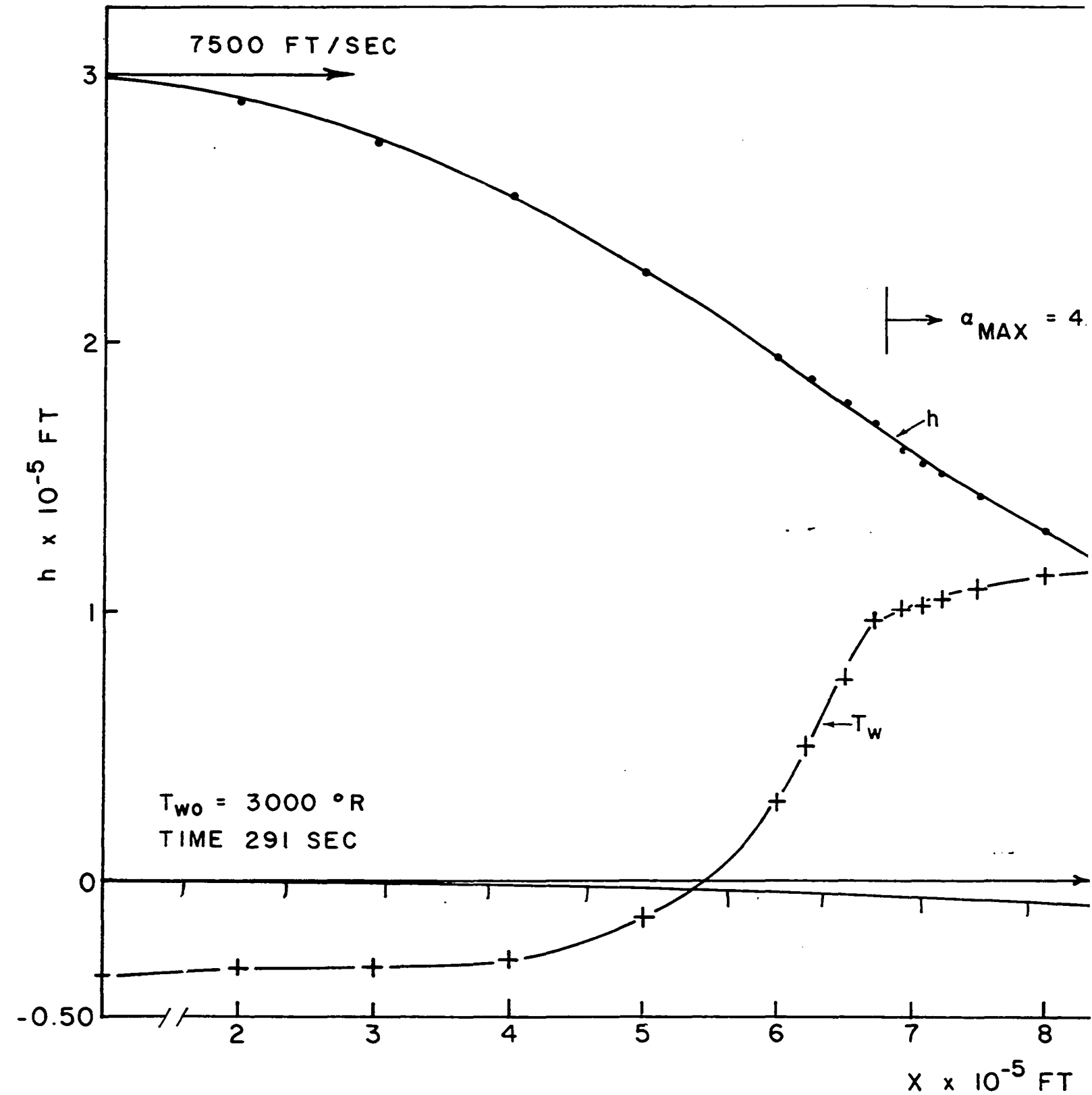
7500 FT/SEC
3
2
1
0
-0.50
h x 10^-5 FT
α MAX = 4
h
Tw
Two = 3000 °R
TIME 291 SEC
2
3
4
5
6
7
8
X x 10^-5 FT

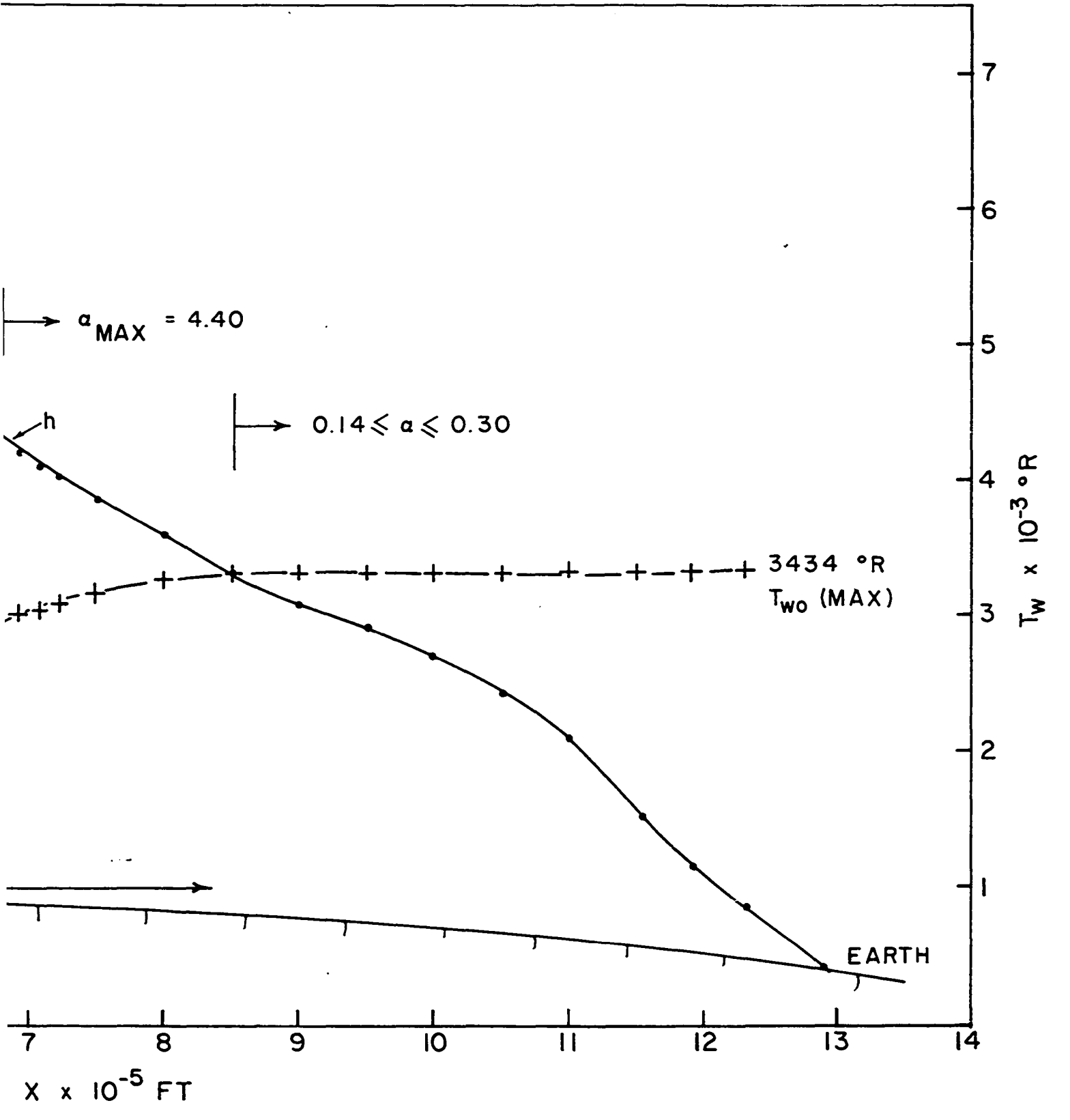
α_{MAX} = 4.40
h
0.14 ≤ α ≤ 0.30
3434 °R
T_{wo} (MAX)
EARTH
7
8
9
10
11
12
13
14
X x 10^{-5} FT
1
2
3
4
5
6
7
T_w x 10^{-3} °R

Figure 25. Altitude and nose cone surface temperature versus range

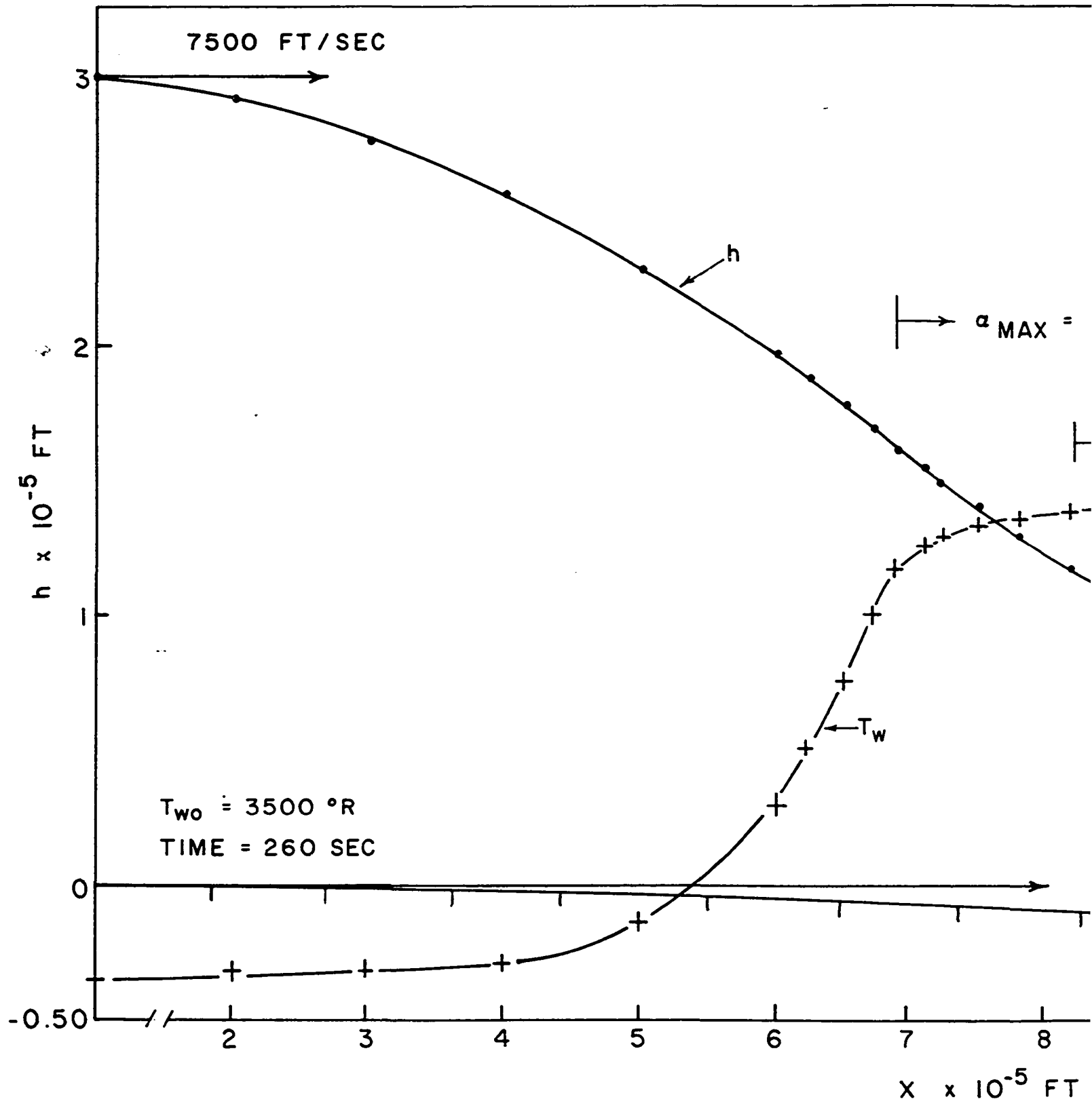
7500 FT/SEC
h
α_{MAX} =
T_W
T_{WO} = 3500 °R
TIME = 260 SEC
h x 10^{-5} FT
X x 10^{-5} FT
3
2
1
0
-0.50
2
3
4
5
6
7
8

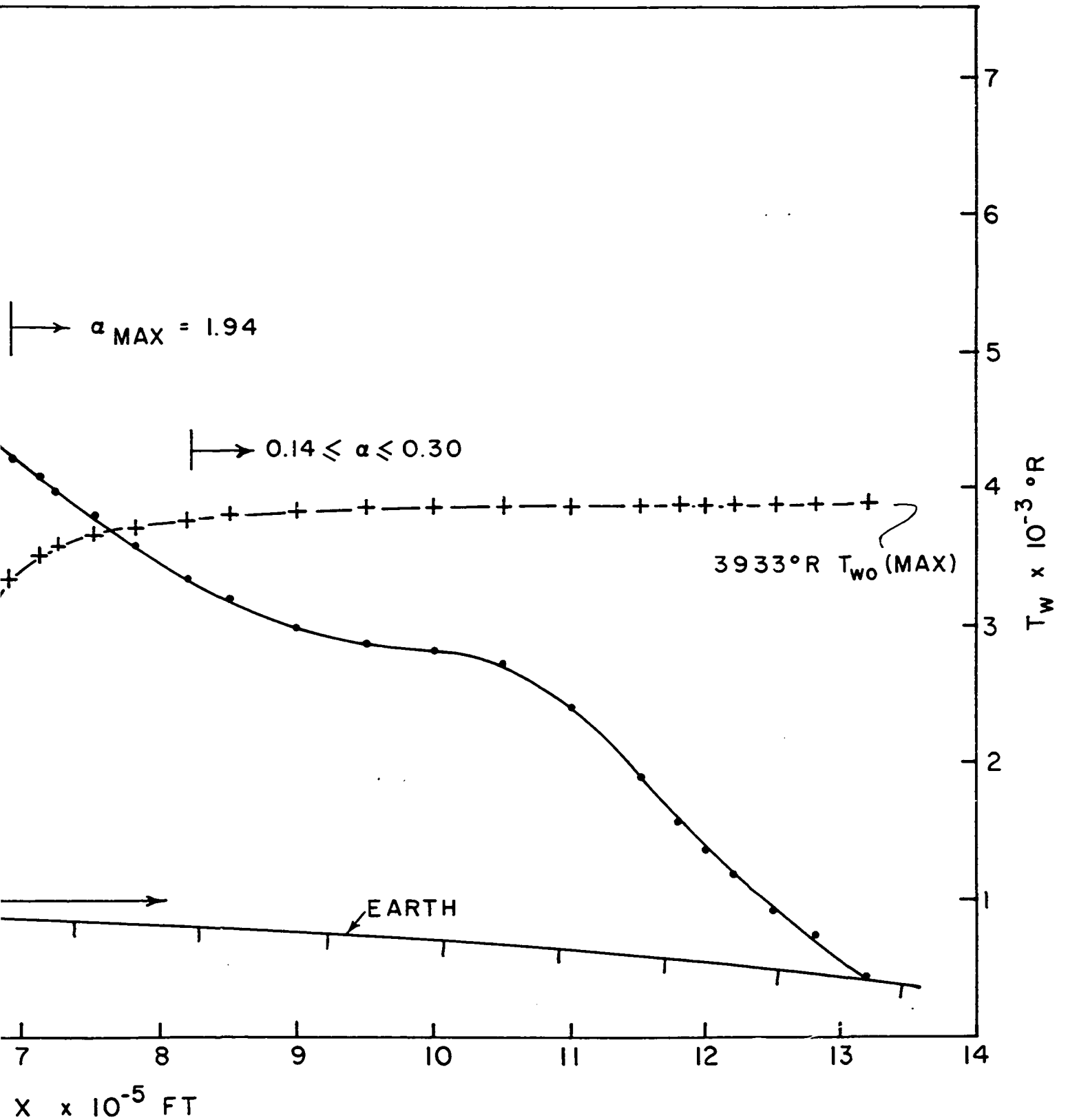
α_{MAX} = 1.94
0.14 ≤ α ≤ 0.30
3933°R T_{wo} (MAX)
EARTH
7
6
5
4
3
2
1
$T_w \times 10^{-3}$ °R
7
8
9
10
11
12
13
14
X x 10^{-5} FT

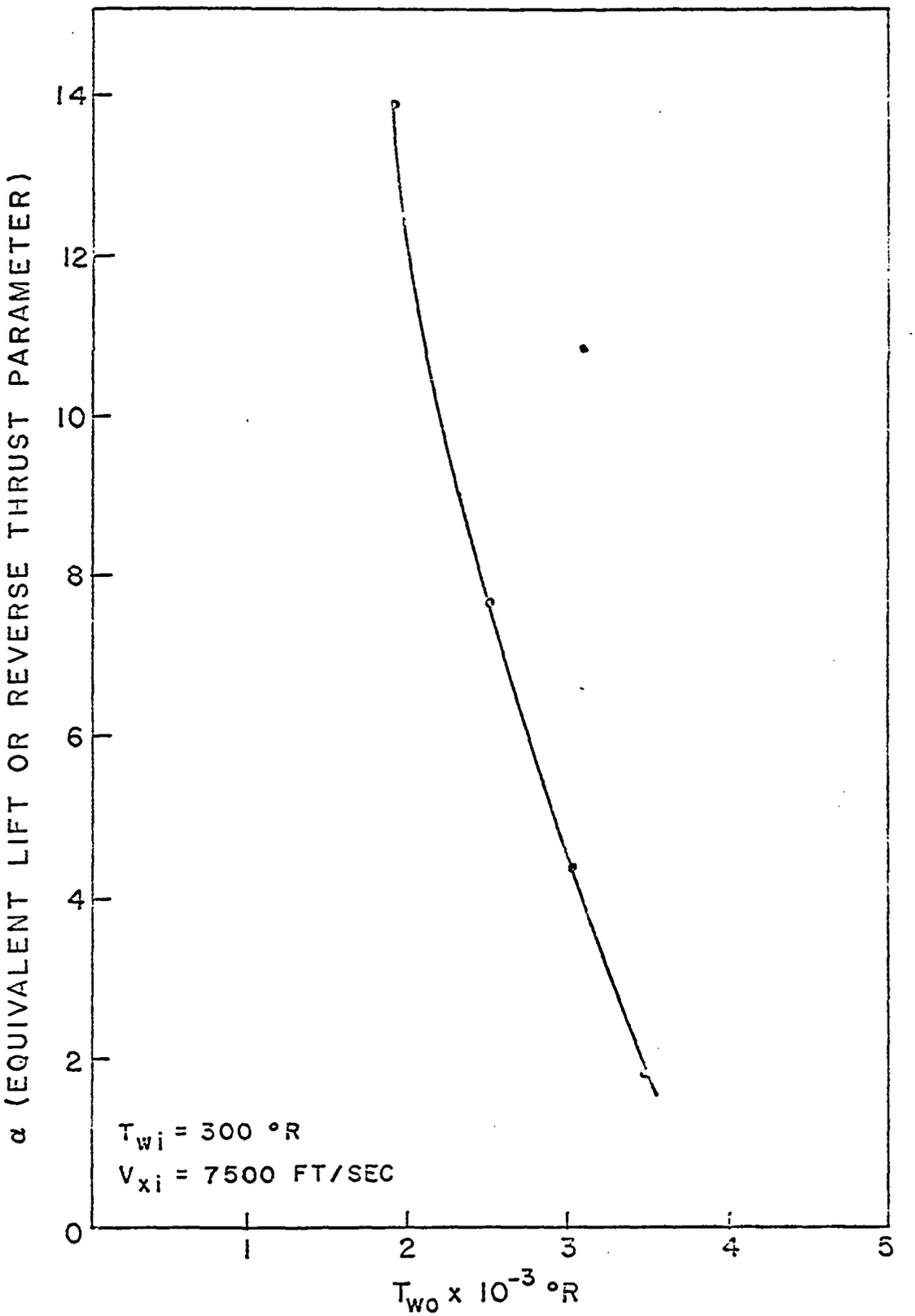

Figure 26. α versus preassigned T_{wo}

BIBLIOGRAPHY

1. Battle, C. T., Bryson, A. E. and Mikami, K. Optimum lateral turns for a re-entry glider. Aerospace Engineering 21:18-23. 1962.

2. Bliss, G. A. Lectures on the calculus of variations. University of Chicago Press. 1946.

3. Brainin, S. M. and Mason, M. Descent trajectory optimization for soft lunar landings. Aerospace Engineering 21:55-57, 82-91. 1962.

4. Breakwell, J. V. The optimization of trajectories. North American Aviation, Inc. Report AL-2706. 1957.

5. Dorrance, W. H. Two-dimensional airfoils at moderate hypersonic velocities. Journal of the Aeronautical Sciences 19:593-600. 1952.

6. Ehriche, Krafft A. Principles of guided missiles. Vol. 1. New York, N.Y. D. Von Nostrand Company, Inc. 1960.

7. Friedmann, Herbert. Physics of the atmosphere and space. Astronautics 5:42, 128, 130. 1960.

8. Hall, Newman A. Thermodynamics of fluid flow. 2nd ed., Englewood Cliffs, N.J. Prentice-Hall, Inc. 1956.

9. Knudsen, J. G. and Katz, D. L. Fluid dynamics and heat transfer. New York, N.Y. McGraw-Hill Book Company, Inc. 1958.

10. Lass, Harry. Vector and tensor analysis. New York, N.Y. McGraw-Hill Book Company, Inc. 1950.

11. Lees, L. Recent developments in hypersonic flow. Jet Propulsion 27:1162-1178. 1957.

12. Leitmann, G. On a class of variational problems in rocket flight. Journal of the Aerospace Sciences 26:586-591. 1959.

13. Ling, Lu and Wang, Kenneth. Aerodynamic heating of reentry vehicles. Journal of the Aerospace Sciences 30:1180-1182. 1960.

14. Linnell, R. D. Two-dimensional airfoils in hypersonic flows. Journal of the Aeronautical Sciences 16:22-30. 1949.

15. Miele, A. General variational theory of the flight paths of rocket-powered aircraft, missiles, and satellite carriers. Purdue University Report No. A-58-2. 1958.

16. _____. Generalized variational approach to the optimum thrust programming for the vertical flight of a rocket. ZFW 6:69-70. 1958.

17. _____. Lagrange multipliers and quasi-steady flight mechanics. Purdue University Report No. A-58-3. 1958.

18. _____. Some recent advances in the mechanics of terrestrial flight. Jet Propulsion 28:581-587. 1958.

19. Nathan, A. and Lindorfer, W. Optimization of missile intercept range. Aerospace Engineering 21:74-75, 104-111. 1962.

20. Poritsky, H. Optimum thrust orbits. Proceedings of the Fourth U.S. National Congress of Applied Mechanics 1:347-358. 1962.

21. Probstein, R. F. and Kemp, N. H. Viscous aerodynamic characteristics in hypersonic rareified gas flow. Journal of the Aerospace Sciences 27:174-192. 1960.

22. Rosenberg, R. M. An optimum problem in dynamics. Proceedings of the Fourth U.S. National Congress of Applied Mechanics 1:359-369. 1962.

23. _____. On optimum rocket trajectories and the calculus of variations. Aerospace Engineering 19:20-21, 65-66. 1960.

24. Rosser, J. B. Newton, R. R. and Gross, G. L. Mathematical theory of rocket flight. 1st ed. New York, N.Y. McGraw-Hill Book Company, Inc. 1947.

25. Scala, S. M. The hypersonic environment. Aerospace Engineering 22: 10-20. 1963.

26. Sharpiro, Ascher H. Dynamics and thermodynamics of compressible flow. Vol. 1. New York, N.Y. Ronald Press Company. 1953.

27. Stechert, D. G. Ballistic missile and space technology. 1st ed. New York, N.Y. Academic Press, Inc. 1960.

28. Stewartson, K. On the motion of a flat plate at high speed in a viscous compressible fluid. Journal of the Aeronautical Sciences 22:303-309. 1955.

29. Stojanovic, Dragutin. Similar temperature boundary layers. Journal of the Aerospace Sciences 26:571-574. 1959.

30. Strand, T. Design of missile bodies for minimum drag at very high speeds-thickness ratio, lift, and center of pressure given. Journal of the Aerospace Sciences 19:568-578. 1952.

31. Truitt, Robert W. Fundamentals of aerodynamic heating. New York, N.Y. McGraw-Hill Book Company, Inc. 1962.

32. Van Wylen, Gordon J. Thermodynamics. New York, N.Y. John Wiley and Sons, Inc. 1959.

33. Whittaker, E. T. A treatise on the analytical dynamics of particles and rigid bodies. Cambridge, England. Cambridge University Press. 1937.